ISDN 1039-3218

Nutrient Status of the Sediments of Port Phillip Bay

G.J. Nicholson, A.R. Longmore and R.A. Cowdell
Marine and Freshwater Resources Institute
PO Box 114
Queenscliff
Victoria 3225 Australia

Technical Report No.26

Port Phillip Bay Environmental Study
CSIRO Environmental Projects Office
Building 9, Forestry Site, Banks Street
Yarralumla, ACT, Australia

PO Box 225, Dickson, ACT 2602, Australia

September 1996

ABSTRACT

Nutrient fluxes from the sediments of Port Phillip Bay were estimated from the results of sediment coring and benthic chamber deployments between July 1993 and January 1996. Sediment coring estimated fluxes caused by diffusive processes only whereas benthic chambers measured fluxes caused by diffusion, advection and bio-irrigation. Diffusive fluxes differed between sites whilst temperature and site differences were evident from benthic chamber flux rates. During summer periods fluxes measured from chamber deployments were generally more than twice the magnitude of the fluxes measured from sediment coring. The greatest fluxes measured from chamber deployments were at sites near major terrestrial inputs of nutrients to the Bay when water temperatures were near their annual maximum. Denitrification within the Bay was very efficient with about 60 - 70% N lost to the system annually. Benthic-associated primary production was found at three sites sampled.

CONTENTS

CONTENTS (cont'd)

CONTENTS (cont'd)

TABLES

FIGURES

FIGURES

INTRODUCTION

General

Port Phillip Bay (PPB), located on the central south coast of Victoria, Australia, is an almost land-locked marine embayment of 1950 km^2 area (Figure 1). Urban and industrial development surrounds most of the Bay, with the city of Melbourne (population 3,000,000) along the northern and eastern shorelines and the city of Geelong (population 200,000) sited in the south-west. Water exchange with Bass Strait is restricted by the 3 km wide entrance, with an estimated Bay turnover time of about one year (Hunter 1992).

The catchment of the Bay, encompassing forested, agricultural, urban and industrial land, has an area of about 10,000 km^2. Approximately 65% of the catchment is drained by the Yarra River and it's tributaries, with most of the remainder accounted for by the Patterson, Werribee and Little Rivers and Kananook and Kororoit Creeks.

More than half of Melbourne's wastewater, including about 90% of industrial liquid waste, passes through the Western Treatment Plant (WTP). This facility is situated on the western foreshore of PPB occupying an area of 10,800 ha of which 6,700 ha is used for treatment purposes. It discharges treated effluent (lagoon settlement and summer land irrigation/winter grass filtration) directly to the Bay. There are a number of other smaller treatment plants that discharge to the Bay indirectly through water courses. Their total input is very small.

The major nutrient loads enter the Bay via riverine transport and sewage treatment facilities. Rivers, streams and drains discharge annually from 2000 to 3000 tonnes of nitrogen (N) and 500 tonnes of phosphorus (P) to the Bay, while about 3600 tonnes N and 1000 tonnes P enter the Bay in effluent discharged from the WTP (Murray 1994). Groundwater N load is probably about 50 t y^{-1} or less, and P load about 10 t y^{-1} (Otto 1992). Deposition of N from the atmosphere is about 1000 t y^{-1} (Skyring *et al*. 1992).

Whilst most of the N enters the Bay as ammonium, it is rapidly taken up by primary producers and converted to particulate organic N (PON) and dissolved organic N (DON) forms. Dissolved organic N make up about 90% of the total N and is present in many unknown and probably refractory forms. Phosphorus is almost the opposite of N, being present mainly as dissolved inorganic P (DIP) with very little dissolved organic P (DOP). The distribution of biomarkers in the sediments of the Bay indicates that the major source of sedimented organic matter is from diatoms (O'Leary *et al*. 1994). The decomposition of sedimented organic matter of marine planktonic origin follows a fixed stoichiometric molar relationship, termed the Redfield ratio, *viz* 138O_2:106C:16N:1P (Hecky *et al*. 1993) :16Si (Justic *et al*. 1995). Nitrogen is the limiting nutrient in the Bay (Axelrad *et al*. 1981, Longmore *et al.* 1989).

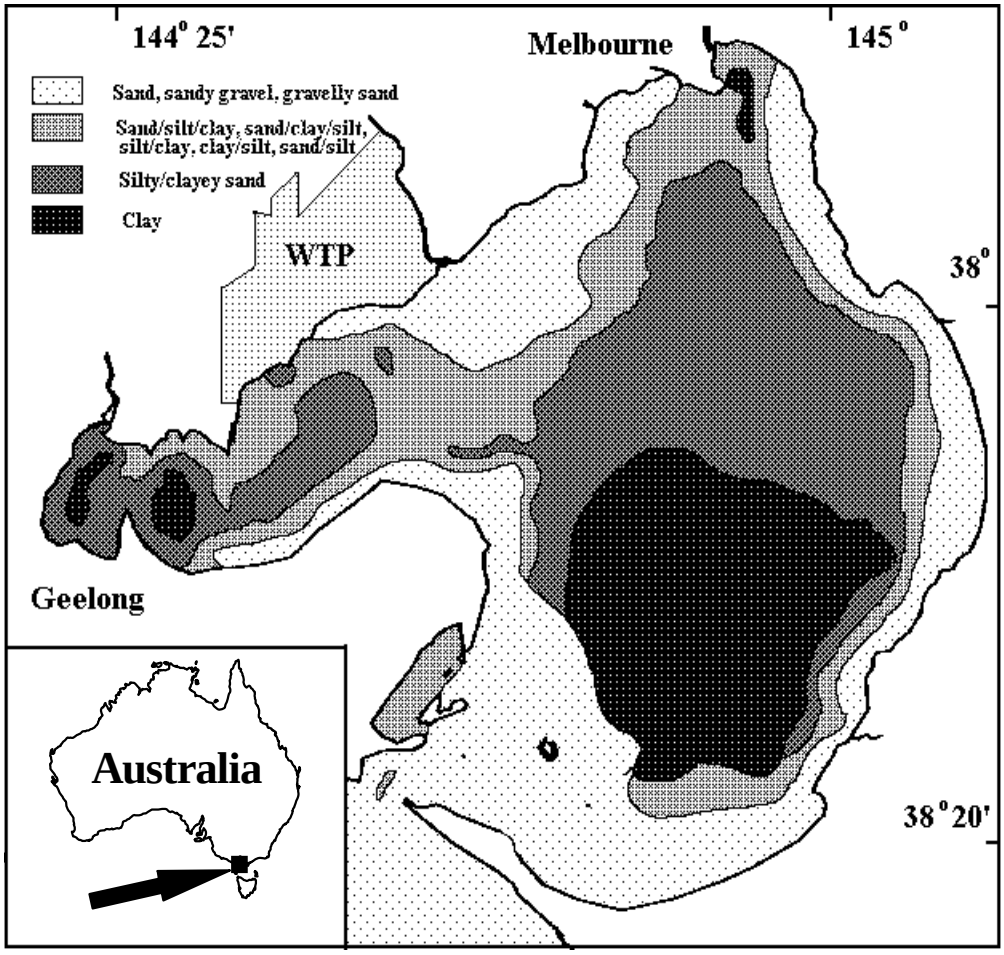

Figure 1: The distribution of sediment types in PPB (from Beasley 1966).

Sediments

The four broad categories of sediment types in PPB are shown in Figure 1. The deeper central section has a large deposit of fines with the 15 m depth contour approximating the boundary of silty/clayey sand. Sections of the Geelong Arm and Corio Bay where fines are deposited are shallower than this but may be areas of lower current and wave energy. Appendix 1 contains diver observations of sediment type at a number of sites (Figure 2) within PPB.

Previous work

Little is known about the contribution that nutrient fluxes derived from the breakdown of sedimented organic matter make to the water column of the Bay. Bauld and Millis (1977) has demonstrated mineralisation, nitrification and denitrification in sediments off the WTP. They found nutrient levels in the interstitial water to be 10 to 20 times higher than in the water column, but decreasing off-shore. Results from two more comprehensive studies of Bay sediments, in which sediment cores were brought ashore and incubated, indicated a net flux of inorganic P into the sediments and a net flux of inorganic N out of

the sediment (Gorfine *et al.* 1996, Longmore *et al*. 1994). It was estimated that from 6000 to 18,000 tonnes of inorganic N transferred annually from the sediments to the water column. This amount is of the same order as that discharged to the Bay from land (Skyring *et al*. 1992).

Tasks

Task N3.1, determining the nutrient status and nutrient pool sizes within the sediments, was investigated by chemical analysis of extracted interstitial water from cored and sectioned sediment collected from a number of sites within the Bay. Task N3.2, determining nutrient fluxes between the sediments and the water column, and task N3.3, determining factors controlling nutrient fluxes, were investigated by the deployment of benthic chambers on the sediments of the Bay at a number of locations.

An objective of the PPBES was to develop a set of integrated models of physical, chemical and biological processes within the Bay, which managers could use as extended monitoring tools and as predictive tools in assessing the impacts of nutrient and contaminant loadings. The results presented here have made a fundamental contribution to such models.

METHODS

Fluxes were measured in two ways in this study: diffusive fluxes by calculation from porewater solute concentrations and net fluxes (diffusive and advective) by benthic chamber measurements.

Vertical fluxes of solutes diffusing between sediments and the overlying water can be calculated from Fick's First Law of Diffusion (Revsbech *et al*. 1980, Ullman and Aller 1982, Emerson *et al*. 1984, Sweerts 1991). The major controls on diffusive fluxes are sediment porosity and the Diffusive Boundary Layer (DBL). The DBL is formed when the internal friction of water creates a viscous boundary layer at the sediment-water interface. It forms a partial barrier between the bulk water and the sediment surface. The DBL is typically between 0.1 mm to several millimetres thick and flow velocity of water above the sediment has a major effect on DBL thickness (Jorgensen and Revsbech 1985, Santschi *et al*. 1990, Burke 1995).

Fluxes estimated from measurements using benthic chambers integrate diffusive and bioturbation/bioirrigation processes. Bioturbation refers to the physical effect of biological activity on particle and porewater dynamics at the sediment-water interface. The range of mechanisms of particle and water movement by macro-organisms is varied, and the effects of bioturbation/bioirrigation on mass transport and chemical micro-environments in surface sediments include an increase in surface area, mixing, biodiffusion, enhancement of porewater exchange, horizontal and vertical redox gradients and spherical gradients (Santschi *et al.* 1990). As the DBL is a hindrance to dissolved oxygen (DO) diffusion to the sediments, burrowing animals respond by either building sediment tubes or creating mounds high enough above the sediment to be free of DBL effects (Jorgensen and Revsbech 1985) or by vigorous pumping regimes. The resulting loose packed and oxygen-ventilated sediments may sustain aerobic bacterial populations at depths some centimetres below the sediment-water interface (Bird 1994).

SECTION 1: SEDIMENT SAMPLING

DIFFUSIVE FLUXES

Principles

Fluxes of solutes diffusing from sediments into the overlying water can be calculated from Fick's First Law of Diffusion (Revsbech *et al*. 1980, Ullman and Aller 1982, Emerson *et al*. 1984, Sweerts 1991).

$$J_S = -Ø D_S (ðC/ðx) \quad (1)$$

where J_S = flux (mol cm^{-2} s^{-1})

Ø = porosity of the sediment

D_S = whole sediment diffusion coefficient (cm^2 s^{-1})

ðC/ðx = initial concentration gradient (mol cm^{-3} cm^{-1})

D_S is estimated, because while diffusivities of solutes in particle free water are known (D_O), the effect of tortuosity (*t*) is not known. Tortuosity is defined as the ratio of the distance (dl) that a diffusing species must travel through an interstitial space in a porous medium to the linear distance (dx) that it would travel in a particle free medium (Sweerts 1991).

$$t = dl/dx \quad (2)$$

The method of calculating D_S and *t* is presented by Ullman and Aller (1982):

$$D_S = D_O / t^2 \quad (3)$$

and $$t^2 = ØF \quad (4)$$

where $$F = Ø^{-m} \quad (5)$$

m is an approximate exponent, and depends on the sediment porosity. For sediments of porosity less than or equal to 0.7, **m** = 2 is a good approximation. For sediments of porosity greater than 0.7, **m** = 3 is a good approximation. Ullman and Aller (1982) note different values of **m** used by other workers. The discrepancies are not large and there appears to be a general acknowledgment of different **m** values for different sediment types (or porosities). For surficial marine sediments at least, the empirical correction factors based on porosity as outlined above should yield good estimates of bulk diffusion coefficients for the quantitative modelling of solute behaviour.

Temperature affects molecular diffusion coefficients and has to be corrected for (Krom and Berner 1980). Silicate diffusion coefficients approximately double for every 25^{o}C increase in temperature (Emerson *et al*. 1984, Marinelli 1992).

The temperature correction applied to SiO_4^{4-} diffusion coefficients (Marinelli 1992) is :

$$\mathbf{D_0(SiO_4^{4-}) = 5e^{(0.0277259\ T)}} \qquad (6)$$

where T = temperature in ^{o}C.

Empirical expressions which provide good temperature corrected approximations over the temperature range 0 - 25^{o}C (Krom and Berner 1980) are:

$$\mathbf{D_0(NH_4^{+}) = 19.8 + 0.40(T - 25)} \qquad (7)$$

$$\mathbf{D_0(HPO_4^{2-}) = 7.34 + 0.16(T - 25)} \; . \qquad (8)$$

and

$$\mathbf{D_0(H_2PO_4^{-}) = 8.46 + 0.19(T - 25)} \qquad (9)$$

where HPO_4^{2-} is present as 0.8 of the total PO_4^{3-}, and $H_2PO_4^{-}$ is present as 0.2 of the total PO_4^{3-} at seawater pH (8).

In addition to molecular diffusion, faunal activity can affect the vertical solute transport in the sediment. Thus, the effective or apparent diffusion coefficient (D_e) of sediments with infauna is the sum of D_S and the increased diffusion due to faunal activity (D_i)

$$\mathbf{D_e = D_S + D_i} \qquad (10)$$ (Sweerts, 1991)

The porosity of the sediment is a dimensionless unit and is calculated by:

$$\mathbf{Ø = 1 - (dry/wet)} \qquad (11)$$

where **dry** is the oven-dried (110^{o}C) weight per unit volume of the sediment, and **wet** is the wet weight per unit volume of the sediment, which includes the weight of the extracted porewater.

Many benthic processes occur at millimetre scales or less at the sediment-seawater interface (Berelson *et al*. 1994). The core sectioning table we used enabled us to slice our sediment cores into sections of 1 cm. Therefore, the concentration gradient was calculated as the difference between the overlying water nutrient concentration and the concentration of the nutrient in the interstitial water from the first depth sectioned, and the depth of the interstitial water concentration was taken as the mid-point of the first section, at a depth of 0.5 cm. However, even this depth may be too great for calculating the concentration gradient.

FIELD SAMPLING

Diffusive fluxes of ammonium (NH_4), nitrite (NO_2), nitrite plus nitrate (NO_x), phosphate (PO_4) and silicate (SiO_4) were calculated from porewater profiles obtained from three sediment core collection periods in PPB during July 1993, January 1994 and July 1994.

July 1993

During the period 14 July to 6 August 1993, 22 sites (Figure 2 and Table 1) were analysed for sediment nutrient concentrations. At each site SCUBA divers collected sediment cores in triplicate using polycarbonate corers of 10 cm diameter and 50 cm long. The corers were placed next to each other on the sediment and pushed as far as possible into the sediment, usually to a depth of approximately 40 cm. The corers were withdrawn from the sediment by first digging down by hand alongside the corer and installing a bottom stopper. The top stopper was installed whilst supporting the bottom stopper by hand to ensure that it was not displaced. Once both stoppers were in place the corer was removed from the sediment and transferred on-board for immediate analysis.

The top stopper of the corer to be processed was removed so that excess water above the sediment surface could be drained off by gentle siphoning. The corer was then placed in the extrusion table. This table was designed so that the extruded sediment could be sectioned into 1 cm thick slices. The sectioning and transferring of sediment sections to other containers was always conducted within an atmosphere of N_2 to avoid loss of nutrients by the oxidation of reduced metals (Bray *et al*. 1973). As each section was sliced, approximately 60 cm^3 of the sediment of that slice was immediately placed within a labelled 85 mL capped centrifuge tube, which had been previously flushed and filled with nitrogen gas.

The centrifuge tubes were spun at 11,000 RPM for 5 minutes using a "Hettich Universal 30F" centrifuge. Following centrifugation the volume of the spun-out porewater was measured by measuring cylinder. Usually 10 mL was transferred by syringe filtration through 0.45 *u*m membrane filters to sample cups for immediate analysis of inorganic nutrients in the on-board laboratory. Porewaters from replicate cores were pooled to provide enough sample for Kjeldahl N and total P analysis, stored in labelled resealable plastic bags ("Whirlpaks") and kept frozen until required for on-shore laboratory analysis.

Ammonium was measured using an automated phenol-hypochlorite method (Solorzano 1969, Technicon 1973a) with significant modifications by VFRI to eliminate salinity dependent sensitivity. Nitrite was measured using the method of Bendschneider and Robinson (1952) as automated by Technicon (1972). Nitrate was measured as NO_2 using an automated cadmium coil reduction method (Morris and Riley 1963, Technicon 1972). Phosphate was measured by the automated molybdenum method (Murphy and Riley 1962, Technicon 1973b). Monomeric reactive SiO_4 was measured by the method of Koroleff (1972) as automated by Technicon (1973c). Results were digitised and recorded on an interfaced computer.

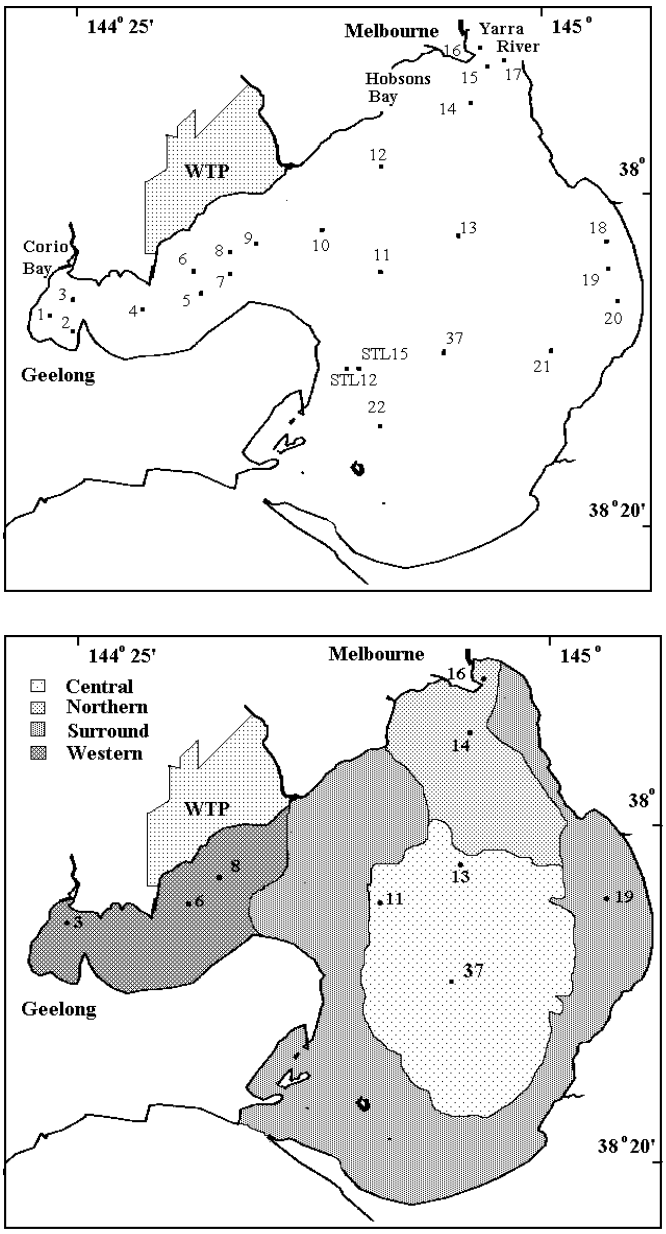

Figure 2: All sites sampled at least once in PPB by sediment coring or chamber deployment are shown in the top diagram. The four regions of the Bay are based on similar inorganic nutrient flux behaviour. The reduced number of sites selected for repetitive sampling by sediment coring and for benthic chamber deployment are shown in the lower diagram.

Table 1: Site locations, the water depth at each site and the sediment type at each site. The sites indicated with bold letters were the sites sampled on all three cruises.

Site	Depth (m)	Latitude	Longitude	Sediment Type
1	8	38º 07.92'	144º 22.5'	Silty/clayey sand
2	9	38 07.80	144 28.98	Silty/clayey sand
3	**7**	**38 05.80**	**144 24.36**	**Silty/clayey sand**
4	8	38 07.00	144 29.70	Silty/clayey sand
5	9	38 05.86	144 33.78	Silty/clayey sand
6	**9**	**38 04.70**	**144 33.78**	**Sand/silt/clay**
7	10	38 04.70	144 36.12	Sand/silt/clay
8	**8**	**38 03.09**	**144 36.36**	**Sand/silt/clay**
9	8	38 03.20	144 38.28	Clay undiff sand
10	11	38 02.10	144 43.20	Undiff sand
11	**17**	**38 05.76**	**144 46.88**	**Sand/silt/clay**
12	12	37 58.10	144 47.64	Undiff sand
13	**20**	**38 02.38**	**144 53.52**	**Silty/clayey sand**
14	**13**	**37 54.13**	**144 54.30**	**Sand/silt/clay**
15	8	37 52.20	144 55.20	Sand/silt/clay
16	**8**	**37 51.70**	**144 54.72**	**Clay**
17	4	37 51.94	144 56.46	Coarse sand
18	9	38 03.85	145 04.98	Medium sand
19	**12**	**38 04.66**	**145 04.98**	**Sand/silt/clay**
20	8	38 06.27	145 06.24	Fine sand
21	21	38 09.50	145 00.78	Clay
22	**6**	**38 13.98**	**144 48.26**	**Medium fine sand**
37	**24**	**38 09.47**	**144 52.25**	**Clay**
*STL12	12	38 09.91	144 44.64	Sand/silt/clay
*STL15	15	38 09.91	144 45.02	Sand/silt/clay

* Small scale project related to but not part of this task.

Standards and blanks were analysed frequently to detect drift and changes in sensitivity. Kjeldahl N and total P were determined using the H_2SO_4/H_20_2 digestion method of Nicholls (1975) as modified by VFRI. Total N was derived by the addition of nitrite plus nitrate to the Kjeldahl N value.

The spun-down sediment was removed from the centrifuge tubes and placed in labelled "Whirlpaks" and frozen. This was analysed later in the shore laboratory for wet to dry weight ratios, total P, Kjeldahl N and organic C. Kjeldahl N and total P in subsamples of dried homogenised sediment were determined by the H_2SO_4/H_20_2 digestion method of Nicholls (1975) as modified by VFRI. Organic carbon was determined by the method of Van Hall *et al*. (1963) as modified by VFRI. Subsamples of dried homogenised sediment were placed on combusted glass fibre filters and acidified with 16% HCl to remove calcareous carbon prior to measurement of organic carbon by high-temperature combustion followed by DNIR detection of CO_2.

A sample of bottom water was collected by Niskin bottle at each site, and analysed directly in the on-board laboratory for NH_4, PO_4, SiO_4, NO_2 and NO_3. Four sub-samples were placed in "Whirlpaks" and frozen for shore laboratory analysis of Kjeldahl N and total P.

January 1994

The procedure for sample collection, preparation and analysis was similar to that used in July 1993. Based on fluxes obtained from July 1993, sediment types and water depths, the Bay was divided into four geographical regions designated as Central, Northern, Surround and Western (Figure 2). A subsample of seven of the original 22 sites was chosen for the second block of fieldwork (3, 6, 11, 13, 14, 16 and 19). Sites were considered representative of their regions. An extra site (Site 37) was chosen to represent the Bay centre (Figure 2, Table 1). The coring was modified at Sites 3, 13 and 37 where one of the triplicate cores was lengthened to obtain deeper sediment samples. Site 3 was sampled to a depth of 50 cm, Site 13 to 60 cm and Site 37 to 65 cm. This was done to measure nutrient concentrations at greater depths.

Iron in the extracted porewaters was measured from one core per site, the deepest where applicable. The iron present was complexed with ferrozine and the absorbance of the resulting coloured solution was measured by UV/vis absorbance spectrophotometry (Stookey 1970).

Sulphate and chloride in the porewaters were measured from replicated cores at Sites 3, 6, 13, 14, 16, 19 and 37. For the determination of sulphate, the sample was acidified with HCl, complexed with $BaCl_2$ and the absorbance of the resulting colour was measured by UV/vis absorbance spectrophotometry (Tabatabai 1974). Chloride was determined by titration with $AgNO_3$ (Standard Methods 1992).

July 1994

The procedures and sites sampled for this collection period were identical to the procedures followed during January 1994, except that sulphate and chloride were not measured.

COMPARISONS BETWEEN SAMPLING CRUISES

Inorganic nutrients

Mean porewater profiles of inorganic nutrients from July 1993, January 1994 and July 1994 at eight sites are presented in Figures 3a to 3h.

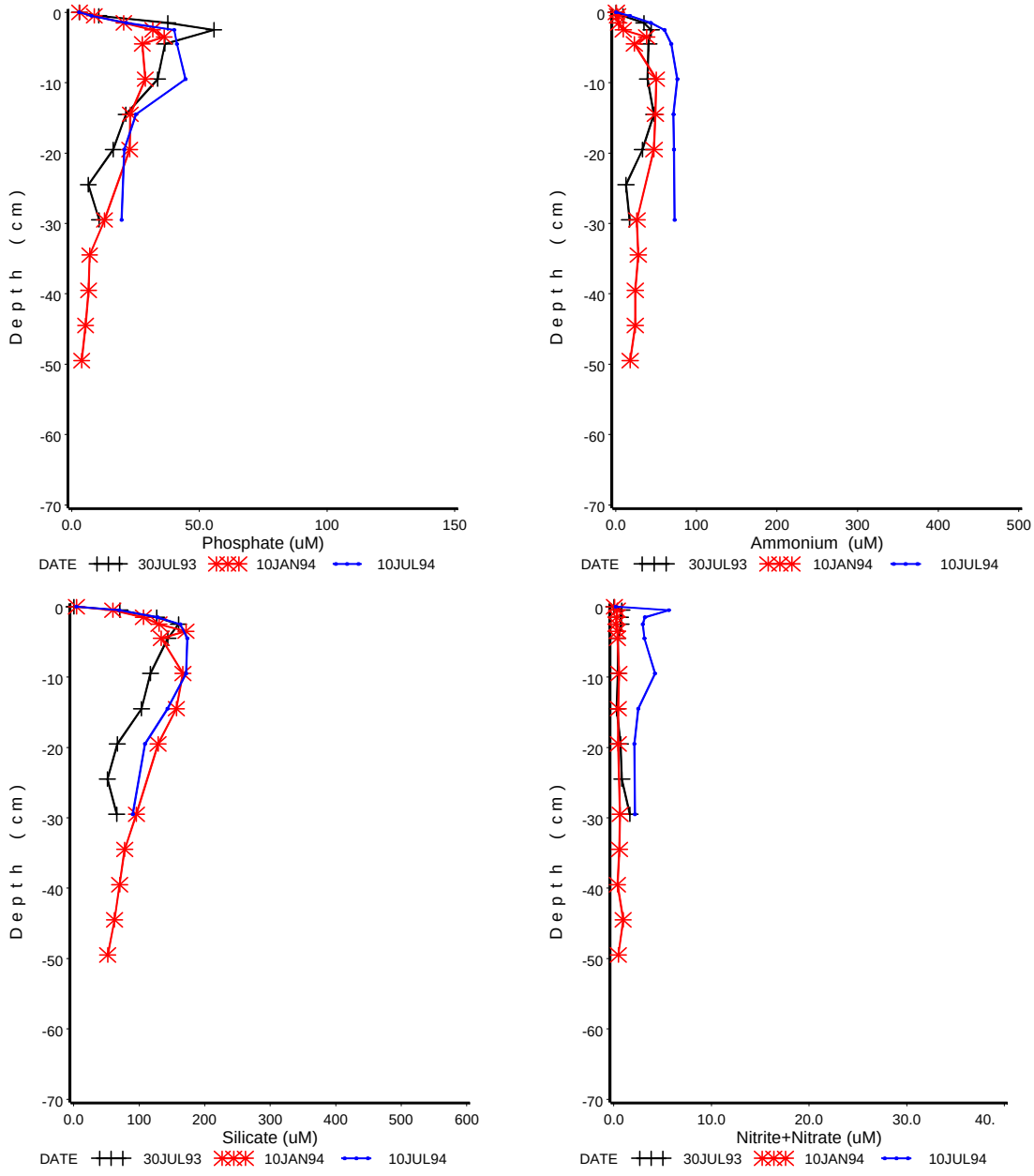

Figure 3a: Mean porewater depth profiles of phosphate, ammonium, silicate and nitrite plus nitrate from three samplings of Site 3 (Corio Bay).

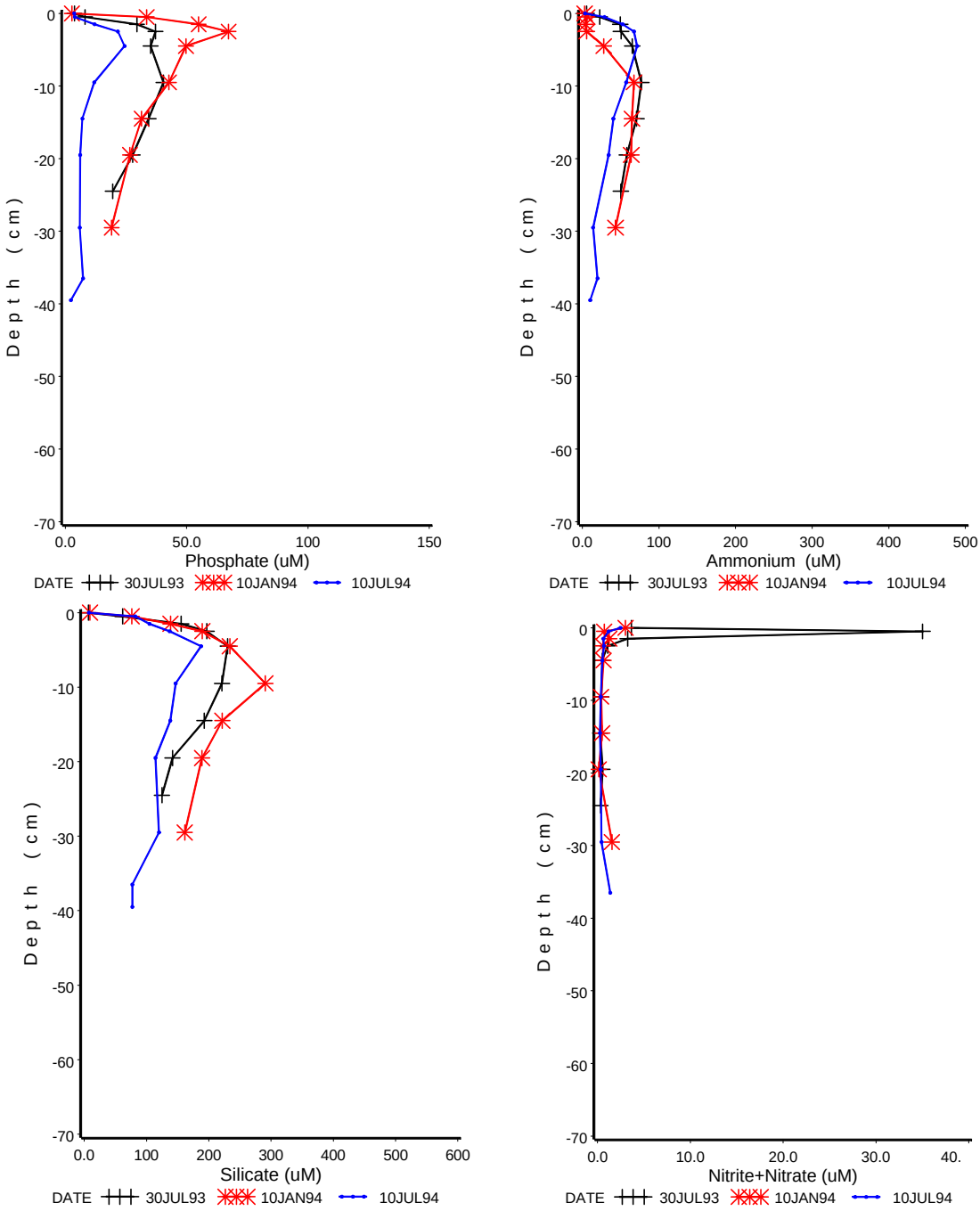

Figure 3b: Mean porewater depth profiles of phosphate, ammonium, silicate and nitrite plus nitrate from three samplings of Site 6 (Werribee).

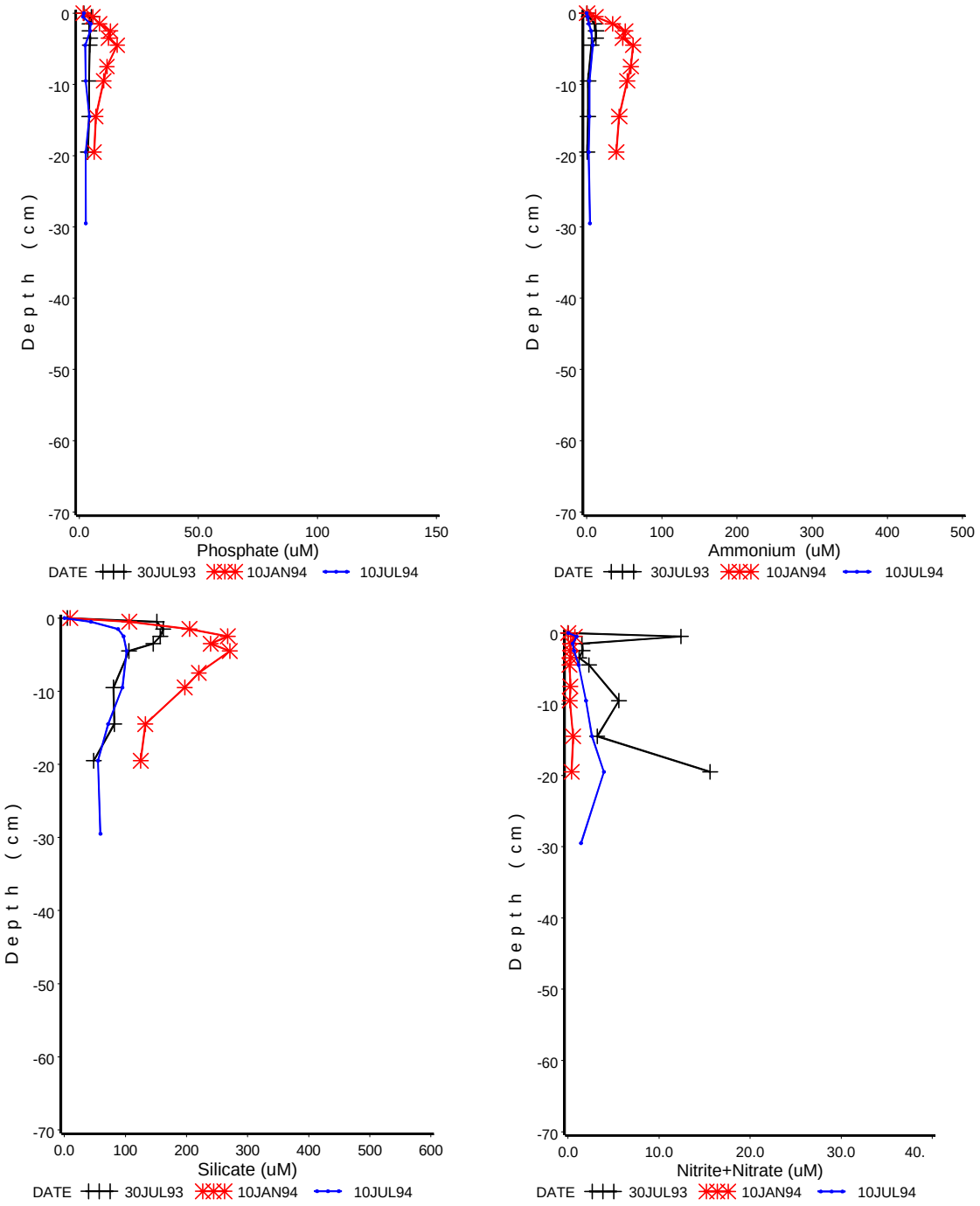

Figure 3c: Mean porewater depth profiles of phosphate, ammonium, silicate and nitrite plus nitrate from three samplings of Site 11 (Central Bay).

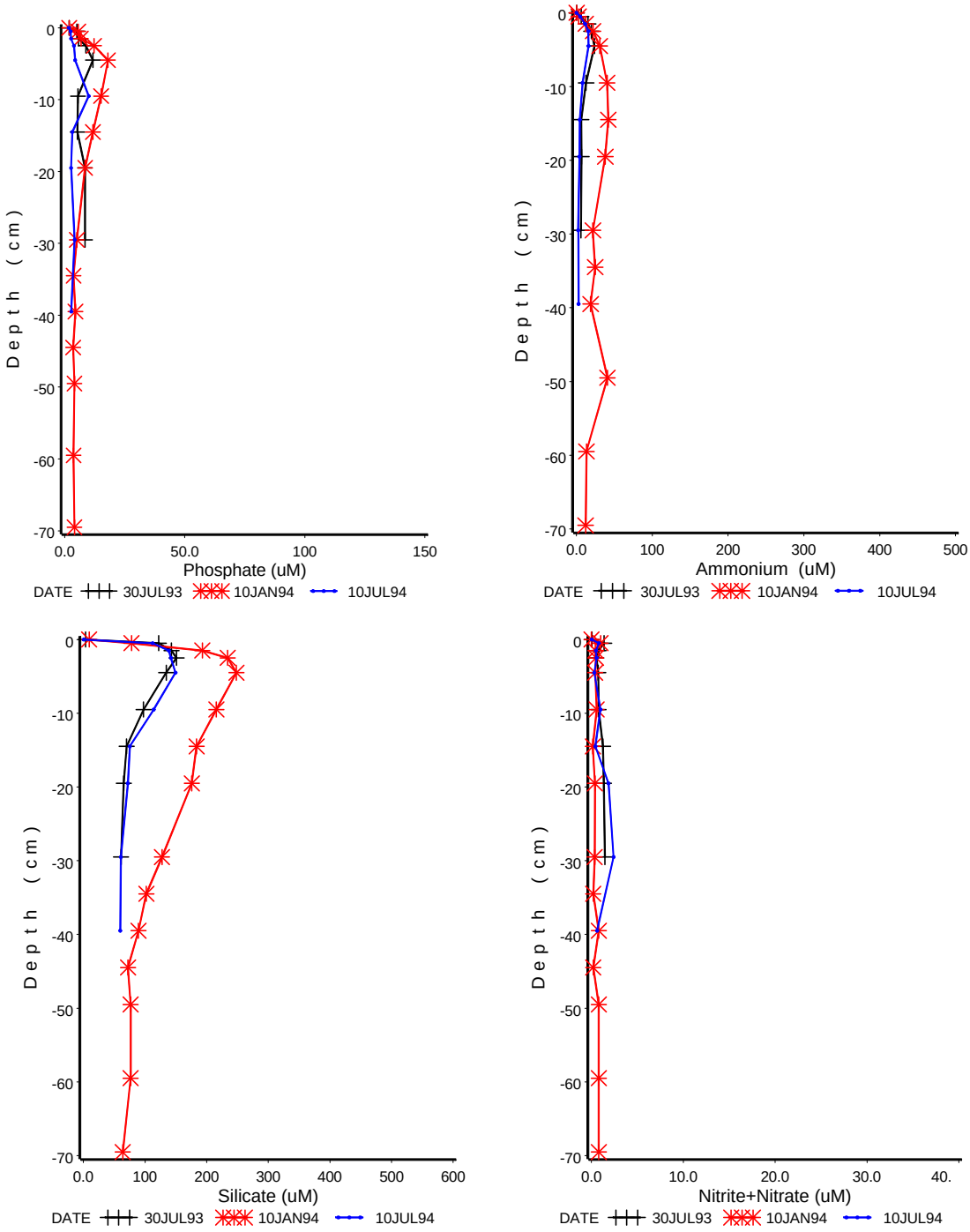

Figure 3d: Mean porewater depth profiles of phosphate, ammonium, silicate and nitrite plus nitrate from three samplings of Site 13 (Central Bay).

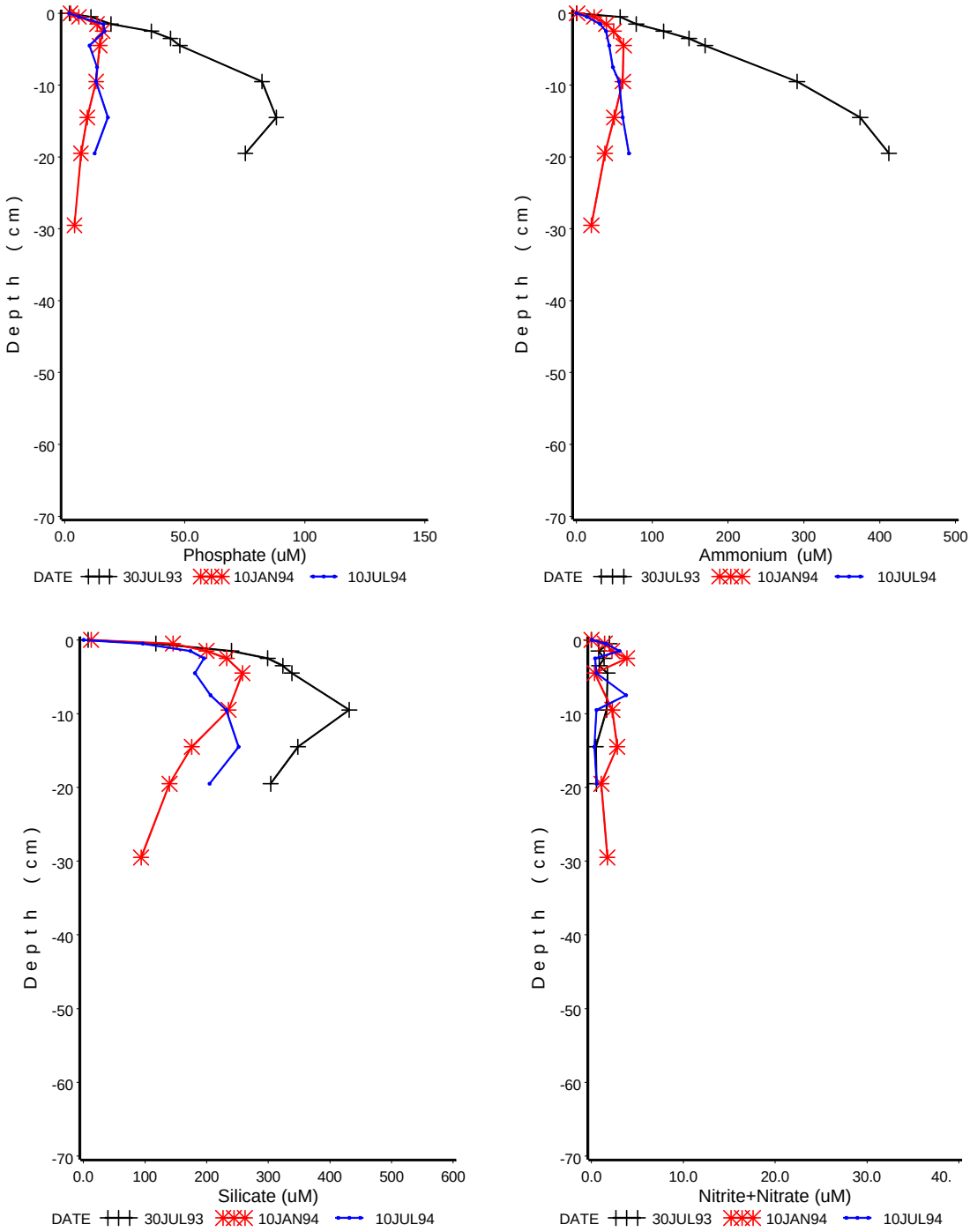

Figure 3e: Mean porewater depth profiles of phosphate, ammonium, silicate and nitrite plus nitrate from three samplings of Site 14 (outer Hobsons Bay).

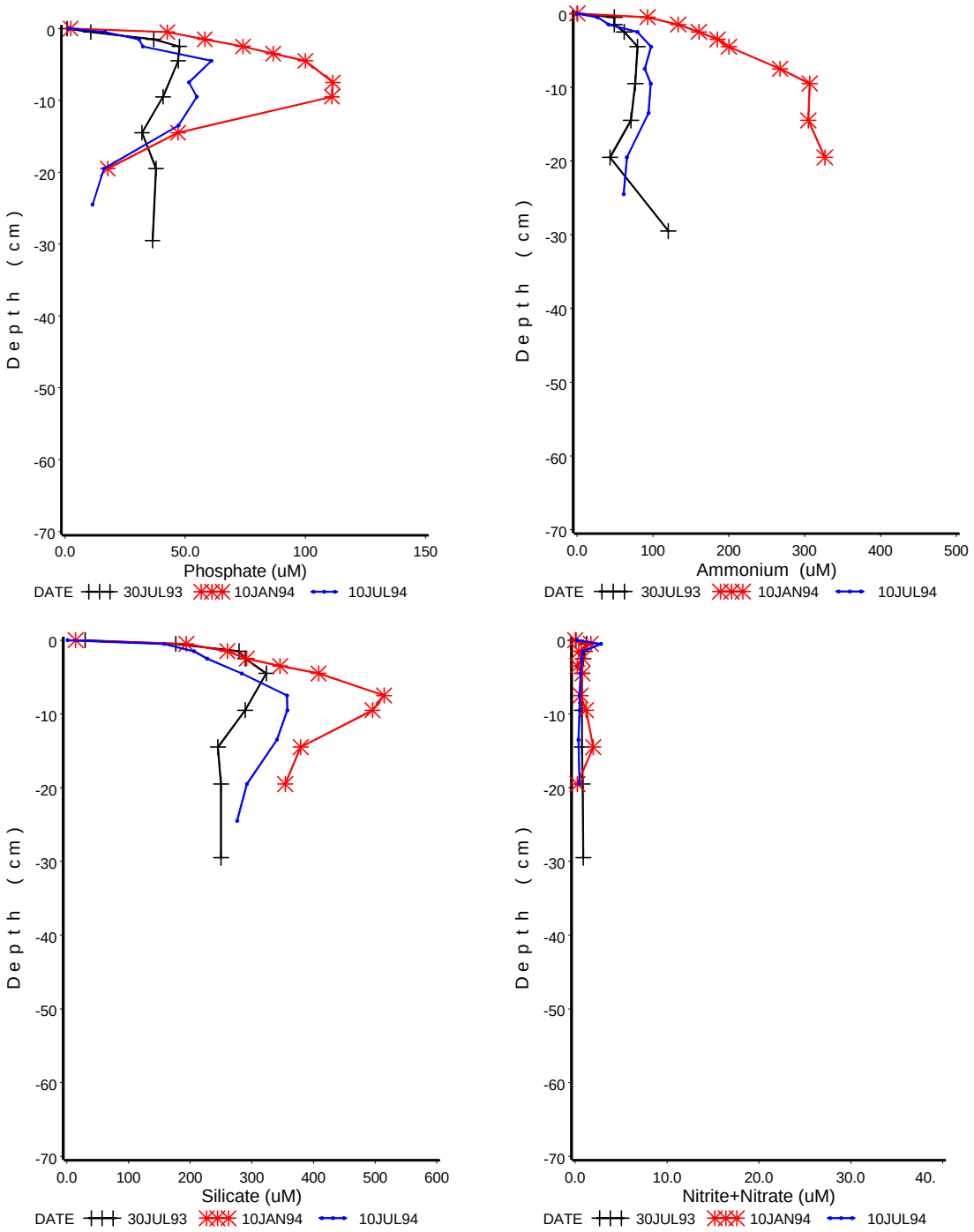

Figure 3f: Mean porewater depth profiles of phosphate, ammonium, silicate and nitrite plus nitrate from three samplings of Site 16 (Yarra mouth).

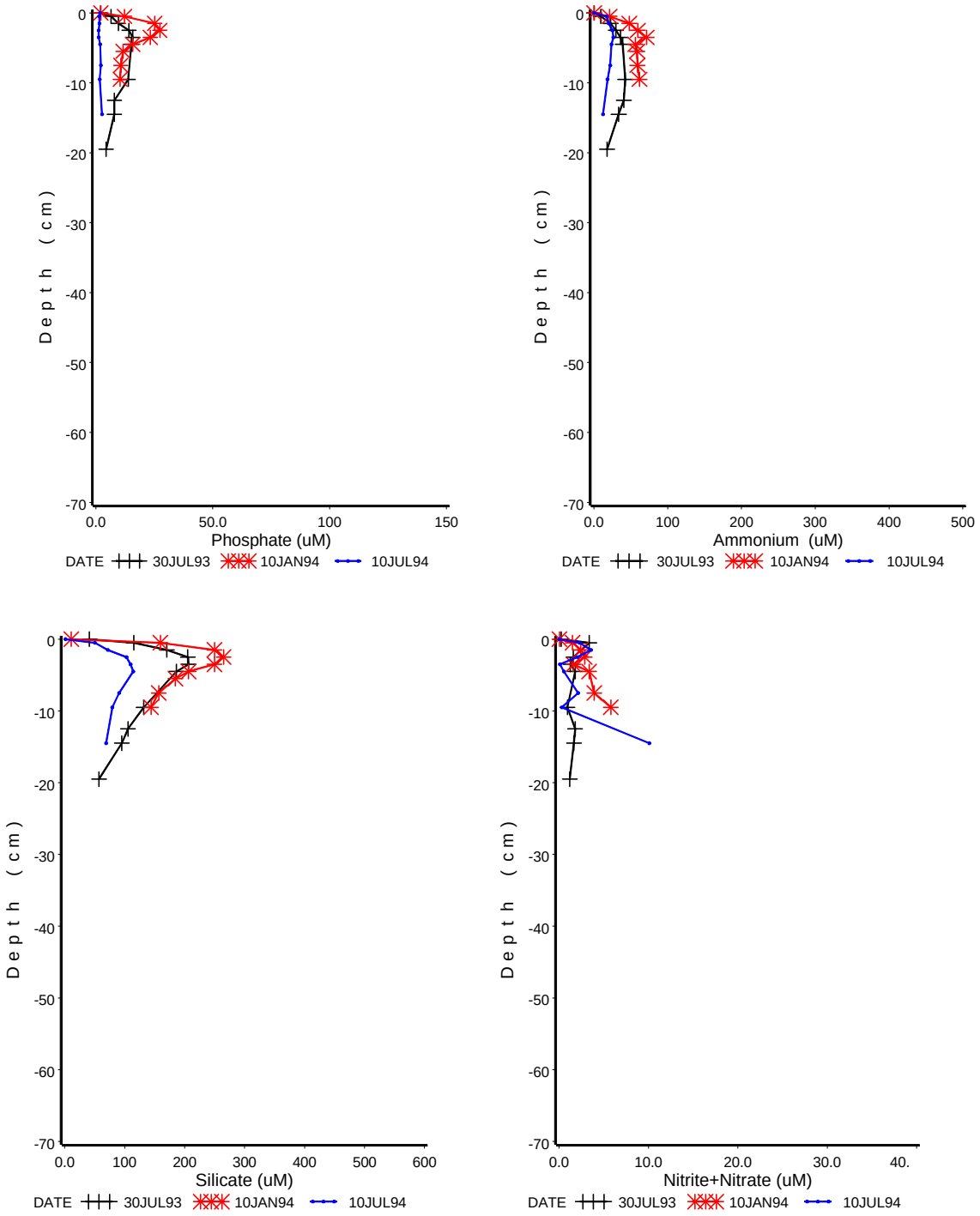

Figure 3g: Mean porewater depth profiles of phosphate, ammonium, silicate and nitrite plus nitrate from three samplings of Site 19 (East coast).

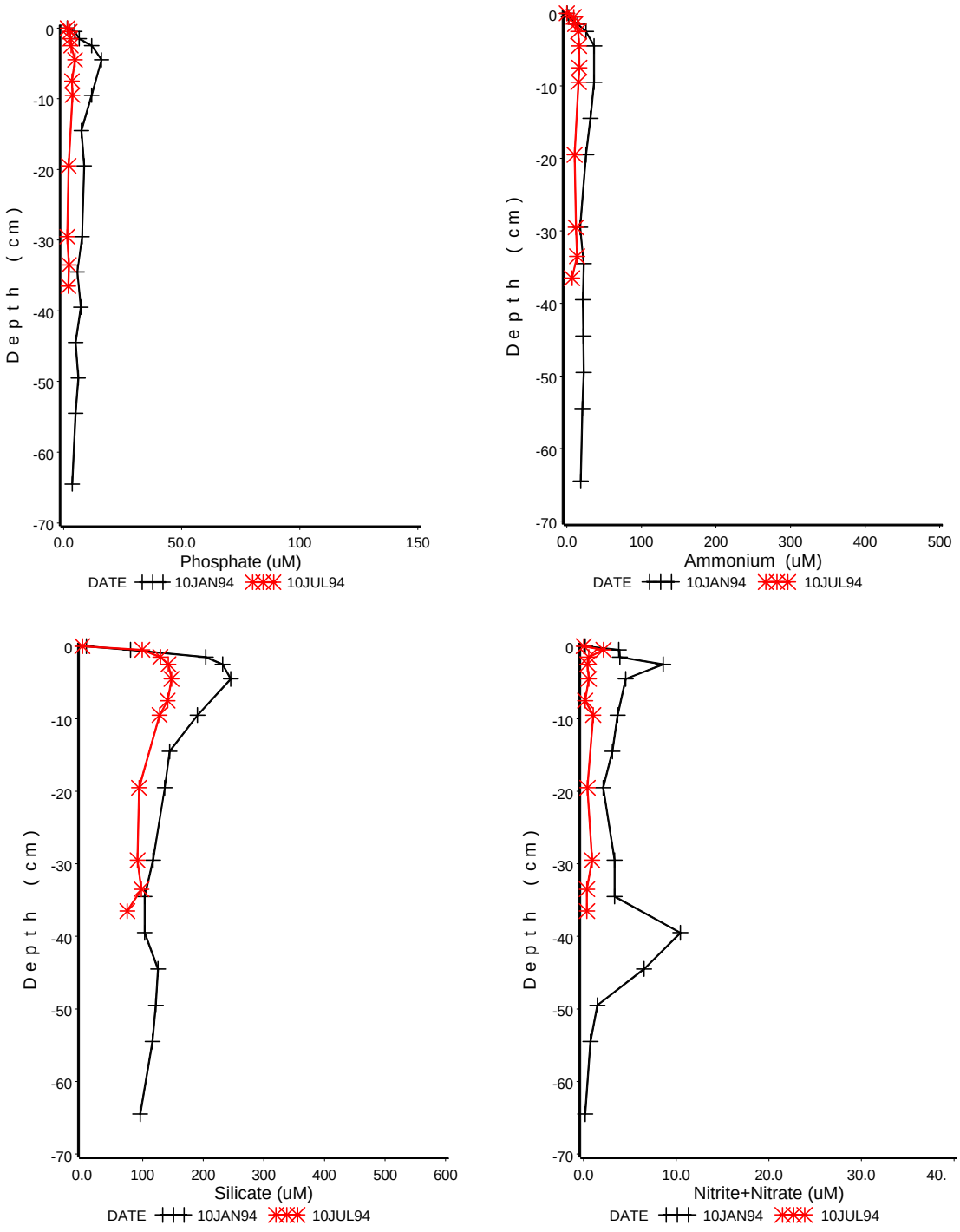

Figure 3h: Mean porewater depth profiles of phosphate, ammonium, silicate and nitrite plus nitrate from January 1994 and July 1994 for Site 37 (Central Bay). This site was not sampled during July 1993.

Diffusive fluxes

Diffusive fluxes were calculated from the concentration gradient between overlying water and porewater at 0.5 cm depth. Mean fluxes of phosphate, ammonium, silicate and nitrite plus nitrate for July 1993, January 1994 and July 1994 are presented in Figures 4a and 4b.

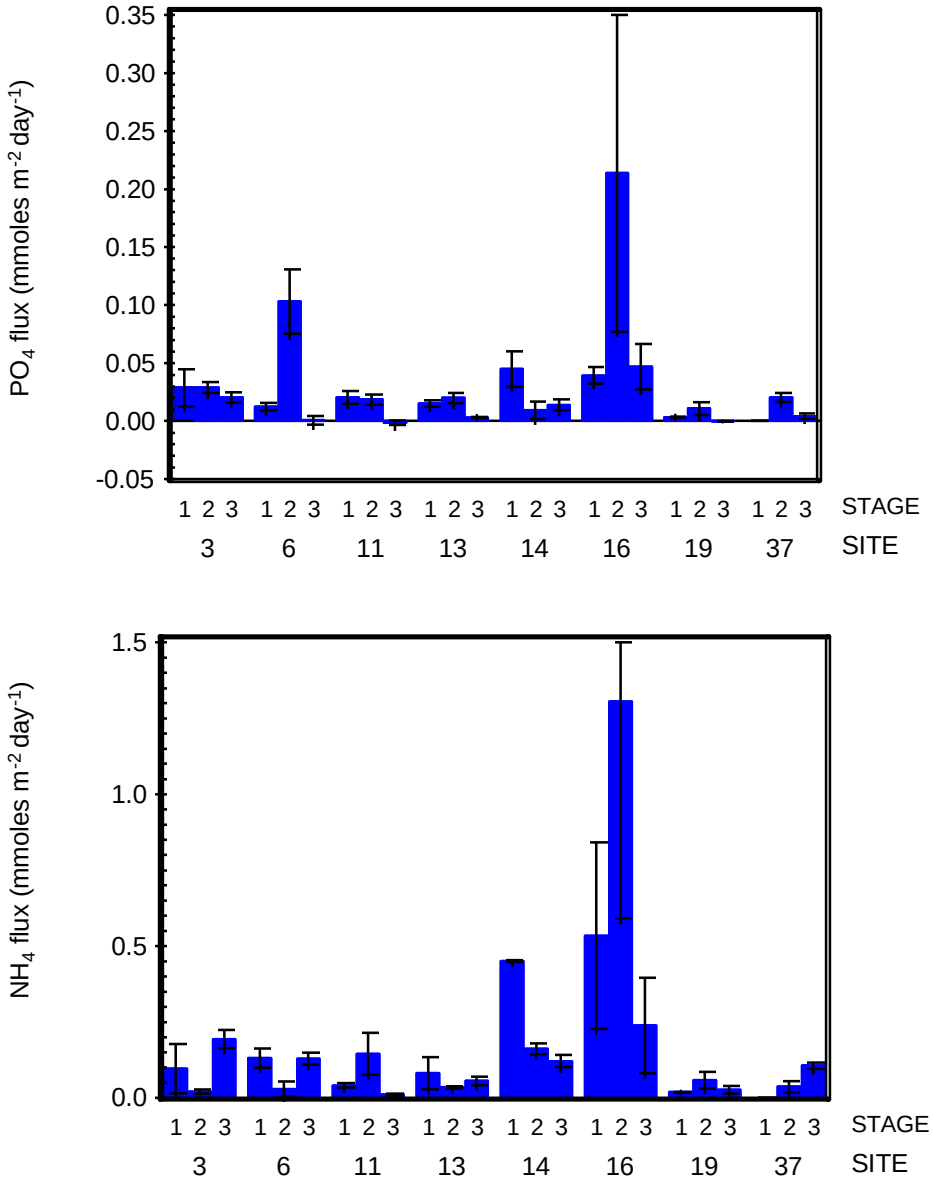

Figure 4a: Mean calculated diffusive fluxes (mmoles m^{-2} day^{-1}) for phosphate and ammonium for the same sites sampled three times (excepting 37) over a 12 month period. Stages 1, 2 and 3 indicate sampling cruises for July 1993, January 1994 and July 1994, respectively. The error bars indicate one standard deviation about the mean.

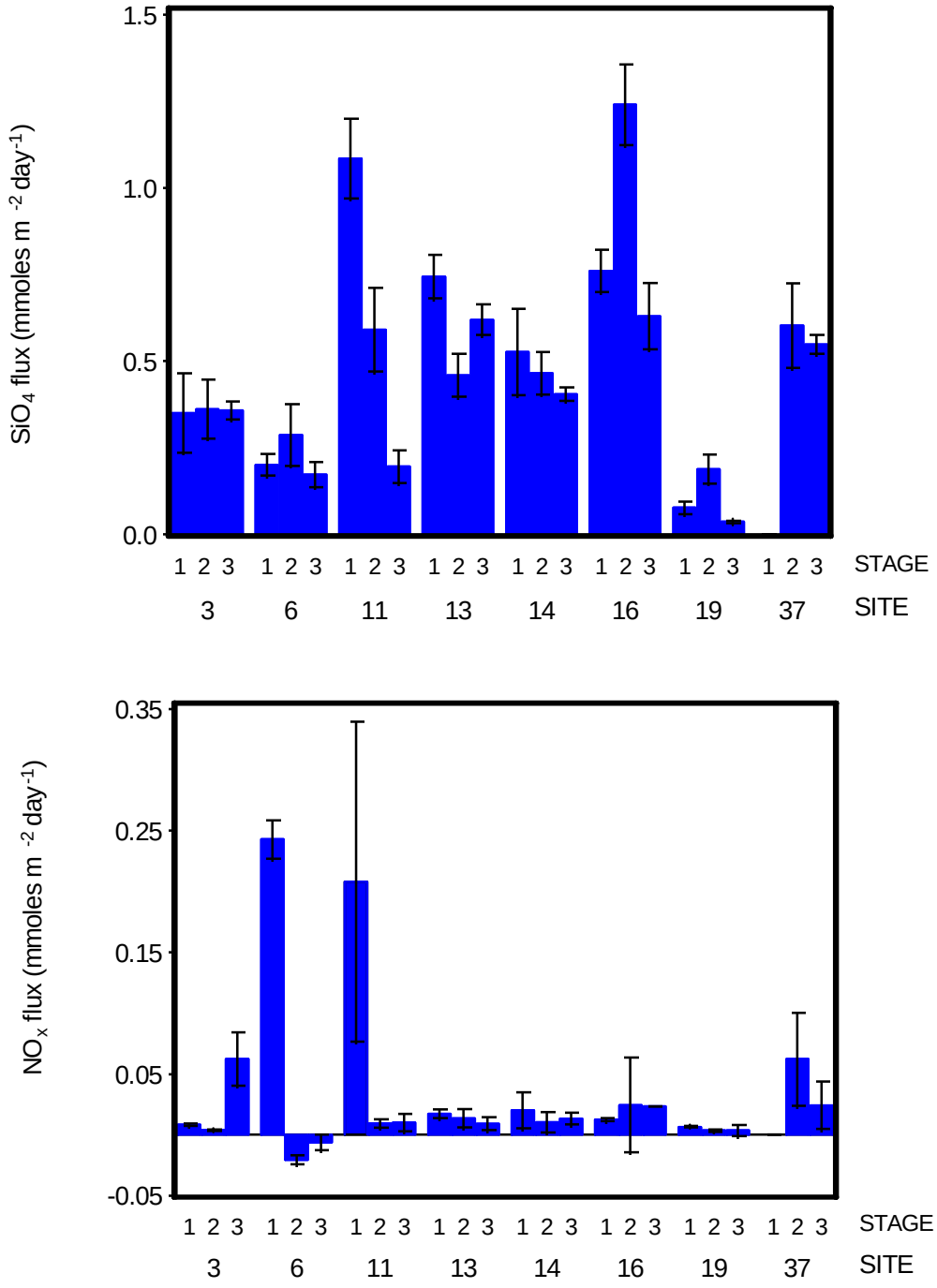

Figure 4b: Mean calculated diffusive fluxes (mmoles m^{-2} day^{-1}) for silicate and nitrite plus nitrate for the same sites sampled three times (excepting 37) over a 12 month period. Stages 1, 2 and 3 indicate sampling cruises for July 1993, January 1994 and July 1994, respectively. The error bars indicate one standard deviation about the mean.

Porewater inorganic nutrient pools

Table 2 and Figure 5 display the contribution of each region to the total inorganic nutrient pool within the porewaters of the Bay to a depth of 20 cm.

Table 2: Porewater pool size (tonnes per region) of PO_4, NH_4, SiO_4 and NO_X for each region to a depth of 20 cm. The date of sampling, nutrient type, number of sample sites within a region, mean mass of the nutrient and highest and lowest values (where applicable) are shown.

Region	Area (km^2)	Date	Nutrient type	Number of sites	Mean mass (tonne)	Highest mass (tonne)	Lowest mass (tonne)
Central	506	Jul93	PO_4 - P	2	15.9	21.2	10.6
		Jan94		3	25.5	19.3	30.7
		Jul94		3	8.8	11.8	6.2
		Jul93	NH_4 - N	2	10.5	16.3	4.6
		Jan94		3	37.8	42.5	34.3
		Jul94		3	9.7	16.1	3.8
		Jul93	SiO_4 - Si	2	246.5	270.6	222.5
		Jan94		3	395.9	435.6	334.2
		Jul94		3	221.6	288.4	145.0
		Jul93	NO_X - N	2	4.0	6.6	1.4
		Jan94		3	1.8	4.6	0.3
		Jul94		3	1.2	1.7	0.8
Northern	240	Jul93	PO_4 - P	2	64.3	80.2	48.4
		Jan94		2	40.9	72.4	9.4
		Jul94		2	23.6	36.6	10.6
		Jul93	NH_4 - N	2	93.4	148.2	38.6
		Jan94		2	64.7	110.3	19.1
		Jul94		2	24.9	32.5	17.4
		Jul93	SiO_4 - Si	2	343.4	373.3	313.5
		Jan94		2	249.2	345.0	153.4
		Jul94		2	190.9	239.1	142.7
		Jul93	NO_X - N	2	0.5	0.6	0.4
		Jan94		2	0.6	0.7	0.5
		Jul94		2	0.3	0.4	0.2

continued

Table 2 (continued):

Region	Area (km^2)	Date	Nutrient type	Number of sites	Mean mass (tonne)	Highest mass (tonne)	Lowest mass (tonne)
Surround	919	Jul93	PO_4 - P	1	37.2		
		Jan94		1	27.7		
		Jul94		1	5.4		
		Jul93	NH_4 - N	1	52.8		
		Jan94		1	50.6		
		Jul94		1	19.6		
		Jul93	SiO_4 - Si	1	416.4		
		Jan94		1	316.5		
		Jul94		1	166.4		
		Jul93	NO_X - N	1	2.6		
		Jan94		1	3.6		
		Jul94		1	3.7		
Western	284	Jul93	PO_4 - P	2	46.5	48.5	44.5
		Jan94		2	35.5	40.1	30.9
		Jul94		2	25.4	39.0	11.8
		Jul93	NH_4 - N	2	34.4	41.8	26.9
		Jan94		2	20.9	21.0	20.8
		Jul94		2	29.4	36.7	22.1
		Jul93	SiO_4 - Si	2	201.2	248.0	154.4
		Jan94		2	176.2	194.8	157.6
		Jul94		2	141.3	161.3	121.3
		Jul93	NO_X - N	2	1.0	1.6	0.4
		Jan94		2	0.2	0.2	0.2
		Jul94		2	1.0	1.8	0.2

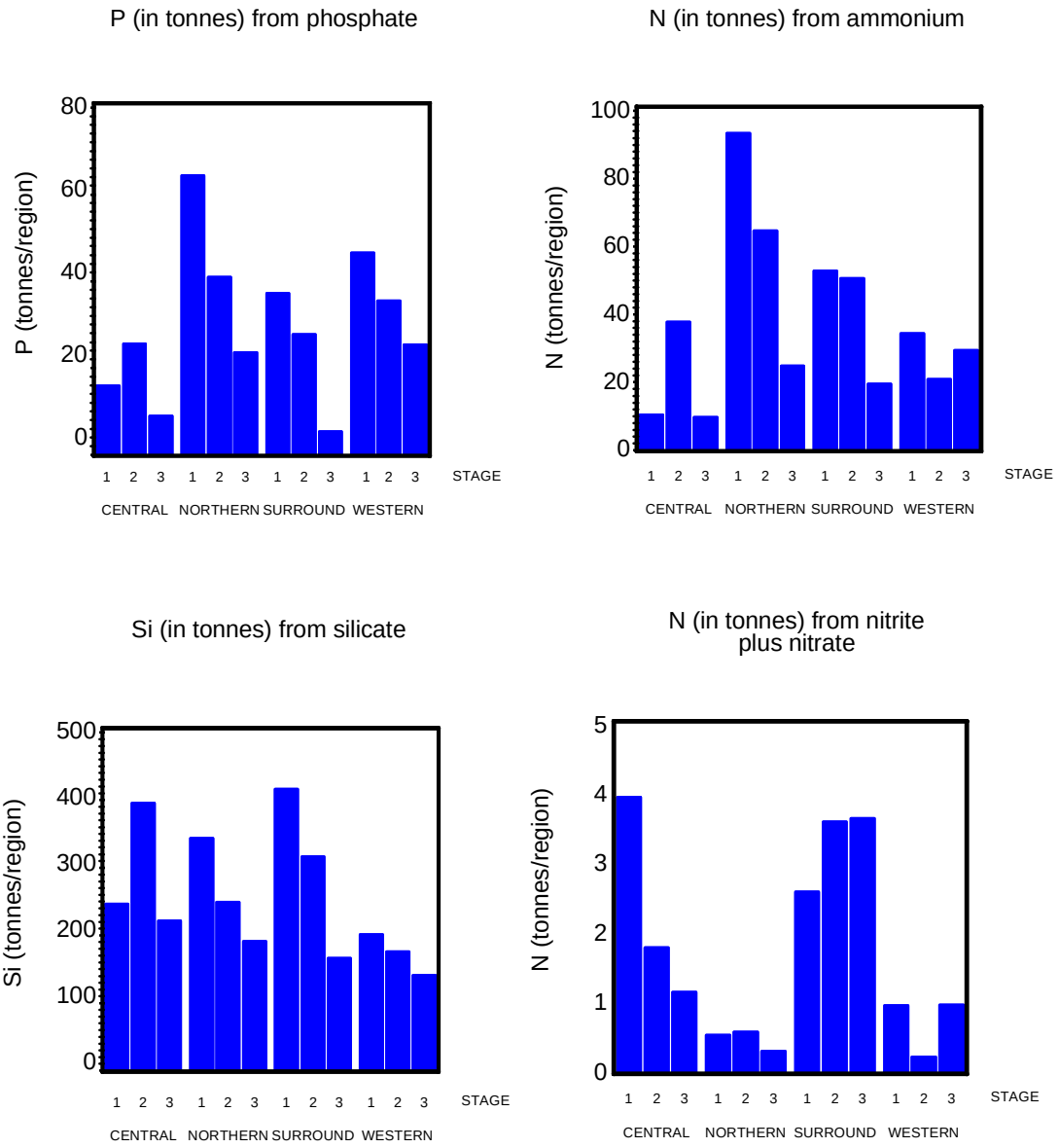

Figure 5: Porewater pools of P, N and Si from phosphate, ammonium, silicate and nitrite plus nitrate from each region within PPB to a depth of 20 cm sampled three times over a 12 month period. Stages 1, 2 and 3 indicate sampling cruises for July 1993, January 1994 and July 1994, respectively.

Dissolved organic nitrogen

Mean profile concentrations of DON in the porewaters of 8 sites sampled during July 1993, January 1994 and July 1994 are presented in Figures 6a and 6b.

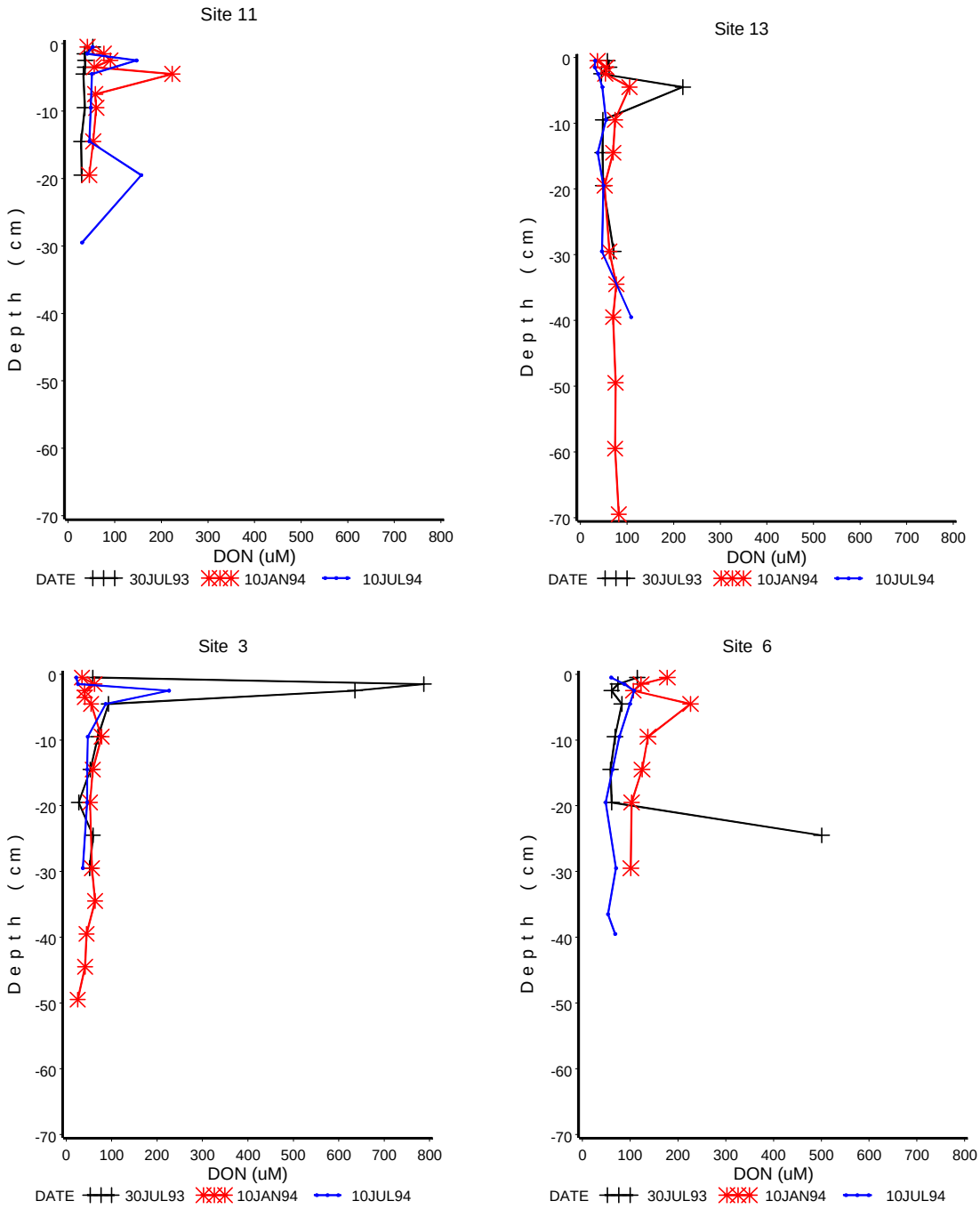

Figure 6a: Mean porewater depth profiles of dissolved organic nitrogen from Sites 3, 6, 11 and 13 sampled during July 1993, January 1994 and July 1994.

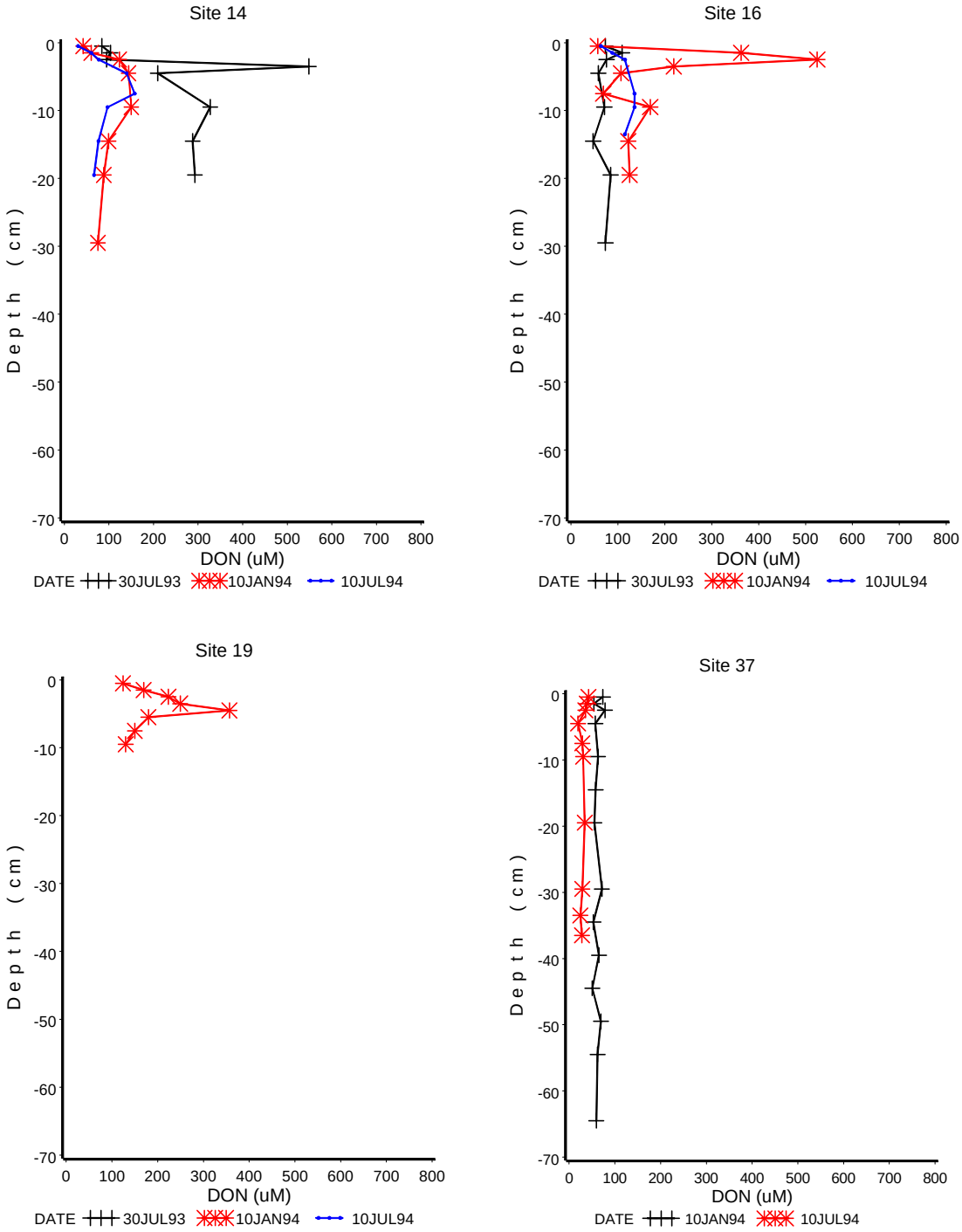

Figure 6b: Mean porewater depth profiles of dissolved organic nitrogen from Sites 14, 16, 19 and 37 sampled during July 1993, January 1994 and July 1994.

Dissolved organic phosphorus

Dissolved organic phosphorus was calculated as the difference between the analytically determined values for total P and inorganic P (as PO_4). By definition, DOP should always be positive. However, our analyses produced a number of negative values for DOP.

The analytical error associated with total P analysis is 3.9% for one standard deviation (1 S.D.) and 3% (1 S.D.) for inorganic P. A more conservative estimate of 4% for each is used in calculating the standard deviation for DOP. The combined error for DOP is calculated as follows:

$$1\ \text{S.D.}(\text{DOP}) = (1\ \text{S.D.}(\text{total P})^2 + 1\ \text{S.D.}(\text{inorganic P})^2)^{1/2} \qquad (1)$$

where the S.D.'s for total P and inorganic P are converted from percentage values to absolute values of total P and inorganic P concentrations obtained from each depth of sectioned cores.

Within three standard deviations (3 S.D.) it is theoretically possible for our estimate of PO_4 to exceed total P and produce a negative DOP. When a DOP value was found to be negative, an addition of its positive 3 S.D. was applied. If the product was found to become positive, then the DOP value was considered as zero. If the product remained negative, then it was rejected and discarded. Unfortunately, this resulted in the loss of some data. We have no explanation for the discrepancies other than analytical imprecision.

Dissolved organic phosphorus

Mean profile concentrations of DOP in the porewaters of 8 sites sampled during July 1993, January 1994 and July 1994 are presented in Figures 7a and 7b.

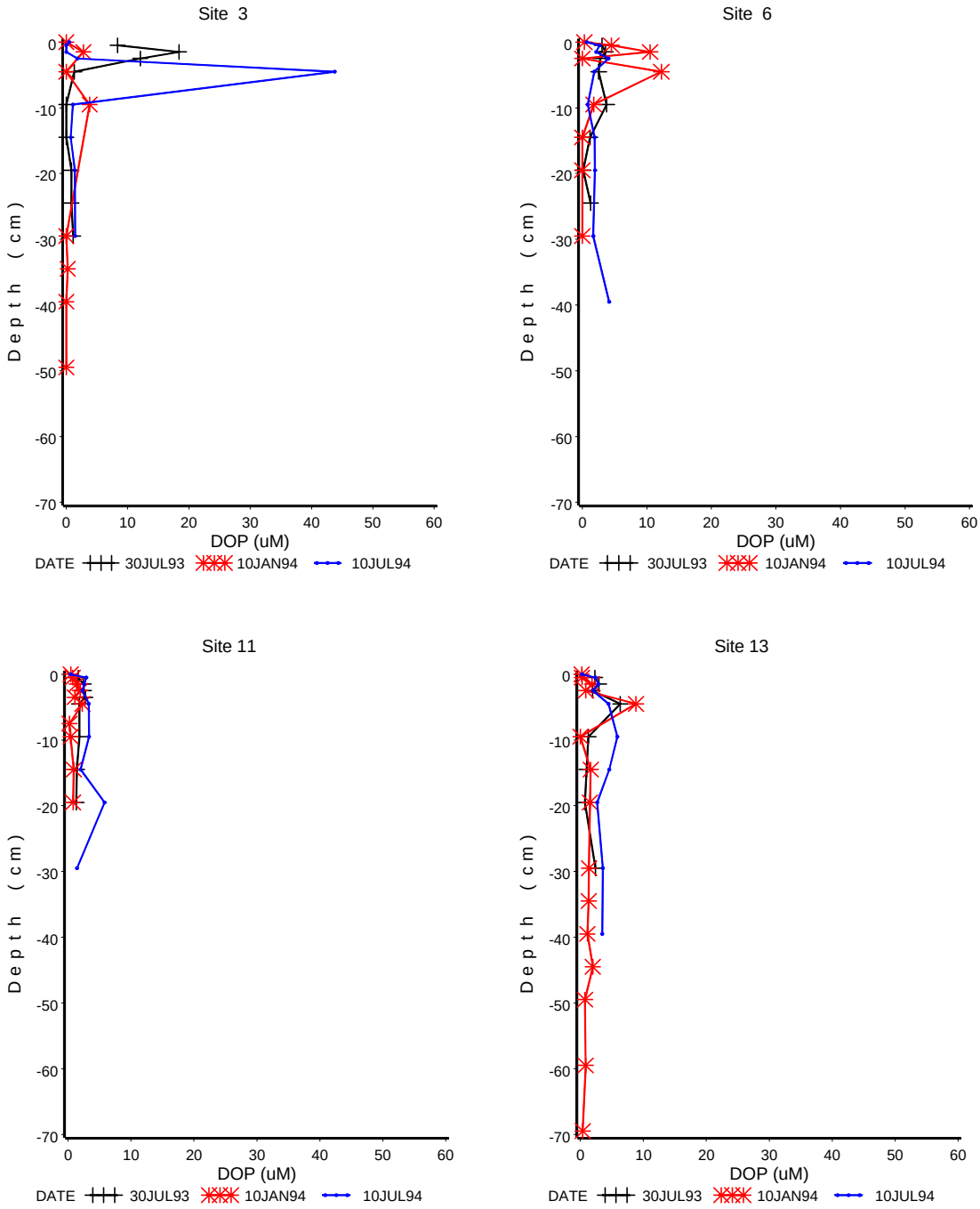

Figure 7a: Mean porewater depth profiles of dissolved organic phosphorus from Sites 3, 6, 11 and 13 sampled during July 1993, January 1994 and July 1994.

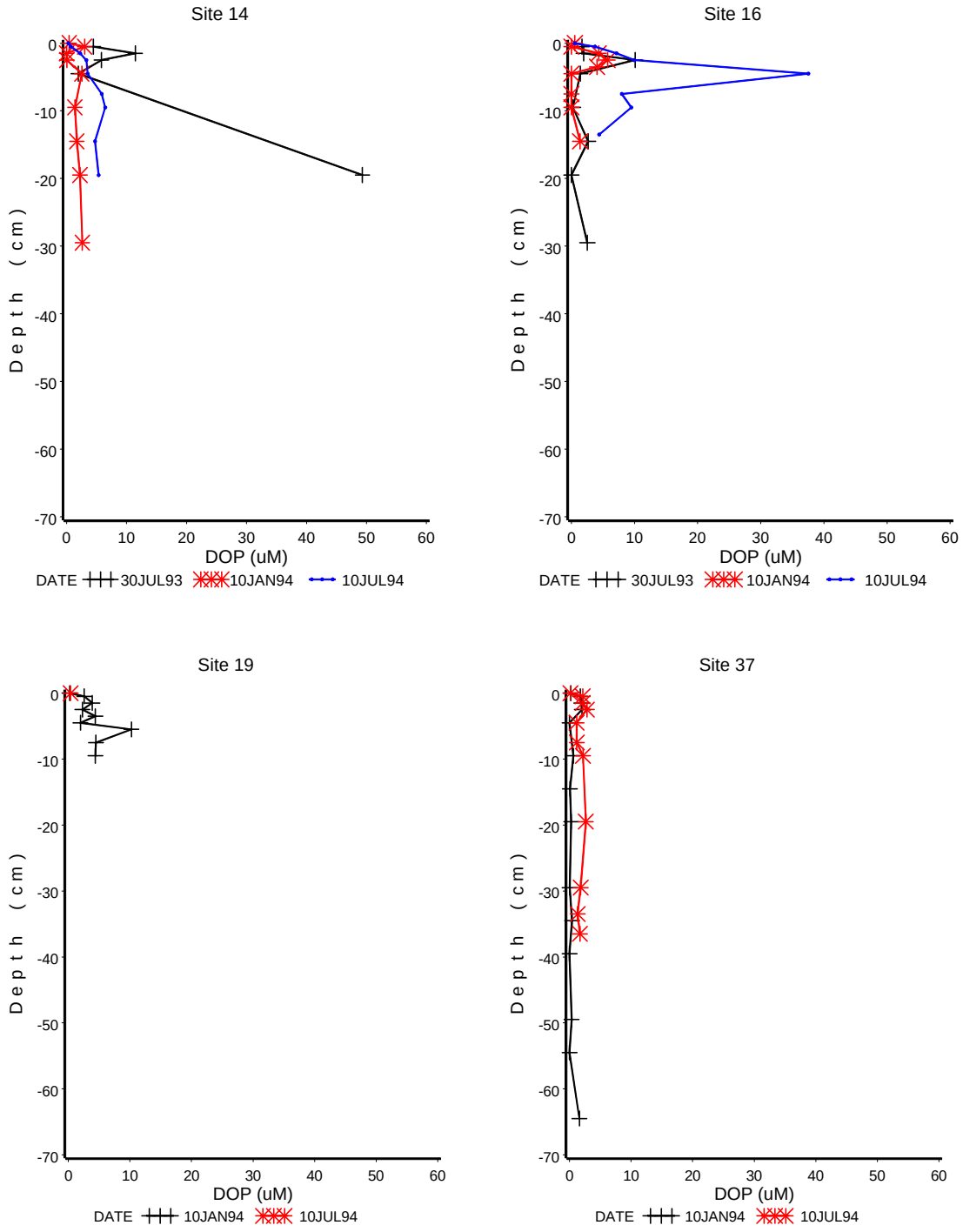

Figure 7b: Mean porewater depth profiles of dissolved organic phosphorus from Sites 14, 16, 19 and 37 sampled during July 1993, January 1994 and July 1994.

Solid-phase nitrogen

Mean profile concentrations of solid-phase nitrogen (SedN) in the sediments of 8 sites sampled during July 1993, January 1994 and July 1994 are presented in Figures 8a and 8b.

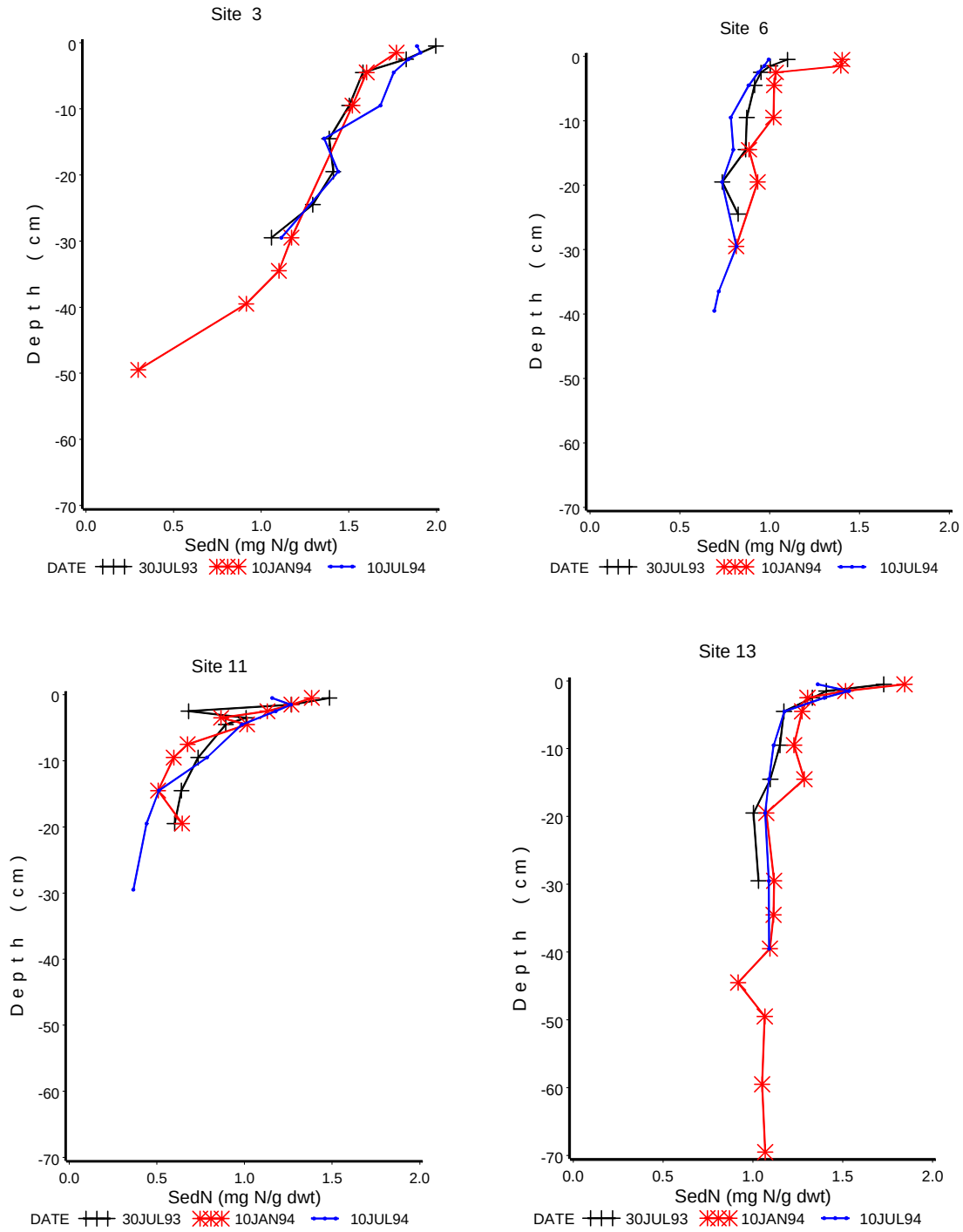

Figure 8a: Depth profiles of solid-phase nitrogen concentrations from Sites 3, 6, 11 and 13 sampled during July 1993, January 1994 and July 1994.

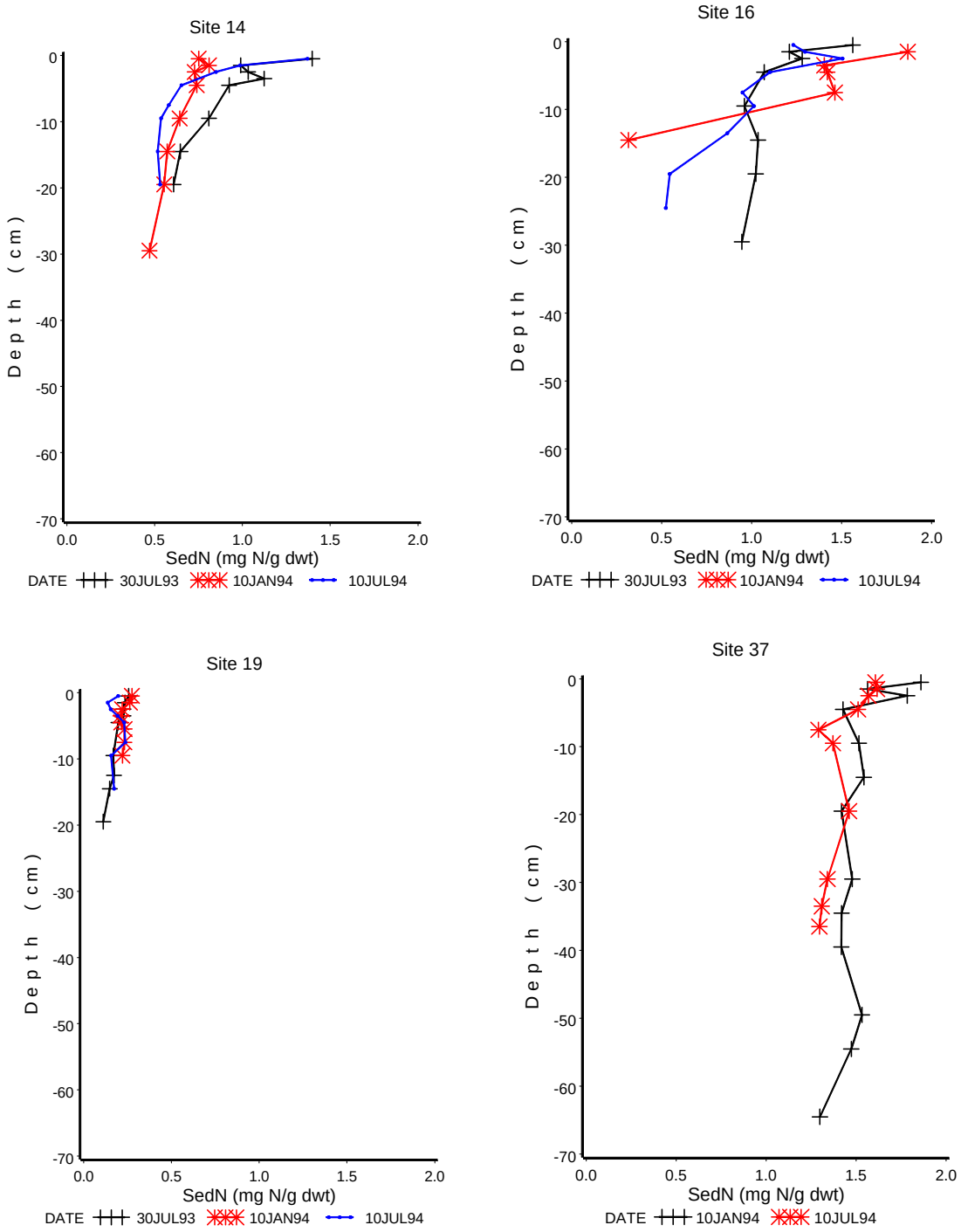

Figure 8b: Depth profiles of solid-phase nitrogen concentrations from Sites 14, 16, 19 and 37 sampled during July 1993, January 1994 and July 1994.

Solid-phase phosphorus

Mean profile concentrations of solid-phase phosphorus (SedP) in the sediments of 8 sites sampled during July 1993, January 1994 and July 1994 are presented in Figures 9a and 9b.

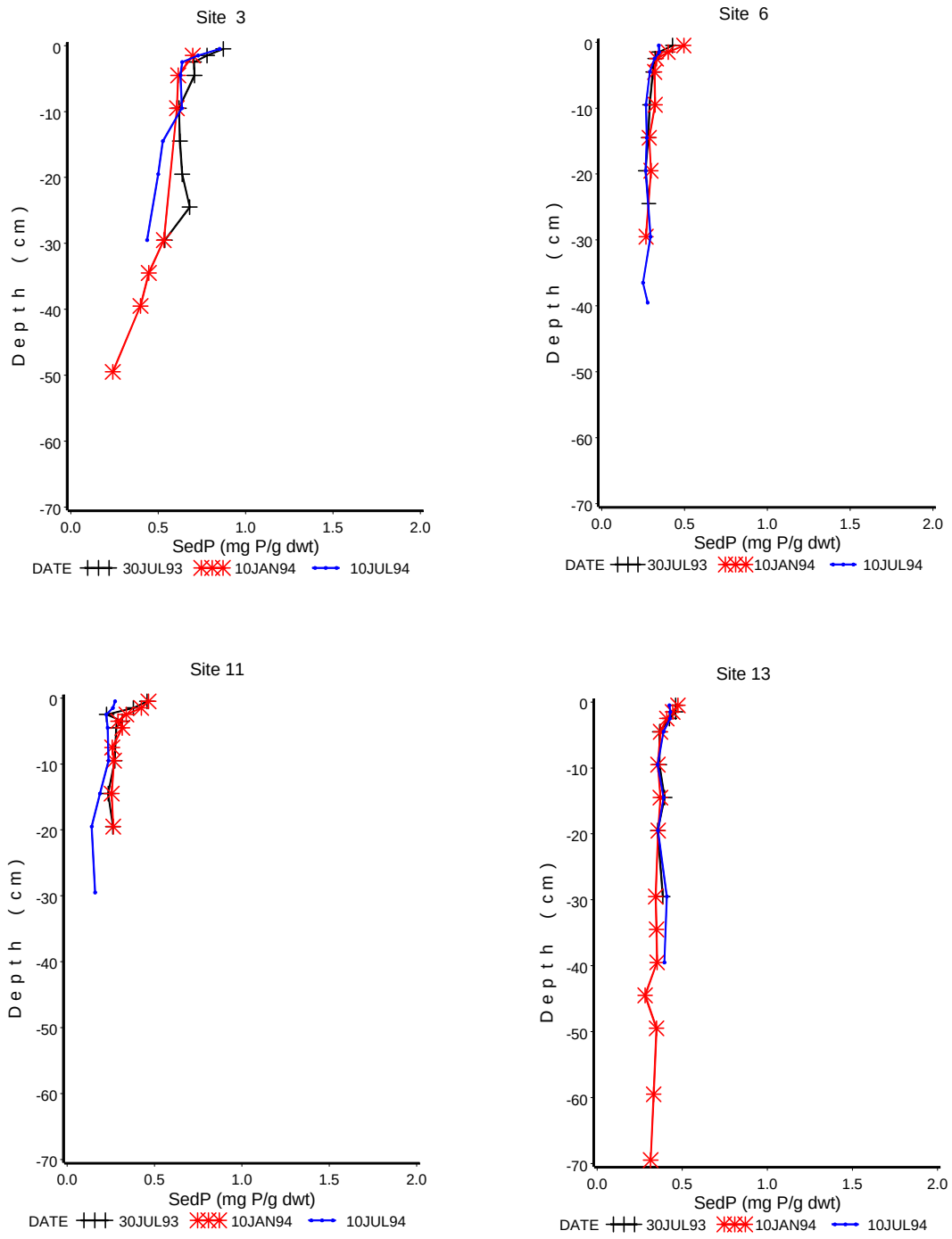

Figure 9a: Depth profiles of solid-phase phosphorus concentrations from Sites 3, 6, 11 and 13 sampled during July 1993, January 1994 and July 1994.

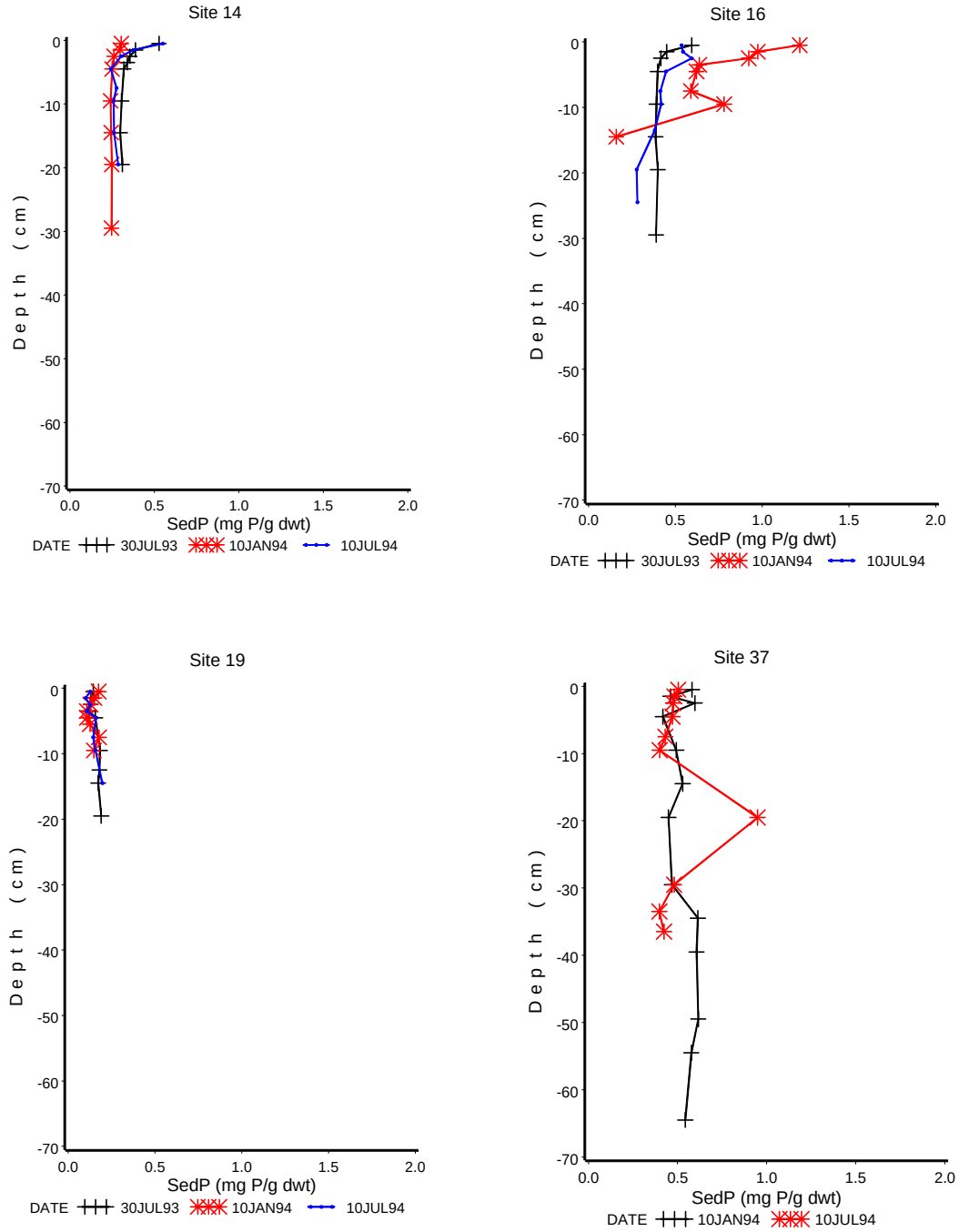

Figure 9b: Depth profiles of solid-phase phosphorus concentrations from Sites 14, 16, 19 and 37 sampled during July 1993, January 1994 and July 1994.

Sediment organic carbon

Mean profile concentrations of sediment organic carbon (SOC) in the sediments of 8 sites sampled during July 1993, January 1994 and July 1994 are presented in Figures 10a and 10b.

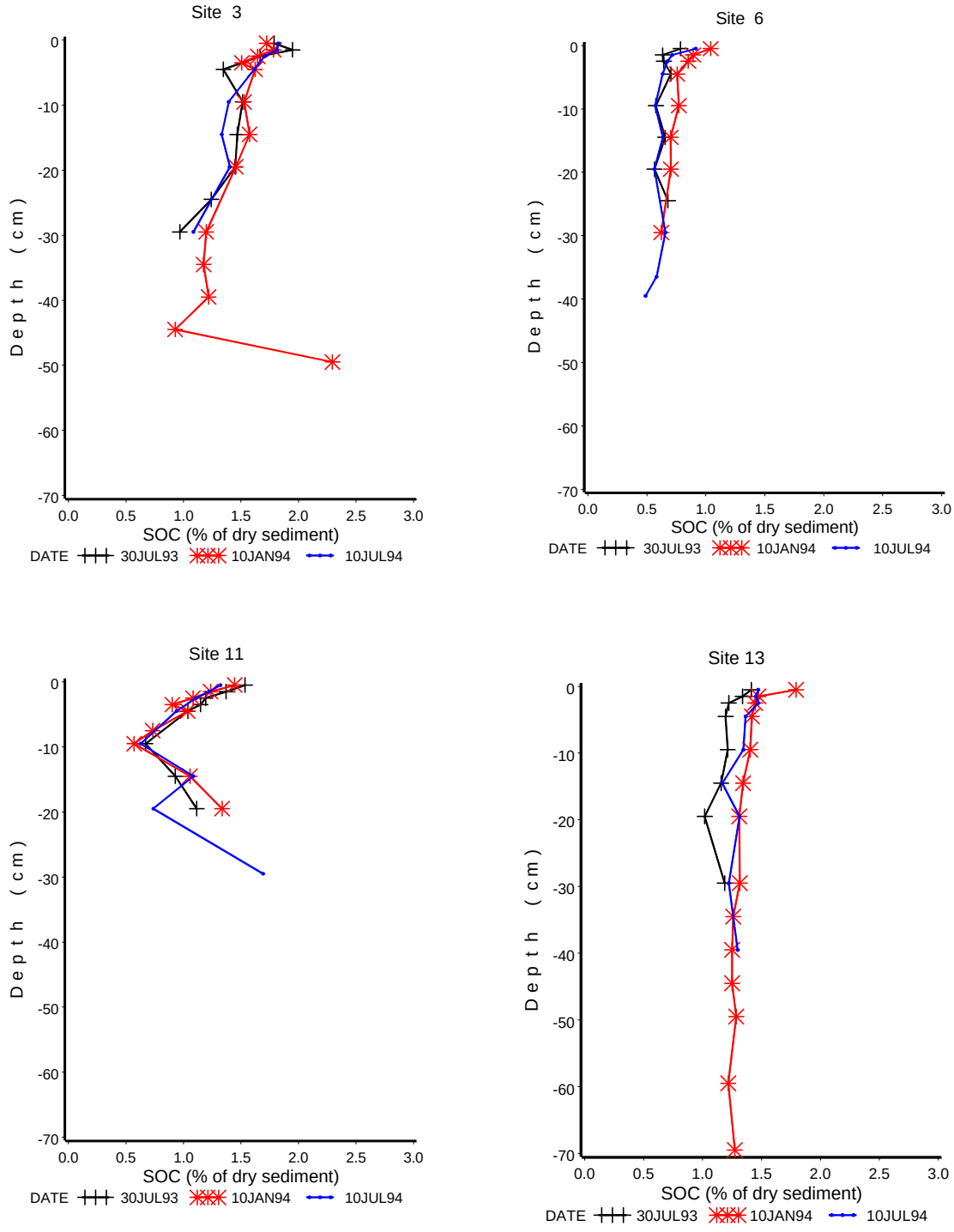

Figure 10a: Depth profiles of organic carbon concentrations from Sites 3, 6, 11 and 13 sampled during July 1993, January 1994 and July 1994.

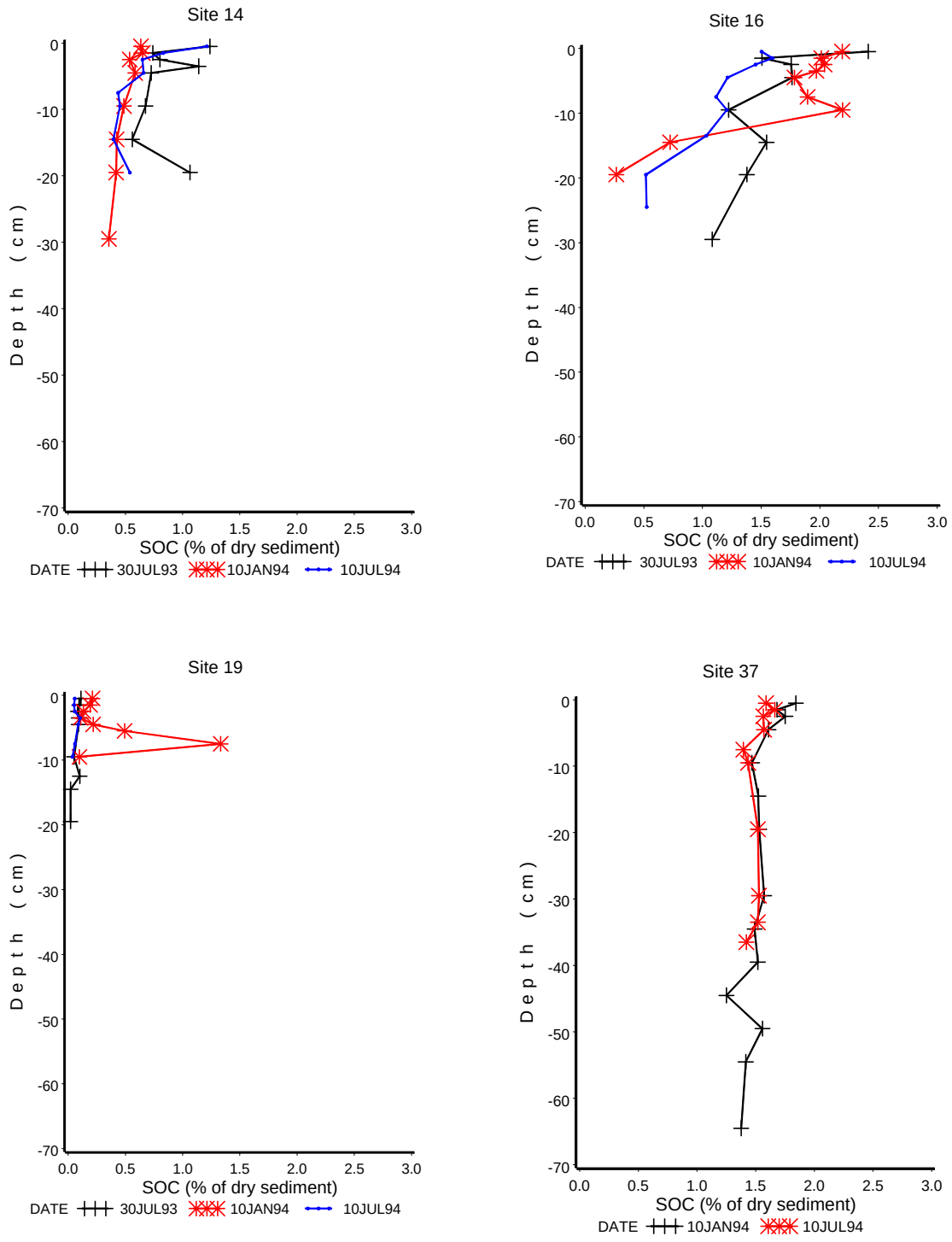

Figure 10b: Depth profiles of organic carbon concentrations from Sites 14, 16, 19 and 37 sampled during July 1993, January 1994 and July 1994.

Pools of solid-phase nitrogen, phosphorus and carbon

Solid-phase nitrogen, phosphorus and carbon (kg m^{-3}) in bottom sediment to a depth of 20 cm for each of the four regions for all data are presented in Figure 11. Approximate mean pool sizes (tonnes) of dissolved inorganic nitrogen (DIN), DIP, DON, DOP, SedN, SedP and SOC are shown in Appendix 2.

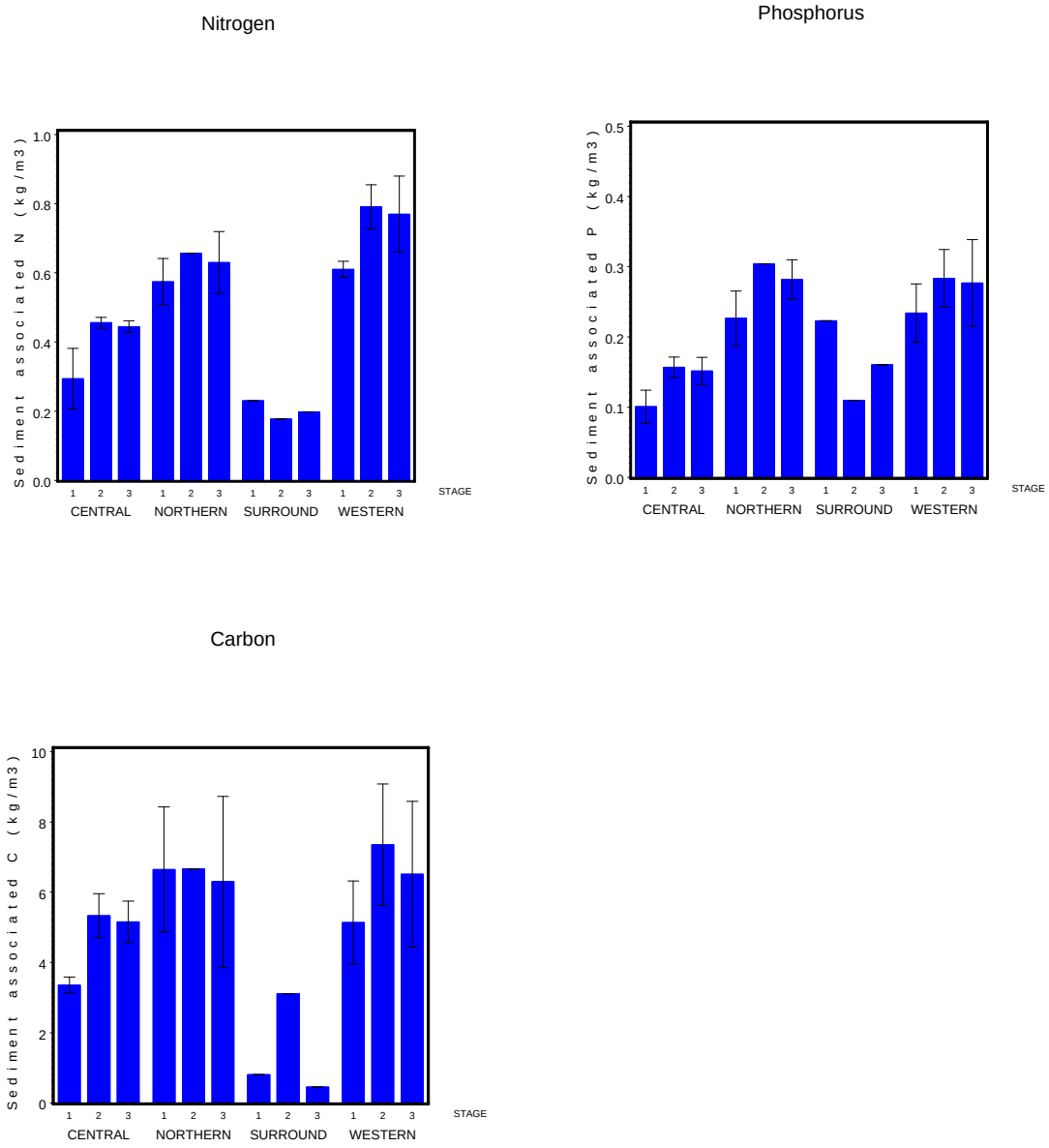

Figure 11: Solid-phase pools (kg m^{-3}) of nitrogen (left top diagram), phosphorus (right top diagram) and carbon (bottom left diagram) to a depth of 20 cm for each of the four regions. Stages 1, 2 and 3 indicate sampling periods of July 1993, January 1994 and July 1994, respectively.

Porewater iron

Concentration profiles of iron in the porewaters from a single core at 8 sites during January 1994 and July 1994 are presented in Figures 12a and 12b.

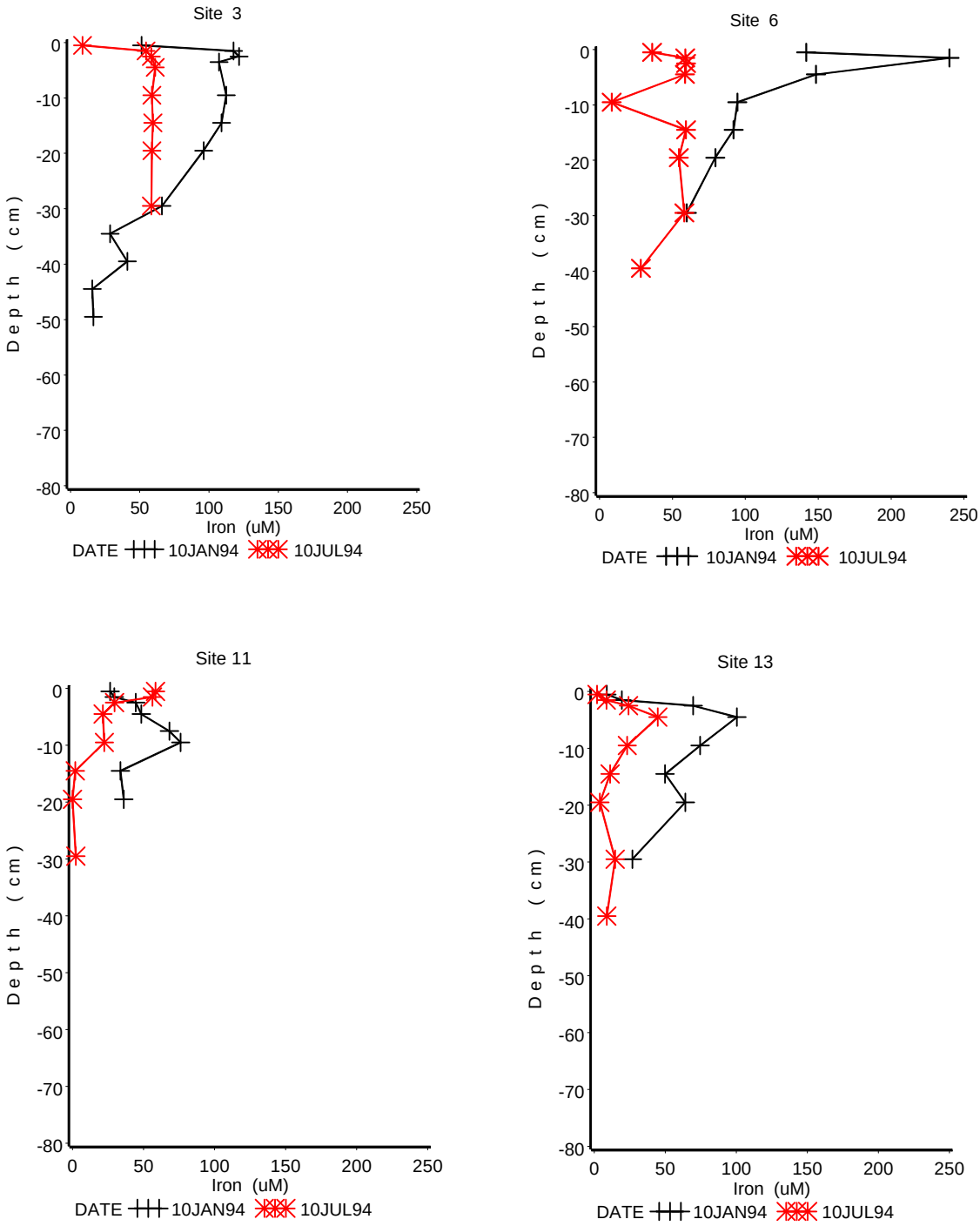

Figure 12a: Porewater depth profiles of dissolved iron sampled from one core at Sites 3, 6, 11 and 13 during January 1994 and July 1994.

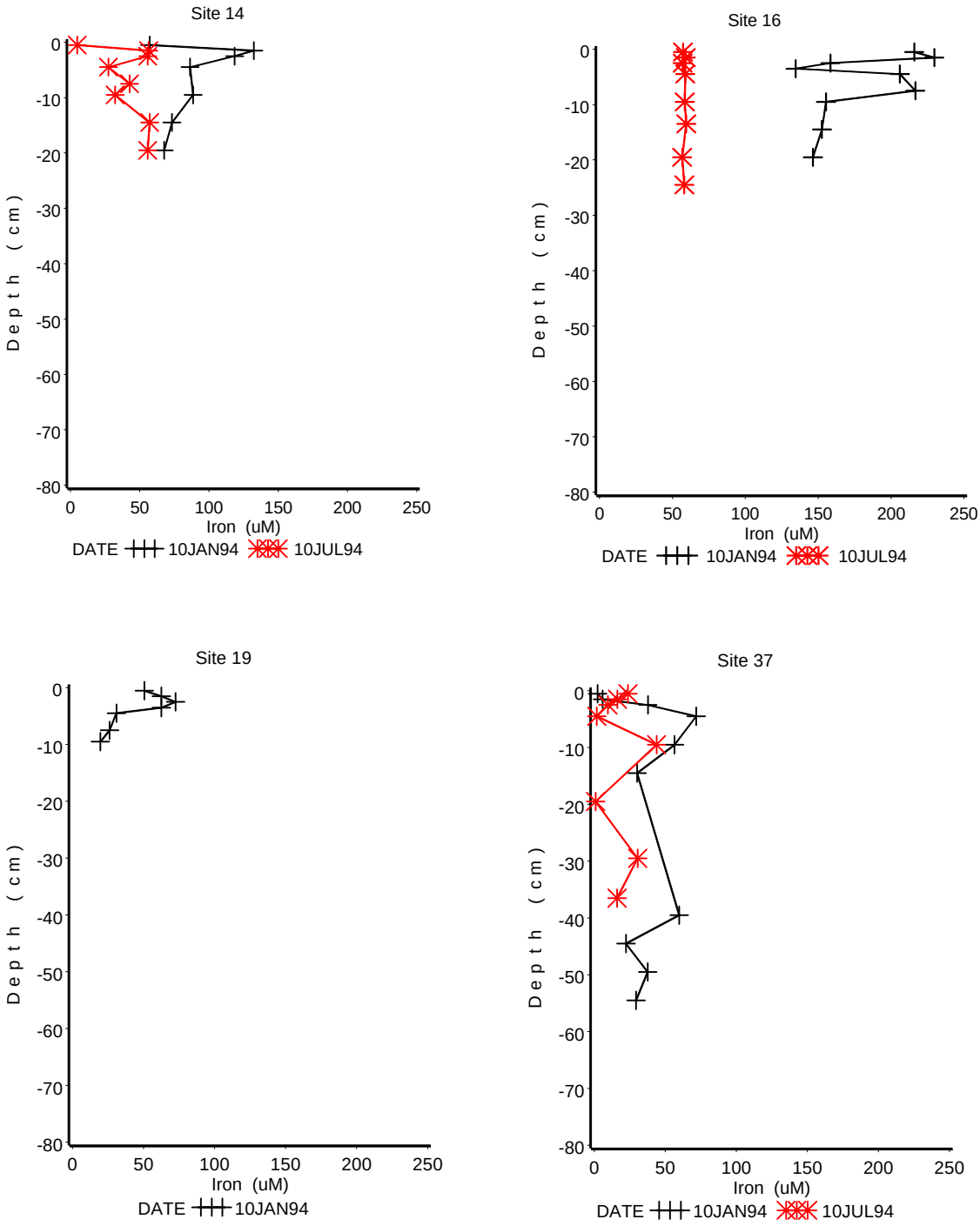

Figure 12b: Depth profiles of dissolved iron sampled from one core at Sites 14, 16, 19 and 37 during January 1994 and July 1994.

Sulphate in porewaters

Sulphate concentrations within the porewaters of Sites 3, 6, 13, 14, 16, 19 and 37 were measured during January 1994, and depth profiles for three cores from each of the 7 sites and a scatter plot of depth versus sulphate for all sites are shown in Figures 13a and 13b.

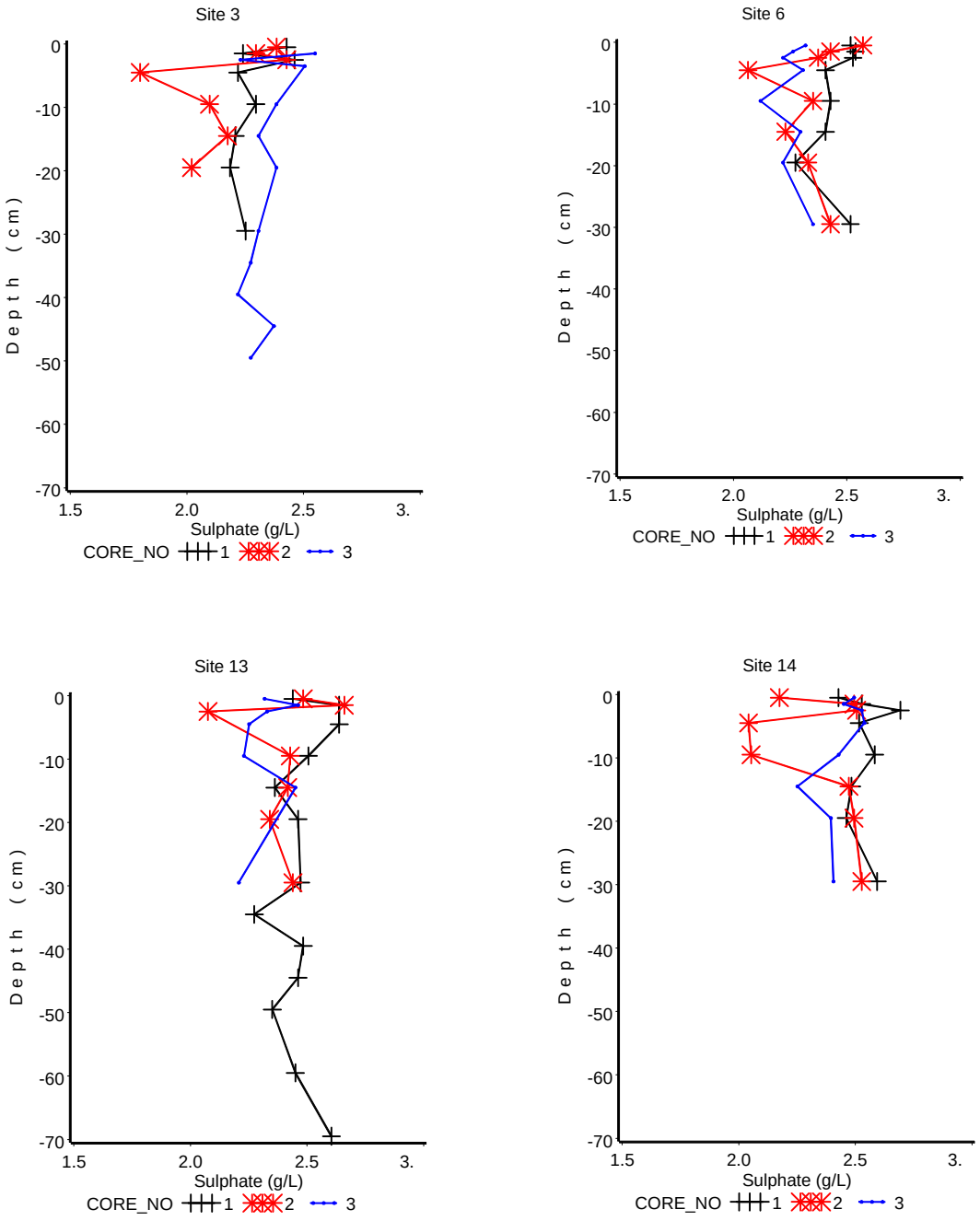

Figure 13a: Depth profiles of sulphate for Sites 3, 6, 13 and 14.

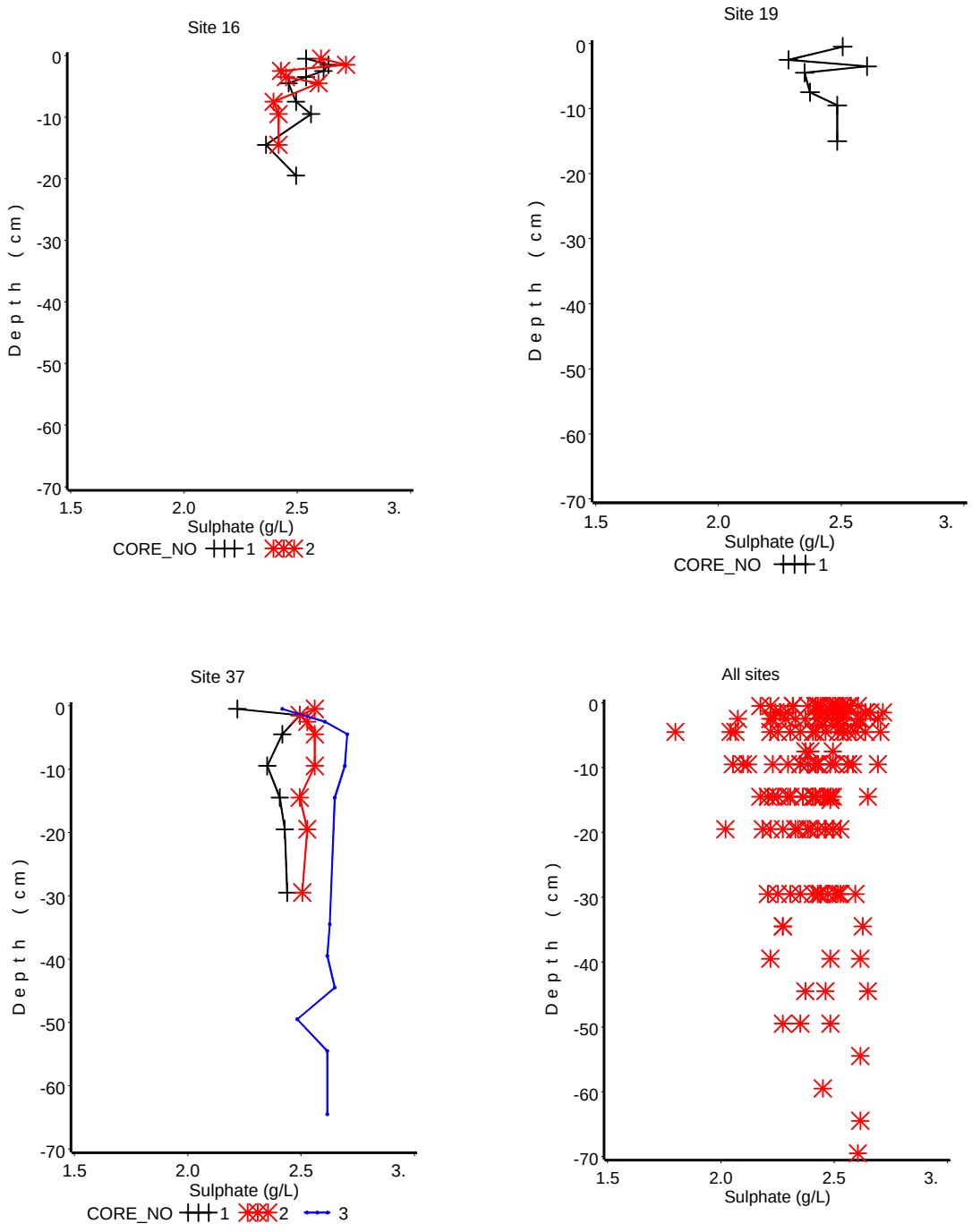

Figure 13b: Depth profiles of sulphate for Sites 16, 19 and 37 and a scatter plot for all sites.

Chloride in porewaters

Chloride concentrations within the porewaters of Sites 3, 6, 13, 14, 16, 19 and 37 were measured during January 1994 and depth profiles for three cores from each of the 7 sites and a scatter plot for all sites are shown in Figures 14a and 14b.

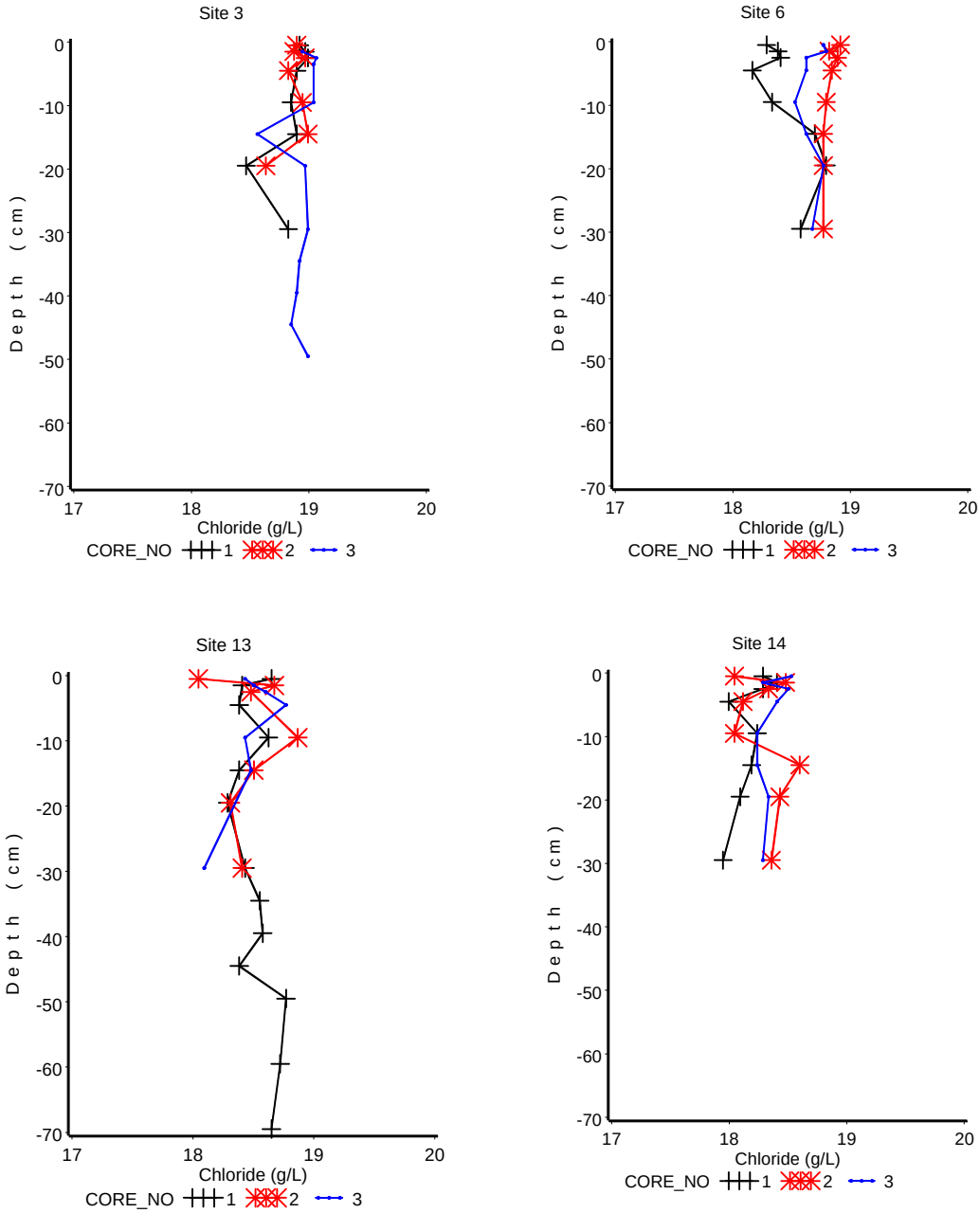

Figure 14a: Depth profiles of chloride for Sites 3, 6, 13 and 14.

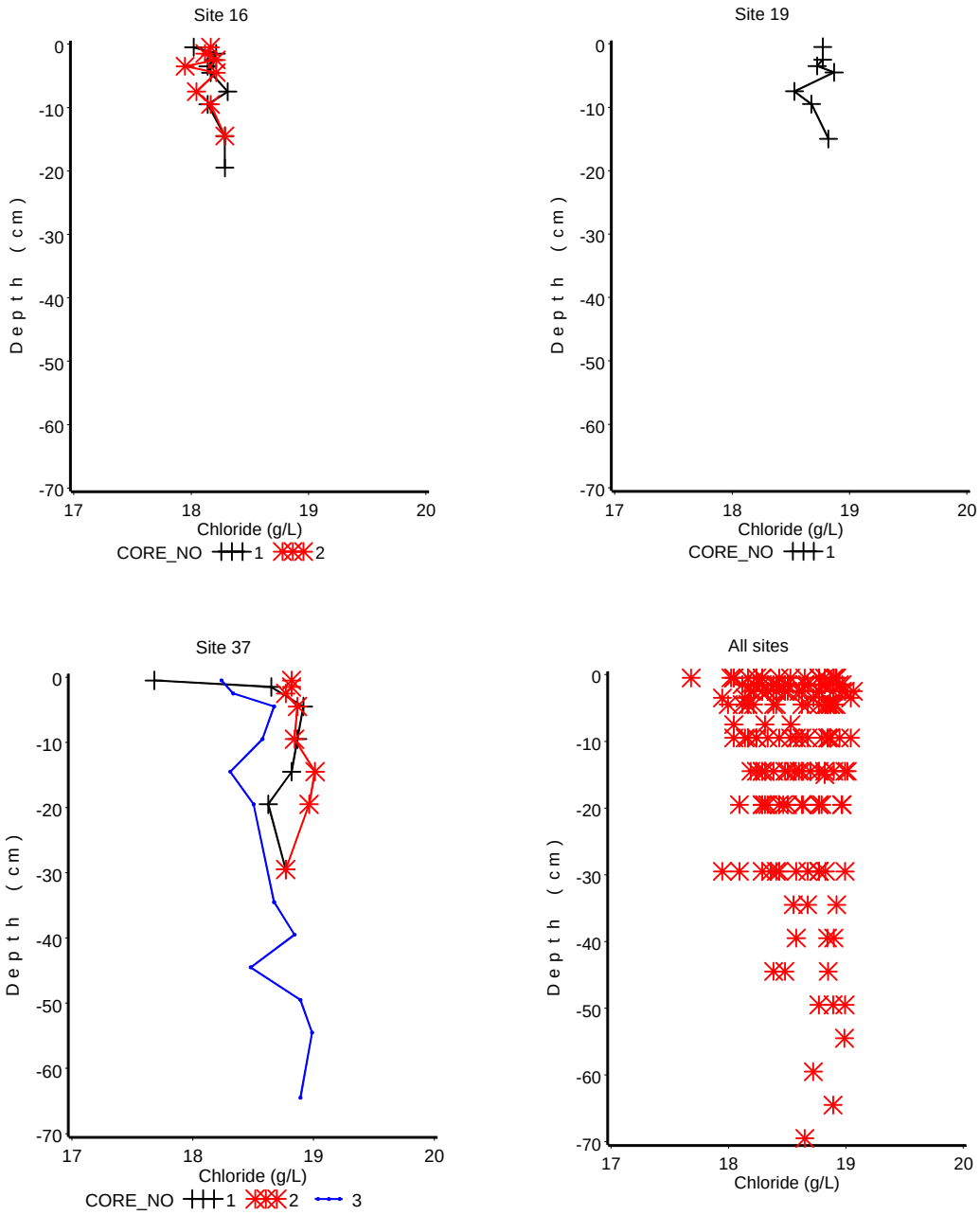

Figure 14b: Depth profiles of chloride for Sites 16, 19 and 37 and a scatter plot for all sites.

Sulphate - Chloride ratios

Sulphate - chloride ratios were calculated and plotted to determine whether there was any seepage of groundwater into the sediments from three cores at Sites 3, 6, 13, 14, 16, 19 and 37. A scatter plot of the data from all of the above sites was also plotted.

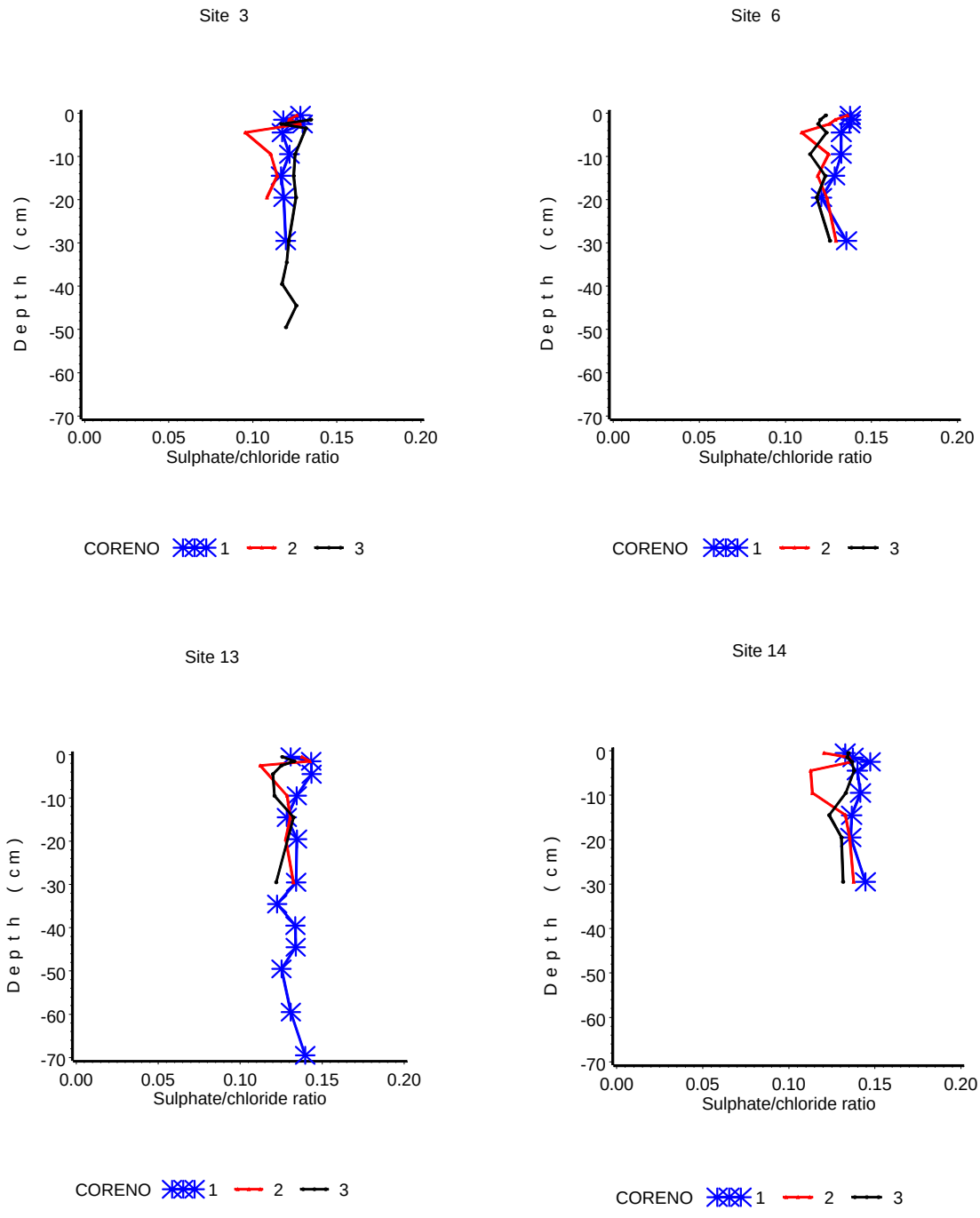

Figure 15a: Depth profiles of the ratio SO_4^{2-} / Cl^- for Sites 3, 6, 13 and 14.

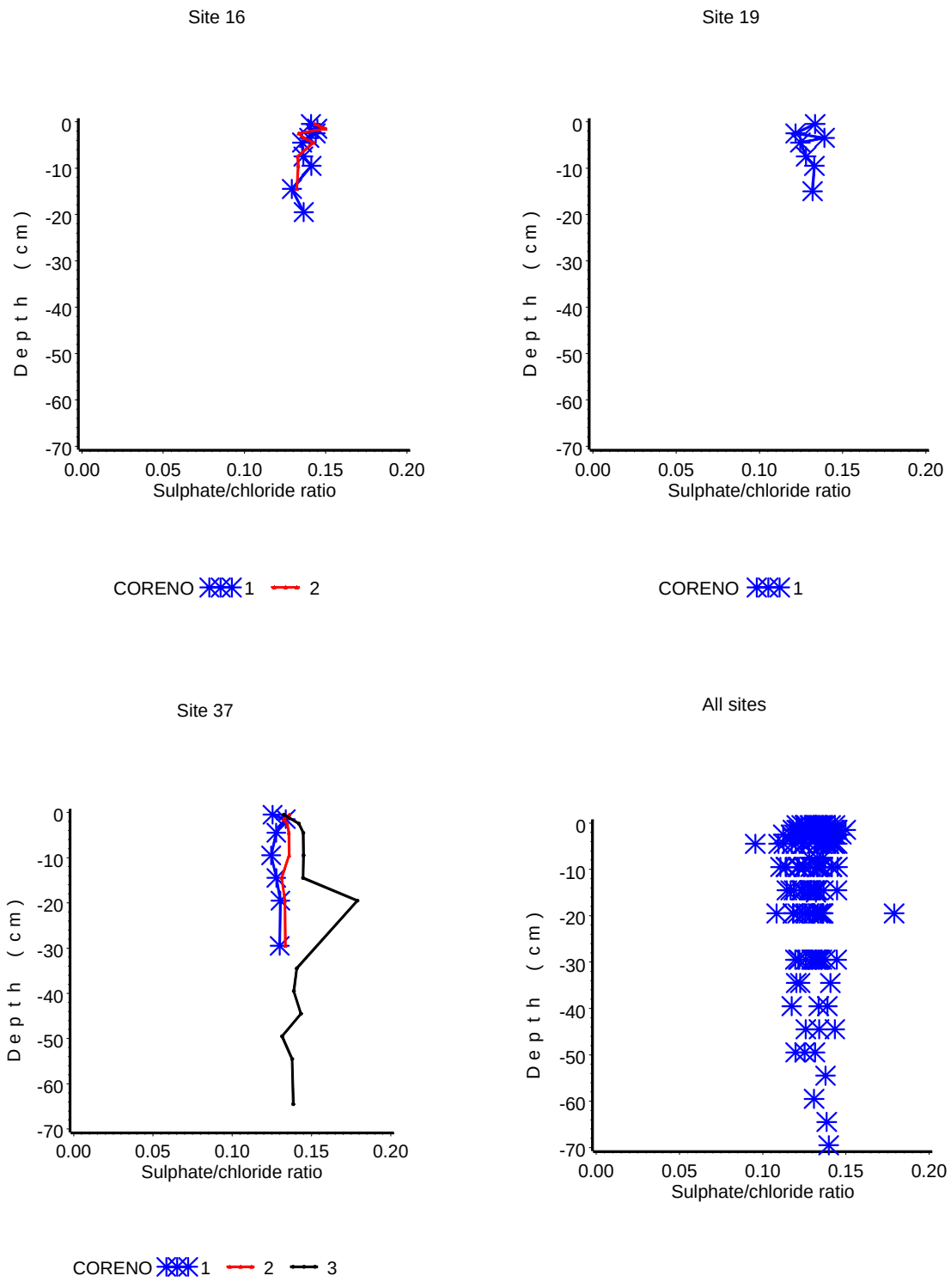

Figure 15b: Depth profiles of the ratio SO_4^{2-} / Cl^- for Sites 16, 19 and 37 and for all sites as indicated in the bottom right-hand corner of this figure.

CORRELATIONS

Soluble and solid-phase correlations

Correlations forced through zero and ratios between diffusive fluxes and between solid-phase parameters from all samples were investigated. Fluxes are in units of mmole m^{-2} day^{-1}. Solid-phase values are converted to units of mole per gm of dry weight sediment. Table 3 presents some results.

Table 3: The goodness of fit, the ratio and the standard error between DIN and phosphate fluxes, silicate and phosphate fluxes, and solid-phase carbon, nitrogen and phosphorus ratios.

Ratio investigated	r^2	ratio	std error
DIN:PO4 fluxes	0.5226	5.88	0.71
SiO4:PO4 fluxes	0.5412	7.01	1.02
SOC:SedP	0.7992	62.66	1.13
SOC:SedN	0.8027	11.20	0.15
SedN:SedP	0.9208	6.28	0.07

SUMMARY

Results

1) The general shape of porewater depth profiles during July 1993, January 1994 and July 1994 for ammonium, phosphate and silicate concentrations (Figs. 3a to 3h) is of a shallow sub-surface maximum, with concentrations usually decreasing with depth below the maximum. The maxima for phosphate profiles were shallower and sharper than for ammonium or silicate. Nitrite plus nitrate profiles showed smaller and fewer maxima.

2) Diffusive fluxes for ammonium, phosphate, silicate and nitrite plus nitrate showed no consistent pattern with respect to sampling period (Figs. 4a and 4b) but spatial trends were evident. Site 16, at the mouth of the Yarra River, had the highest overall fluxes of ammonium, phosphate and silicate but not nitrite plus nitrate. Ammonium dominated the inorganic N diffusive flux at most sites most of the time.

3) The northern region had the smallest area (240 km^2) of the four nominated regions, yet had the greatest porewater pools of P and N (from ammonium) during each sampling period (Fig. 5, Table 2). The pool of nitrite plus nitrate in the northern region was usually less than that in each of the other regions during the three sampling periods. Silicate pools were more uniform.

4) Mean DON porewater profiles (Figs. 6a and 6b) generally showed shallow subsurface maxima at all sites except for Site 6 during July 1993 and Site 37 at all times. The mean porewater profiles for DOP (Figs. 7a and 7b) exhibited shallow sub-surface maxima for 6 out of 8 sites. Porewater DON and ammonium concentrations were similar in magnitude at all sites, whereas DOP concentrations were lower than inorganic phosphate.

5) Mean SedN concentrations were commonly highest at the sediment surface and at most sites decreased rapidly and non-linearly with depth before assuming an asymptotic aspect (Figs. 8a and 8b). Mean SedP profiles were generally uniform with depth (Figs. 9a and 9b).

6) SOC profiles generally showed highest concentrations at the sediment surface which decreased with depth (Figs. 10a and 10b).

7) The northern and the western regions contained the greatest concentrations of solid-phase nitrogen, phosphorus and carbon (Fig. 11). Appendix 2 indicates that most of the N and P in PPB sediments are associated with the solid phase. Pools of DIN, DIP, DON and DOP are greater in the overlying water column than in interstitial waters to a depth of 20 cm.

8) Iron porewater profiles were obtained from only a single core at each of the 8 common sites for January 1994 and July 1994, except for Site 19 which was sampled for iron only during January 1994. The general profile shape was one of a shallow sub-surface maximum (Figs. 12a and 12b). The profiles at all sites indicated that there was generally more iron within the porewaters during January 1994 than during July 1994.

9) The porewater profiles of sulphate were obtained only during January 1994 (Figs. 13a and 13b). The profiles exhibited great variability within and between sites.

10) The porewater profiles of chloride were also obtained only during January 1994 (Figs. 14a and 14b) and no trend was evident in concentrations both within and between sites.

11) The sulphate/chloride ratio (Figs. 15a and 15b) was generally in the order of 0.14, indicating no groundwater dilution of the interstitial waters at the sites sampled.

12) The C:N:P ratio expected from Redfield stoichiometry is 106:16:1. The molar ratio between inorganic N and P fluxes from Table 3 was 5.88, and can be considered an indication of denitrification. The solid-phase ratios C:P and N:P were less than Redfield estimates indicating that the C and N products from the breakdown of organic matter were not as tightly adsorbed to the sediment as P was. The solid-phase C:N ratio was greater than the Redfield ratio indicating more rapid removal of N from the system.

Statistics

Analysis of variance of the calculated diffusive fluxes for ammonium, phosphate, silicate and nitrite plus nitrate with respect to site of sample collection and temperature at sample collection time was conducted. The general linear models procedure (GLM), a factorial analysis of variance with unequal replication (Zar 1984), was used because the data were unbalanced. This procedure implements dummy-variable regression which is applied for the successful analysis of variance (Crum 1986). The GLM procedure within the SAS system (SAS Institute Inc., Cary, North Carolina), which is an integrated system of software for the handling and analysis of data, was used for all flux computations. In all cases the type III sums of squares were used to test the null hypothesis.

Multiple comparison tests such as Duncan's multiple range test and Tukey's 'studentised' range test were made when the analysis of variance indicated that the means tested for a particular effect differed significantly (Walpole and Myers 1978). These *post hoc* or *a posteriori* tests divided the population means into subgroups, and showed which subgroup(s) differed significantly from others (Walpole and Myers 1978, Cody and Smith 1991). Both *post hoc* tests were used because the Duncan's test controls the comparison-wise error rate but not the experiment-wise error rate, while the Tukey's test controls the experiment-wise error rate (SAS Institute Inc., Cary, North Carolina, USA).

1) All samples collected during January 1994 were classified as warm water samples, and samples collected during July 1993 and July 1994 were classified as cold water samples. This was based on the premise that temperature and organic matter deposition are the principal contributing factors in the diagenesis of organic matter. Temperature affects microbially mediated regeneration and diffusion processes (Fisher *et al*. 1982, Valiela 1984, Klump and Martens 1989). The water temperature range during the July 1993 and July 1994 sampling periods was 11 - 11.5 ^{o}C, while water temperature during January 1994 was about 19 ^{o}C. These are close to the minimum and maximum temperatures encountered in the Bay.

The GLM model investigated was:

$$flux = site + date + site*date$$

for the fluxes of ammonium, phosphate, silicate and nitrite plus nitrate. Site, date and site*date interactions were significant at $P < 0.05$ for all fluxes (Table 4).

Table 4: The effects of site, date and site and date interaction for the fluxes of ammonium, phosphate, silicate and nitrite plus nitrate, and the degrees of freedom for each effect.

Effect	Ammonium		Phosphate		Silicate		Nitrite+Nitrate		df
	F	*P*	*F*	*P*	*F*	*P*	*F*	*P*	
Site	20.50	0.0001	22.44	0.0001	55.74	0.0001	3.80	0.0030	7
Date	4.01	0.0253	26.19	0.0001	23.00	0.0001	13.25	0.0001	2
Site*Date	6.51	0.0001	8.90	0.0001	12.46	0.0001	6.81	0.0001	13

Tukey's and Duncan's tests both showed the identical subgroups to be significantly different from other subgroups. The results of Duncan's range test on sites for the four fluxes and the resultant Duncan grouping are shown in Table 5.

Table 5: The Duncan grouping (DG) and the site order (SO) for highest to lowest mean flux values from the 8 sites sampled over the three sample periods. The Duncan group indicators A, B and C are assigned to differentiate subgroups.

Ammonium		Phosphate		Silicate		Nitrite+Nitrate	
DG	*SO*	*DG*	*SO*	*DG*	*SO*	*DG*	*SO*
A	16	A	16	A	16	A	11
B	14	B	6	B	11	A	6
BC	3	BC	3	B	13	AB	37
BC	6	BC	14	B	37	B	3
BC	37	C	13	C	14	B	16
C	11	C	37	D	3	B	14
C	13	C	11	E	6	B	13
C	19	C	19	F	19	B	19

Sites with the same DG letter have similar means. Sites with two DG letters indicate an overlap of means and are not distinctly different from those sites which have one of the two DG letters. Ammonium, phosphate and silicate fluxes that originate from Site 16 are shown to be significantly different in magnitude from those originating at the 7 other sites over the three sample periods.

The results of Duncan's range test for the four fluxes from 8 sites with respect to date sampled are shown in Table 6.

Table 6: The Duncan grouping (DG) and the date order (DO) for highest to lowest mean flux values over the 8 sample sites are shown. The letters 'c' and 'w', in parentheses following the date indicate cold or warm water temperature, respectively. Dates with the same Duncan grouping have means not significantly different.

Ammonium		Phosphate		Silicate		Nitrite+Nitrate	
DG	*DO*	*DG*	*DO*	*DG*	*DO*	*DG*	*DO*
A	Jul93(c)	A	Jan94(w)	A	Jul93(c)	A	Jul93(c)
A	Jan94(w)	B	Jul93(c)	A	Jan94(w)	B	Jul94(c)
A	Jul94(c)	B	Jul94(c)	B	Jul94(c)	B	Jan94(w)

Table 4 shows that site, date and site and date interactivity were significant ($P<0.05$) for all four fluxes. Table 5 indicates that Site 16 was distinguished from the other sites and had the greatest mean fluxes of ammonium, phosphate and silicate. Table 6 indicates that phosphate, silicate and nitrite plus nitrate fluxes varied significantly with date, although only with phosphate were the two cold temperature periods grouped together. In summary, it appears that site effects are more important than sampling period with respect to the magnitude of diffusive fluxes.

SECTION 2: BENTHIC CHAMBER EXPERIMENTS

EQUIPMENT

A diagram of a VFRI benthic chamber used in this study is illustrated in Figure 16. Each chamber was a squat clear polycarbonate cylinder, sealed at the upper end, with an inner diameter of 290 mm and a height of 150 mm. A 50 mm skirt extended outwards 50 mm from near the open end and acted to limit the depth to which the chamber could be pushed into the sediment. When the chamber was pushed into the sediment to the level of the skirt the enclosed volume was approximately 6 L.

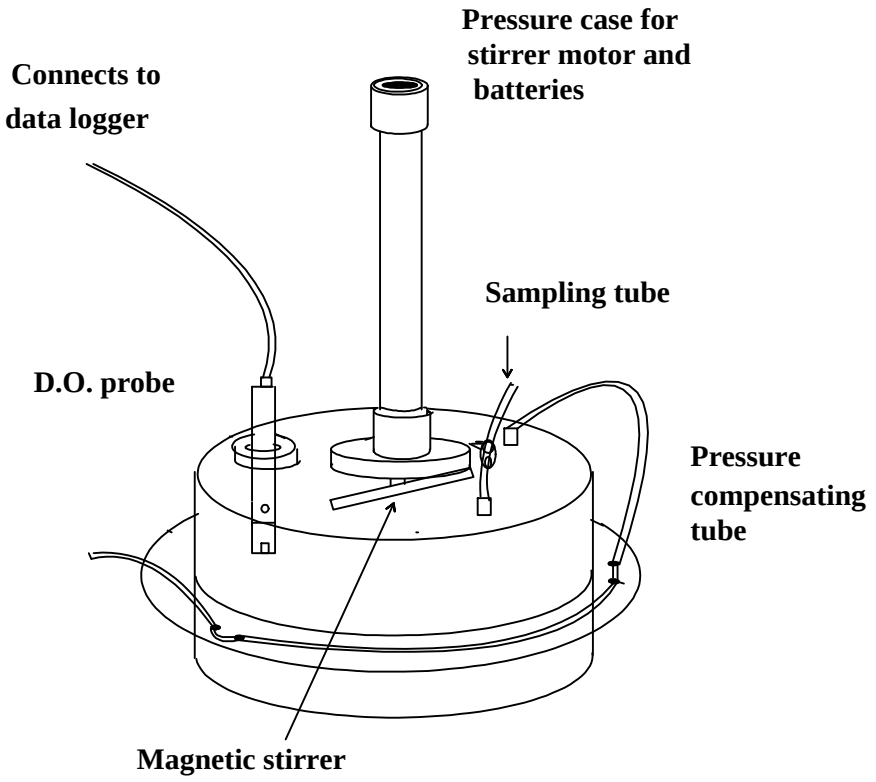

Figure 16: Diagram of a benthic chamber.

The dimensions of the VFRI chambers were similar to the chambers deployed by Berelson (Berelson *et al*. 1994, Berelson *et al.* 1996) during collaborative work in PPB. A direct comparison of results between the chamber types was a major objective and was used to validate VFRI chambers against the established and more sophisticated Berelson design. A stirrer in the chamber was operated magnetically by a battery powered electric motor housed in a water proof casing mounted on the top of the chamber. A sealable sampling tube, a pressure compensating tube and a combined dissolved oxygen and temperature

sensor (YSI Model 5739) were installed in the ports embedded in the chamber top. The pressure compensation tube was composed of silicone rubber of 2 mm internal diameter and about 30 cm in length. It remained unsealed to provide pressure relief if groundwater upwelled into the chamber, or if there were pressure changes resulting from wave action and also to minimise the amount of porewater drawn into the chamber by the action of syringe sampling. Outside water entered the chamber through this tube to replace water withdrawn from the chamber. An accompanying underwater data logger was programmed to read the probes for 3 second periods at 10 minute intervals and to store the data until it was unloaded following logger recovery.

METHODS

At each site SCUBA divers positioned 6 chambers (with probes detached) and the securely weighed down data logger in a 2 m radial configuration on the seabed as illustrated in Figure 17. A numbered YSI probe was placed within the provided port for each numbered chamber. Three chambers were painted black, to prevent photosynthetic processes affecting fluxes.

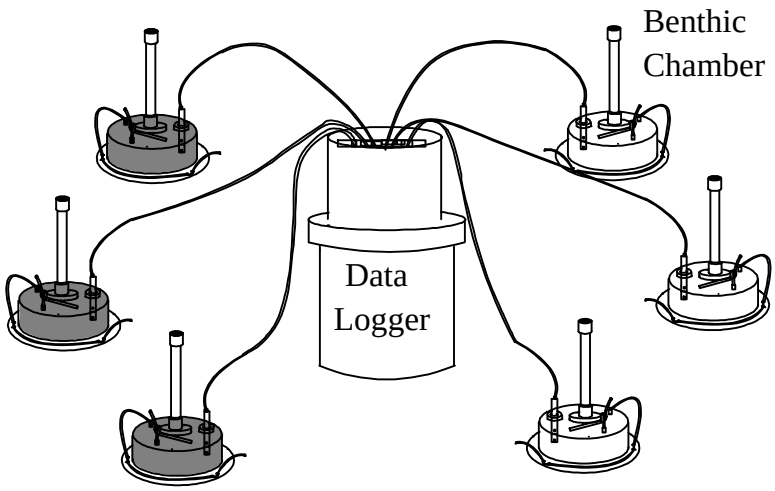

Figure 17: Typical layout of chambers and data logger during field deployment.

Chambers were commonly deployed around the middle of the day and left for 5-24 hours. The logger was usually programmed to start recording about an hour prior to deployment. The stirring paddle revolved at 5 revolutions per minute producing a mean current velocity over the sediment of about 5 cm sec^{-1} and creating a diffusive boundary layer (DBL) of between 0.3 and 0.4 mm thickness. Laboratory *in-situ* measurements by Burke (1995) of the mean DBL thickness over sediment cores from PPB ranged from ~0.3 mm in flowing conditions of 5 - 6.5 cm s^{-1} to ~0.9 mm in stagnant conditions. The chamber stirring rate was chosen to approximate tidal currents in the northern and central part of the Bay of 2 and 5 cm sec^{-1} respectively, and typical wind generated current velocities of

about 5 cm sec^{-1} (Hunter 1992). The DBL is the main modifier of the diffusion of substances between the water column and sediments (Santschi *et al*. 1990). However, doubling the thickness of the DBL by slowing the stirring rate did not lower measured fluxes (Berelson *et al*. 1994). This indicates that processes other than diffusion, such as bio-irrigation of interstitial waters, play a major role in nutrient recycling in PPB.

At the beginning of deployment a seawater sample was collected by Niskin bottle from immediately above the seabed. Subsamples were then taken for DO, salinity and pH measurements. Dissolved oxygen samples were collected in glass bottles filled to overflowing. Fixative reagents were added and the stoppered bottle was stored underwater at ambient temperature until analysis the following day. Salinity samples were collected in stoppered glass bottles and stored at ambient temperature until required for analysis. Samples for pH were collected in 60 mL, de-ionised water rinsed brown high density polyethylene bottles ('Nalgene'), refrigerated and analysed as soon as possible (usually the same day). Appropriate care was taken to ensure as little air as possible was introduced to this sample and the bottle was filled to the brim before sealing.

Further subsamples, filtered through 0.45 *u*m membrane filters, were collected for analysis of Fe, Mn, NH_4, NO_2, NO_3, PO_4, SiO_4 and alkalinity. Samples for Fe and Mn were stored in 60 mL acid-washed, de-ionised water rinsed brown high density polyethylene bottles and refrigerated until required for analysis. A sample for inorganic nutrients was stored in a 100 mL 'Whirlpak' and frozen until required for analysis. Samples for alkalinity were stored in 30 mL 'Nalgene' bottles, refrigerated and analysed as soon as possible (usually the same day). Appropriate care was taken to ensure that as little air as possible was introduced to this sample and the bottle was filled to the brim before sealing. Also, at the beginning of deployment, each chamber was spiked with 20 mL of a 10,000 ppm Cs (as CsCl) solution. Five minutes after injection, samples were withdrawn from each chamber by 60 mL plastic syringe and filtered through 0.45 *u*m membrane filters into 30 mL 'Nalgene' bottles. These were stored refrigerated until required for Cs analysis to determine chamber volume by the dilution of Cs.

Dissolved oxygen was measured by the Winkler titration method (Strickland and Parsons 1968) with a VFRI modified redox endpoint detection. Salinity was measured using a "Yeokal 603 Mk II" high precision inductively coupled salinometer. The pH was measured at 25^{o}C using a Model 8102 Ross combination pH electrode calibrated to $\pm$ 0.002 pH units. Iron and Mn concentrations were determined using a VFRI modified extraction method of Statham (1985) in which the metals were chelated, extracted into freon, back extracted into HNO_3 and analysed by graphite furnace atomic absorption spectroscopy. Inorganic nutrients were analysed on-shore by the analytical methods outlined in Section 1 of this report. Alkalinity was determined by Gran titration in a thermostatically controlled vessel following the method of Dickson (1981). Total carbon dioxide was subsequently calculated from pH and alkalinity. Cesium was determined by direct sample aspiration for emission atomic absorption spectrometry (Varian 1979).

At the end of the deployment, divers using plastic 60 mL syringes collected samples from each chamber for all the analyses described above. All syringes were detergent-washed and de-ionised water rinsed and appropriately labelled. The logger was unloaded as soon as possible following retrieval.

CHAMBER DEPLOYMENTS

Benthic chambers were deployed at five sites from 5 - 13 October 1994, at four sites from 20 February to 3 March 1995, at two sites from 11 - 12 May 1995 and at two sites from 30 August - 1 September 1995 and 18 - 23 January 1996. A once a month deployment was made at one site between October 1994 and June 1995.

5 - 13 October 1994 series

Sites 6, 14, 16, 19 and 37 (Table 1, Figure 2) were sampled to estimate fluxes typical of late winter/early spring. As a result of probe failure DO fluxes could not be calculated for Site 14. Water temperature during this period was about 12^{o}C.

20 February - 3 March 1995 series

Sites 6, 8, 16 and 37 (Table 1, Figure 2) were sampled at a water temperature of about 19^{o}C. The objective was to estimate spatial variability of fluxes during summer. Comparisons of VFRI chambers with a Berelson chamber were also made during this deployment.

11 - 12 May 1995 series

This series of samples were designed to to detect the effects of benthic infauna on fluxes at Sites STL12 and STL15 (Table 1, Figure 2) with the chambers being deployed at each site for 5 hours. These sites, close each other and at similar depths of 12 and 15 m, had been used in a previous study to investigate benthic biomass and diversity. The sediments were soft and differed only moderately in composition at each site, but in the previous study were dissimilar in infauna species diversity and number of individuals, the 12 m site having a greater magnitude of both (Rosenberg *et al*. 1992, Currie and Parry 1995).

October 1994 - June 1995 series

This was a monthly deployment of the chambers at Site 6 (Table 1, Figure 2), with water temperature over this period ranging between 12 and 20^{o}C. The objective was to estimate seasonal variability in fluxes at one site.

30 August - 1 September 1995 series

This was a late winter deployment at Sites 16 and 37. The chambers were deployed and retrieved at Site 16 on 30 August and deployed at Site 37 on 31 August and retrieved on 1 September. The water temperature in the Bay during this period was about 11^{o}C.

18 - 24 January 1996 series

This was a summer deployment at Sites 16 and 37. The chambers were deployed and retrieved at Site 16 on 18 January, and deployed at Site 37 on 23 January and retrieved on 24 January. The water temperature over this period was about 19^{o}C.

BENTHIC CHAMBER FLUXES

Principles

Chamber fluxes are calculated to units of millimoles m^{-2} day^{-1}. Negative flux values indicate solute movement from the water column into the sediments.

$$\mathbf{Flux = ((C_2 - C_1)/(T_2-T_1)).V.24.(1/A)}$$

where C_2 = concentration of solute at time T_2 (*u*mol L^{-1})

C_1 = concentration of solute at time T_1 (*u*mol L^{-1})

T_2 = end time (hr)

T_1 = initial time (hr)

V = chamber volume (L)

A = seafloor area covered by chamber (m^2)

Dissolved oxygen was measured once every 10 minutes. Changes in the DO concentration with time for each deployment are plotted in Figures 18 - 23. The initial stages of the profiles were nearly linear. A regression of the profile for each dark and light (clear) chamber over the first few hours of deployment indicated that this was the straightest section of the plot, and this section was used for the calculation of DO flux.

The continual decrease of DO within chambers from deployments of 20 hours or more (Figs. 18 - 23) indicated that there was no significant replacement by leakage around the chamber lip or groundwater intrusion of oxygen consumed by diagenetic processes. Leakages would be seen by a flattening out of profiles during the intermediate times of the deployment period. The diagenesis of N and P in sedimented diatomaceous organic matter follows first-order reaction kinetics and it would be reasonable to assume that as

the DO concentration decreases, the rate of mineralization of organic N and P also decreases. Fluxes of nutrients, metals, alkalinity and CO_2 were estimated from only two points, based on samples collected by syringe at the beginning and at end of deployment of usually about 20 hours duration. Flux calculations of these solutes contained a systematic error on top of any analytical error.

Preliminary inspection of longer duration deployments indicated that at some sites where fluxes were large, subsequent deployment periods could be reduced to five hours (Figs. 20, 21b, 21c and 22). Where possible, intermediate samples were obtained as a verification of values obtained from initial and final samplings and as a means of reducing the magnitude of systematic errors.

RESULTS

DISSOLVED OXYGEN CONCENTRATION CHANGES

5 - 13 October 1994

Dissolved oxygen profiles for light and dark chambers from the first late winter/early spring deployment during October 1994 at Sites 6, 16, 19 and 37 are illustrated in Figure 18. Site 14 was also sampled during this period, but due to technical problems DO data was unavailable. Not all of the data from each of the sites are plotted because either leakage of seawater into the chamber enclosure, or disturbance of the chambers was suspected.

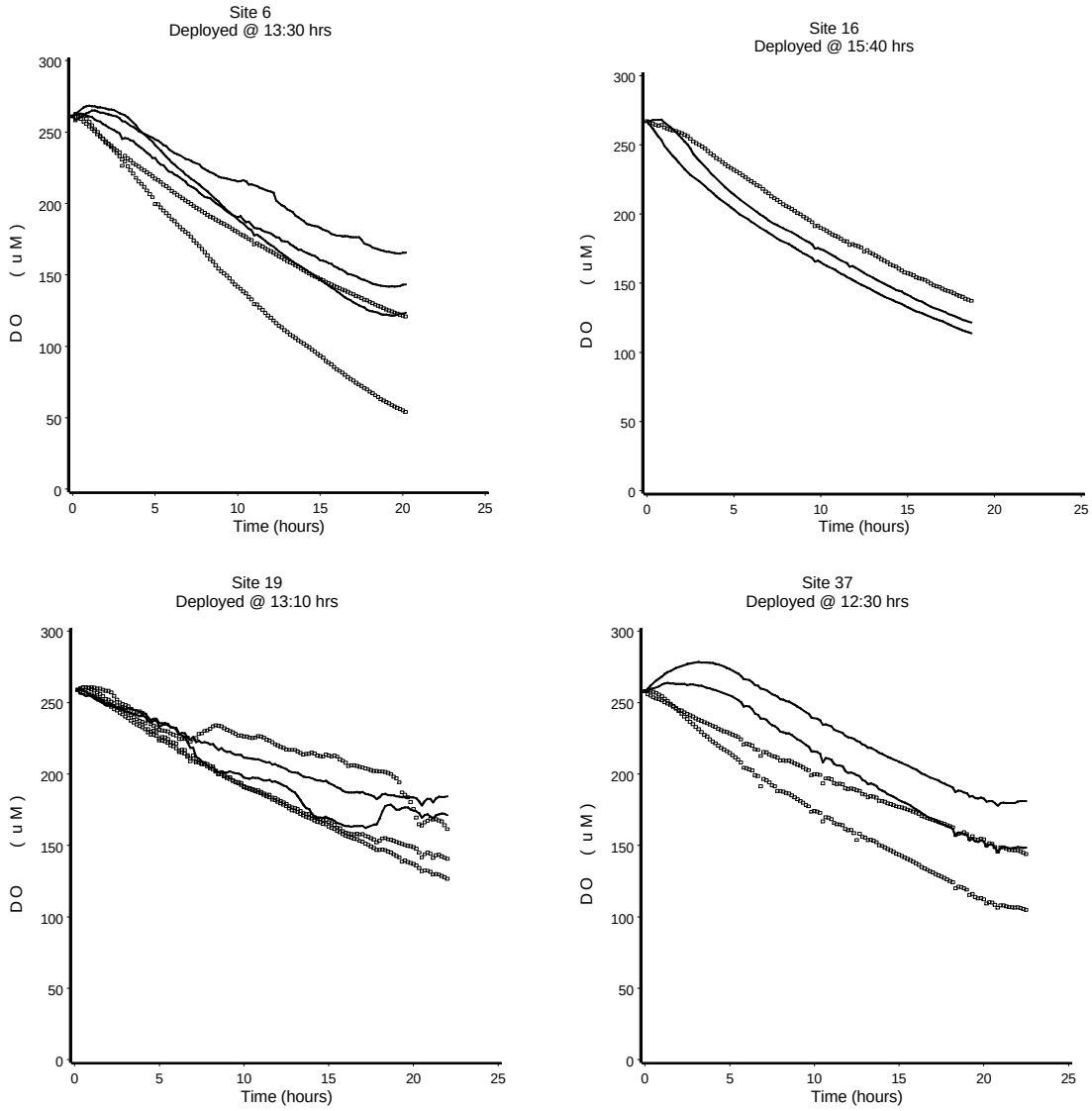

Figure 18: Dissolved oxygen concentrations mearured over time in light chambers (solid lines) and dark chambers (squares) for Sites 6, 16, 19 and 37 during October 1994.

20 February - 3 March 1995

Dissolved oxygen profiles for light and dark chambers during the deployment in February and March 1995 at Sites 6, 8, 16 and 37 are illustrated in Figure 19. The distinctive light chamber profile at Site 16 is due to introduction of oxygenated water into the chamber, most probably by a burrowing animal. Dissolved oxygen flux for this chamber was calculated from the linear portion of the profile during the initial five hours of deployment.

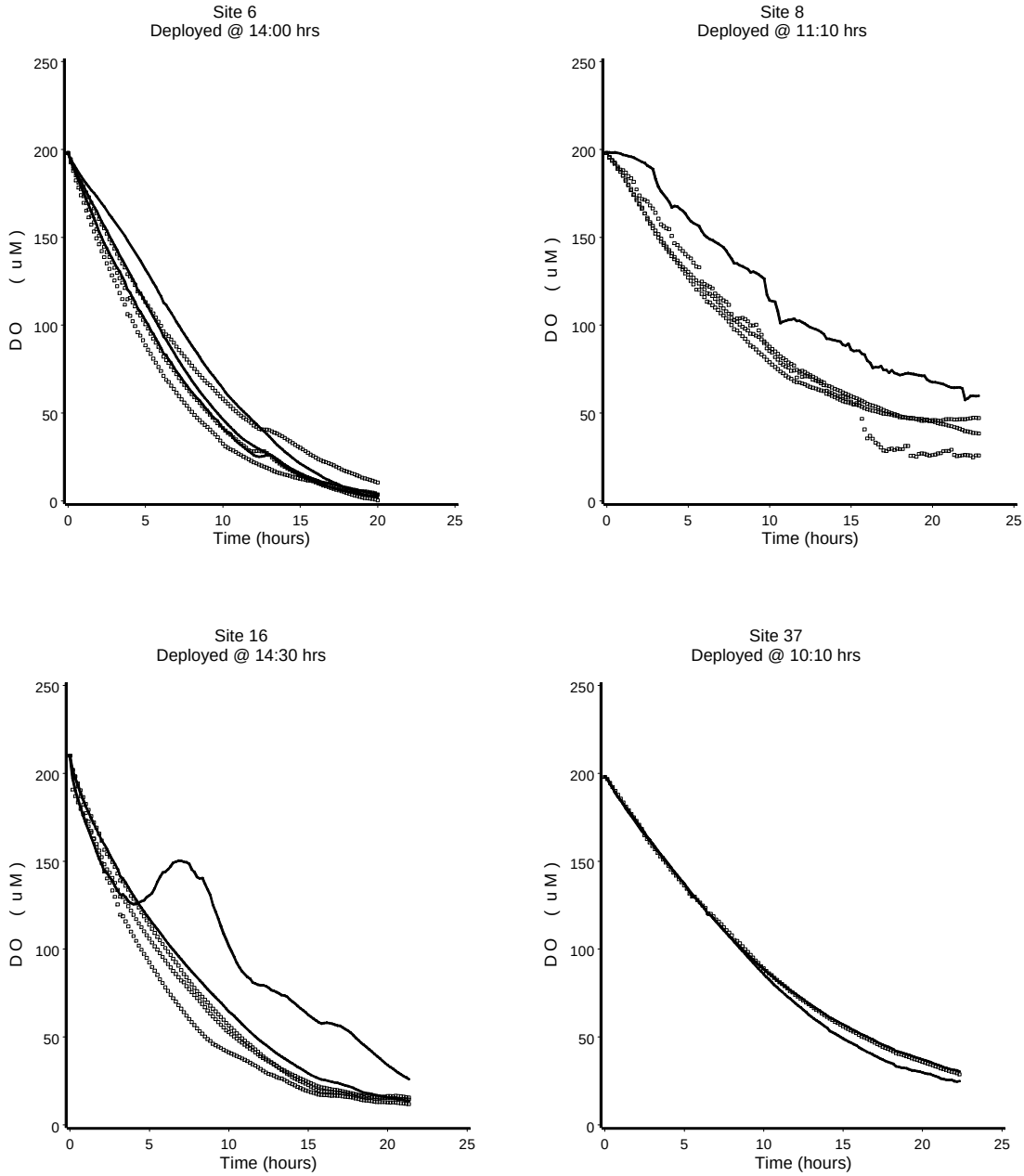

Figure 19: Dissolved oxygen concentrations measured over time for light chambers (solid lines) and dark chambers (squares) at Sites 6, 8, 16 and 37 during February - March 1995.

11 -12 May 1995

The object of this exercise was to observe whether any difference in solute fluxes was a reflection of benthic biomass. Site STL12 was considered to have the greater biomass. The DO profiles are shown in Figure 20.

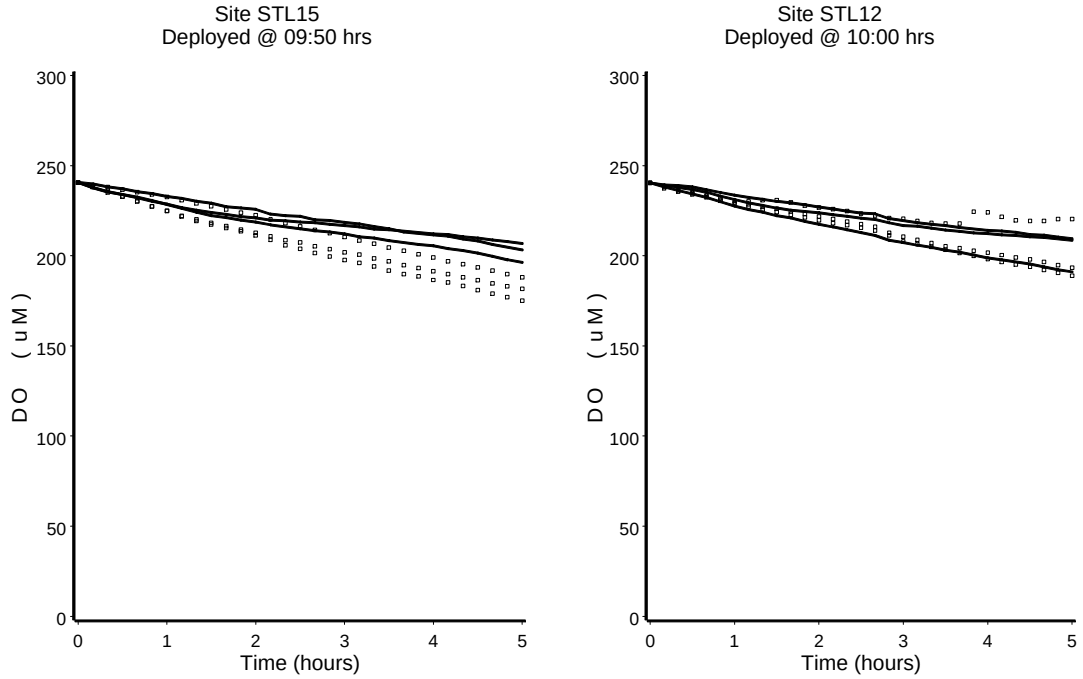

Figure 20: Dissolved oxygen concentrations measured over time in light chambers (solid lines) and dark chambers (squares) at Sites STL12 12 and STL15 during May 1995.

October 1994 - June 1995

Dissolved oxygen profiles from the monthly deployments at Site 6 (Werribee) from October 1994 to June 1995 are shown in Figures 21a - 21c. The shape of the profiles from the light chambers during October, November and particularly January in Figure 21a shows that O_2 production occurred during daylight hours.

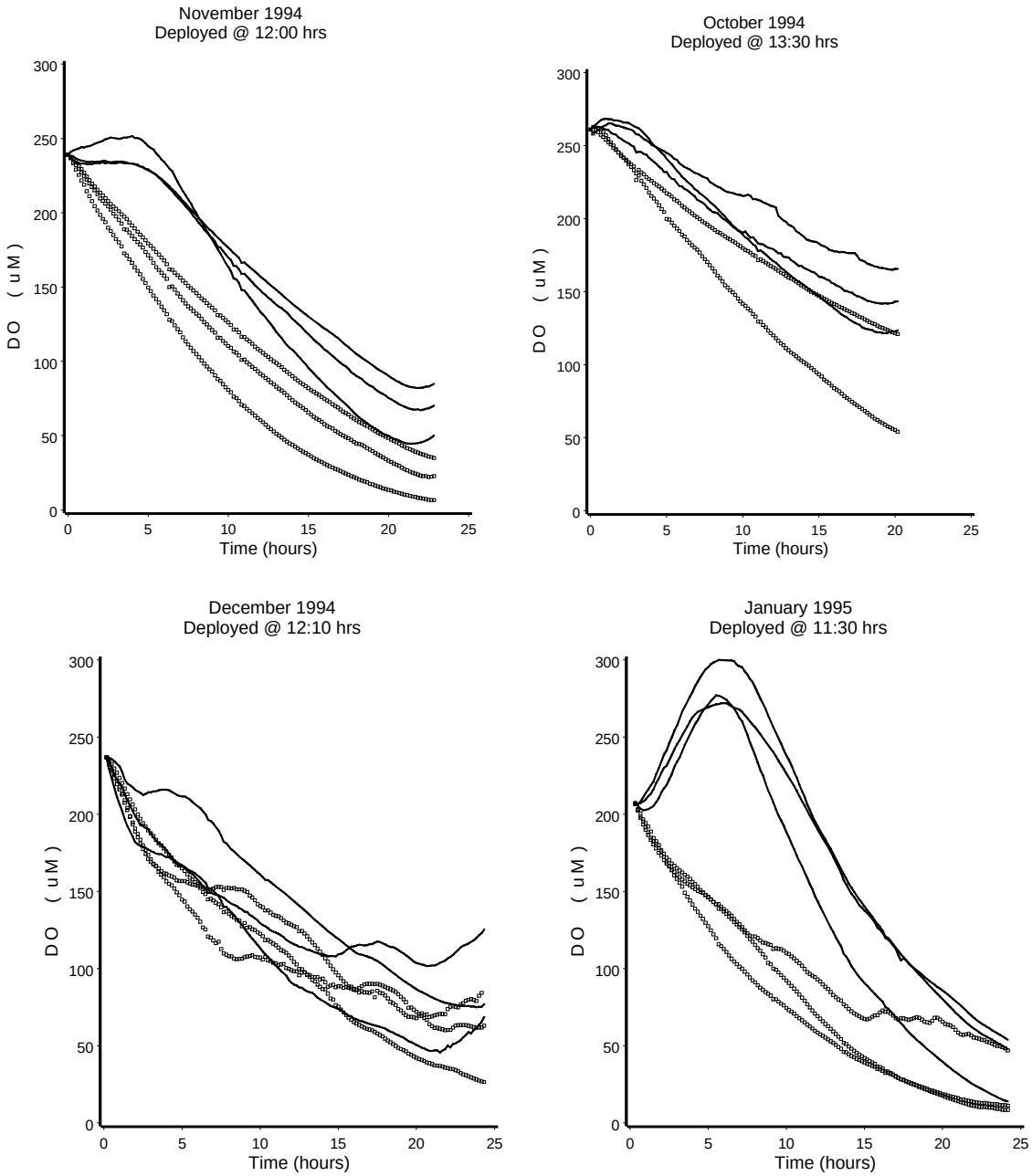

Figure 21a: Dissolved oxygen concentrations measured over time in light chambers (solid lines) and dark chambers (squares) at Site 6 for October, November and December 1994, and January 1995.

Duration of chamber deployments at Site 6 was reduced to 5 hours in April, May and June 1995 as the fluxes obtained from previous deployments were comparatively large and it appeared unnecessary to carry the deployment through to 20 hours or more.

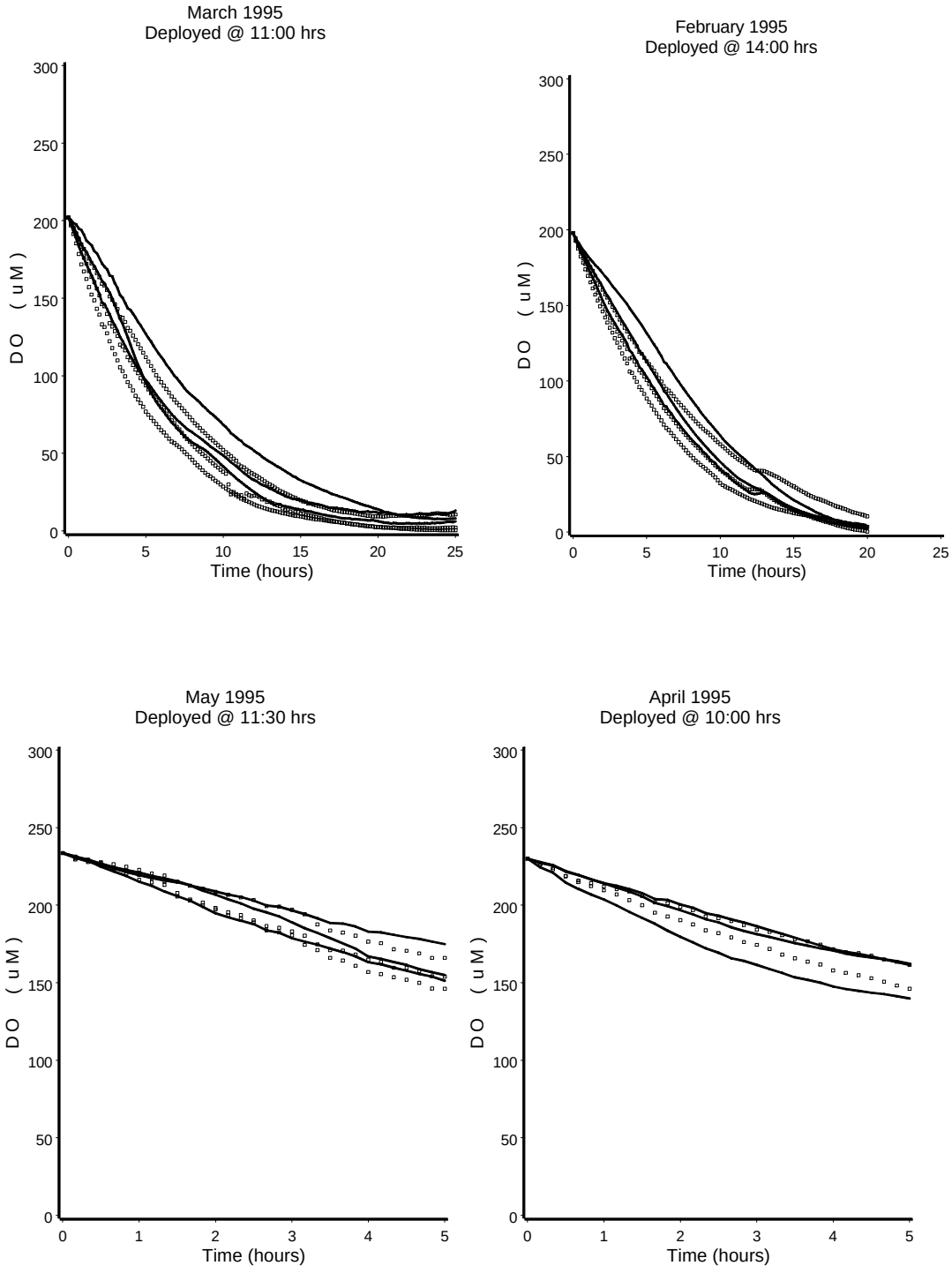

Figure 21b: Dissolved oxygen concentrations measured over time in light chambers (solid lines) and dark chambers (squares) at Site 6 for February, March, April and May 1995.

Only two light chambers were deployed during June 1995 at Site 6 (Fig. 21c). Visibility during diving for the placement of the chambers was very poor, and inadvertently a light chamber was placed over a benthic-dwelling tube worm (*Sabella spallanzanii*). The DO profile from that chamber is distinctive, particularly after two hours when the O_2 uptake increased as the worm probably became more stressed.

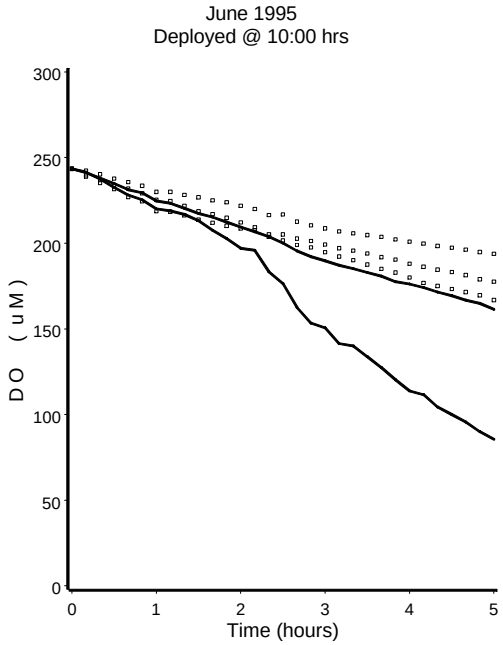

Figure 21c: Dissolved oxygen concentrations measured over time in light chambers (solid lines) and dark chambers (squares) at Site 6 for June 1995.

30 August - 1 September 1995

The DO profiles from the second late winter deployment are shown in Figure 22. The visibility during chamber deployment and retrieval at Site 37 was poor. The profile from one of the dark chambers at this site is distinctly different from all of the others, and it is likely that the chamber was inadvertently placed over some type of sedentary epifauna. The data from this chamber were not used for flux calculations.

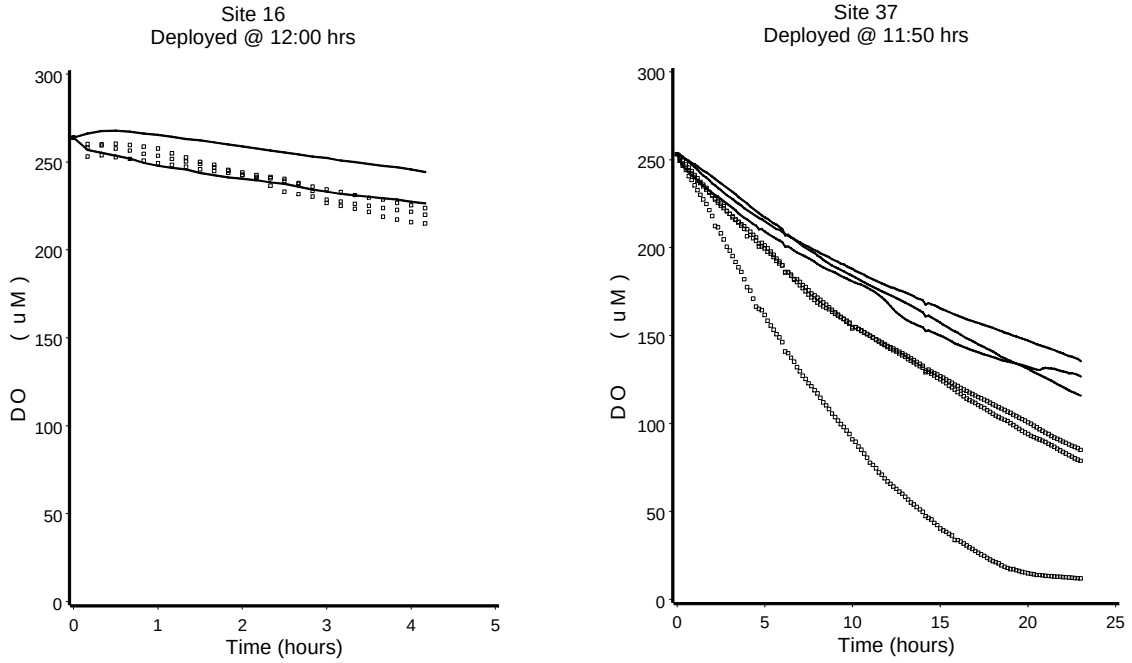

Figure 22: Dissolved oxygen concentrations measured over time in light chambers (solid lines) and dark chambers (squares) at Sites 16 and 37 for August 1995.

18 January - 24 January 1996

The DO profiles from this deployment are shown in Figure 23. The shape of the profiles from the light chambers at Site 37 shows that O_2 production occurred during daylight hours, and very likely originated from the widespread benthic mat noticed at this site.

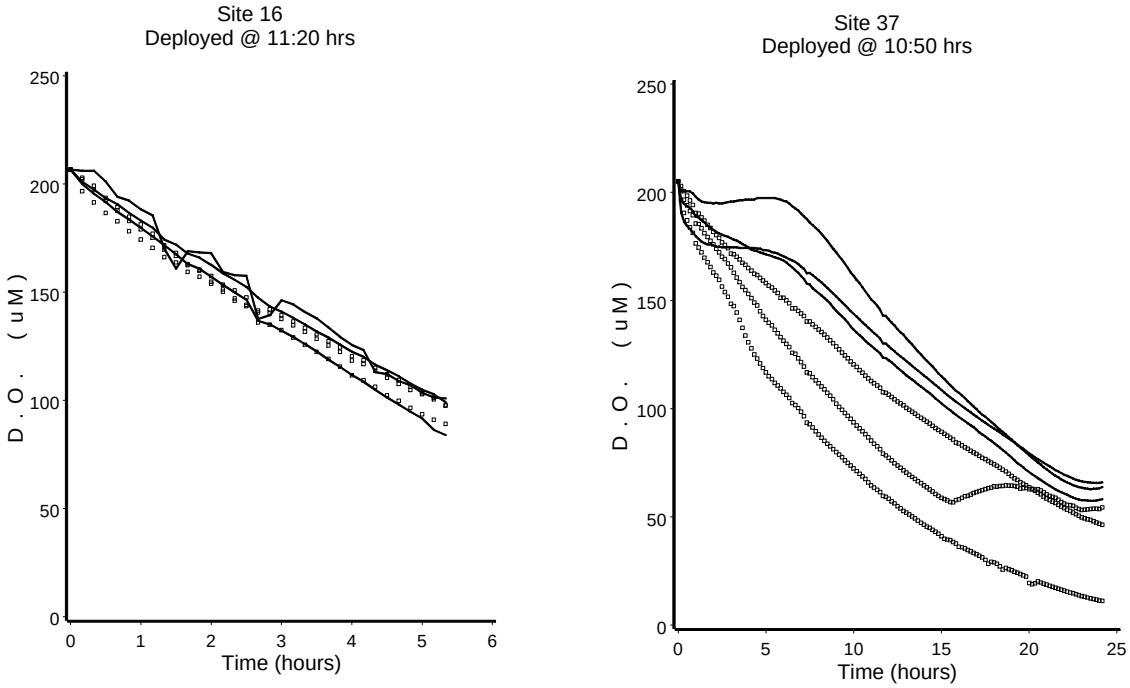

Figure 23: Dissolved oxygen concentrations measured over time in light chambers (solid lines) and dark chambers (squares) at Sites 16 and 37 for January 1996.

SOLUTE FLUXES

5 - 13 October 1994

Fluxes of DO, ammonium, phosphate, nitrite plus nitrate, silicate, total carbon dioxide, iron and manganese, from five sites during 5 - 13 October 1994, are shown in Figure 24. Due to technical difficulties, DO flux data for Site 14 was unavailable.

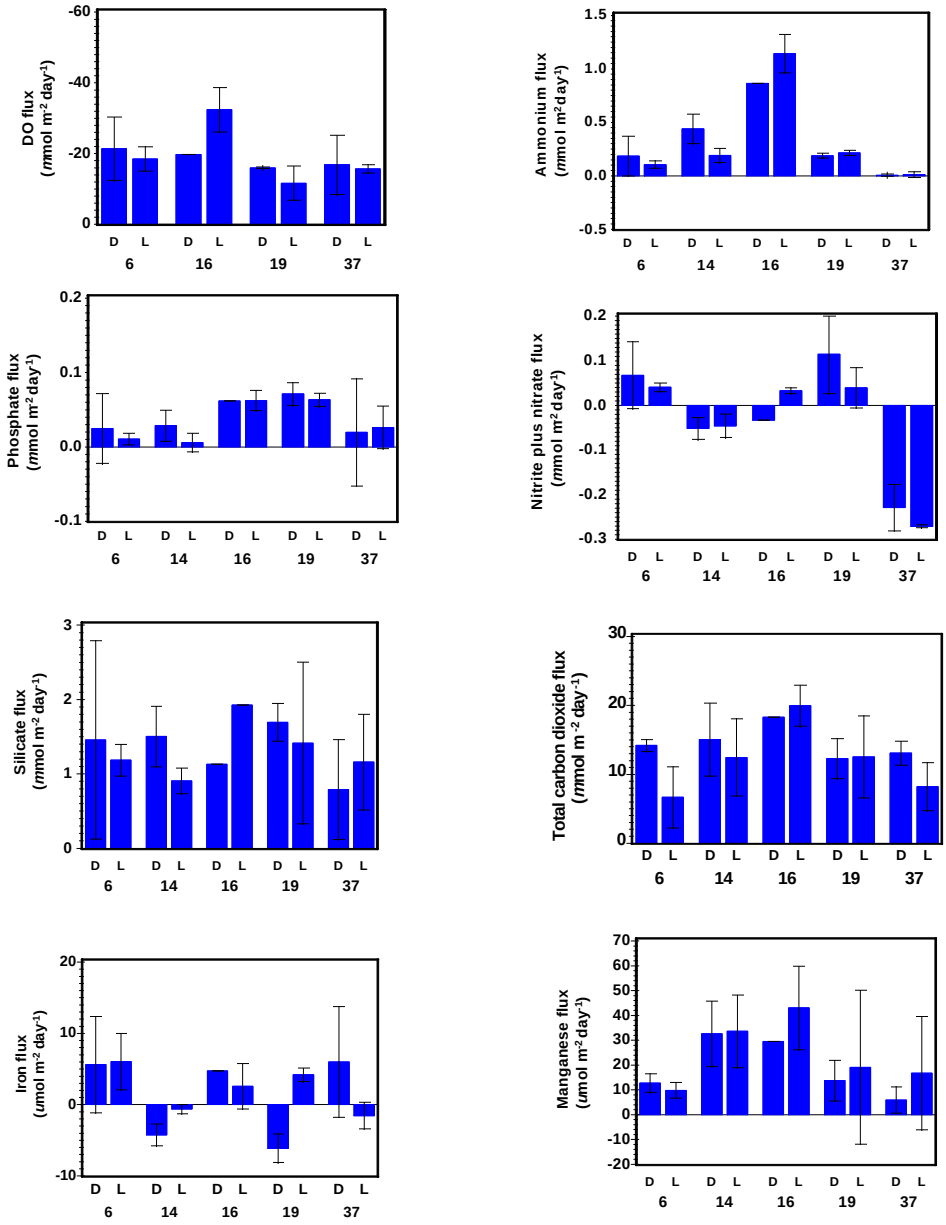

Figure 24: Fluxes (*m*mol m^{-2} day^{-1}) of DO at Sites 6, 16, 19 and 37, and ammonium, phosphate, nitrite plus nitrate, silicate, total carbon dioxide and fluxes (*u*mol m^{-2} day^{-1}) of iron and manganese at Sites 6, 14, 16, 19 and 37, from dark (D) and light (L) chambers deployed during October 1994. The error bars indicate one standard deviation about the mean.

20 February - 3 March 1995

Fluxes of DO, ammonium, phosphate, nitrite plus nitrate, silicate, total carbon dioxide, iron and manganese, from four sites during 20 February - 3 March 1995, are shown in Figure 25.

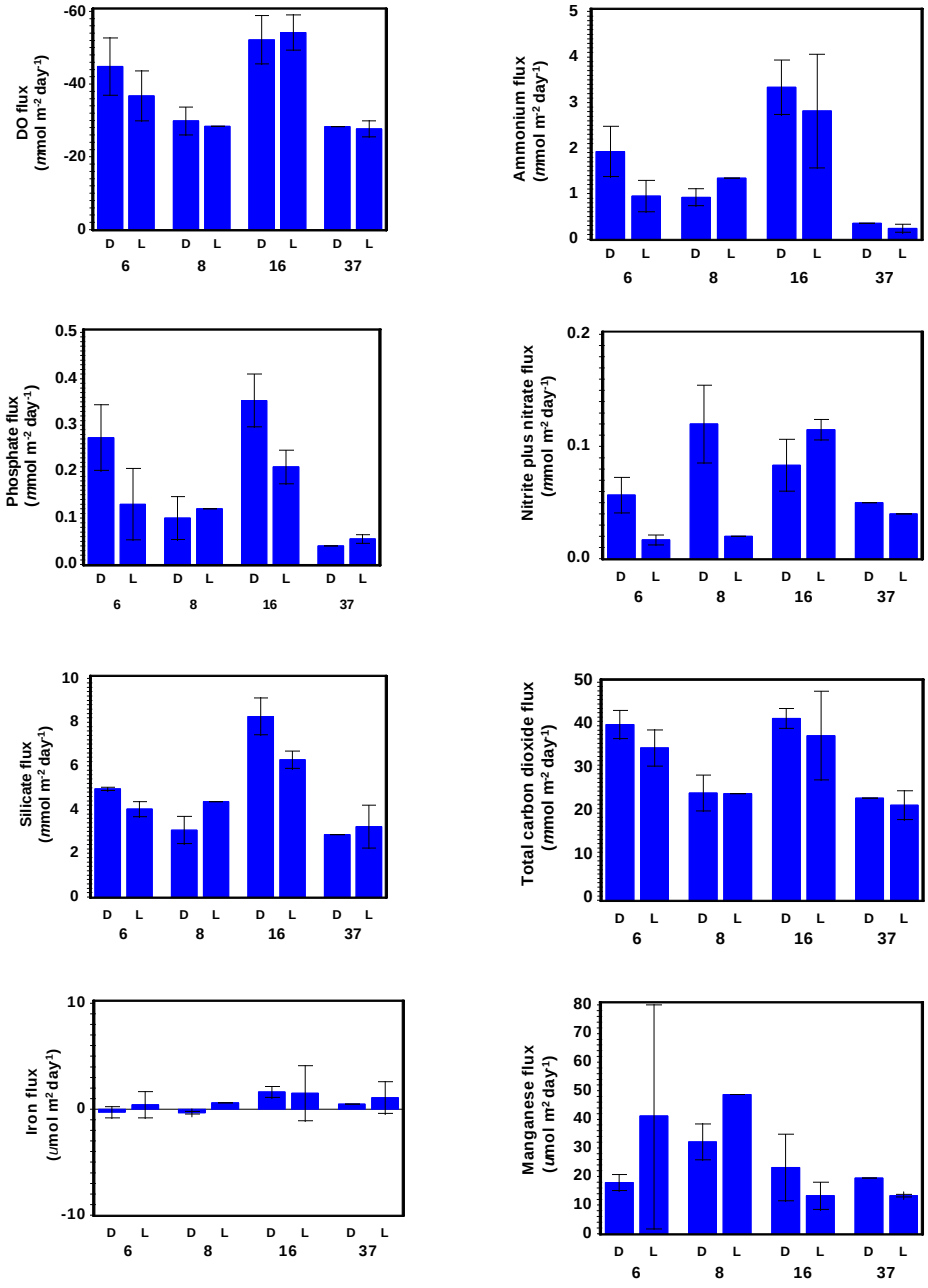

Figure 25: Fluxes (*m*mol m^{-2} day^{-1}) of DO, ammonium, phosphate, nitrite plus nitrate, silicate, total carbon dioxide and fluxes (*u*mol m^{-2} day^{-1}) of iron and manganese at Sites 6, 8, 16 and 37, from dark (D) and light (L) chambers deployed during February - March 1995. The error bars indicate one standard deviation about the mean.

October 1994 - June 1995

Fluxes of DO, ammonium, phosphate, nitrite plus nitrate, silicate, total carbon dioxide, cesium, iron and manganese measured in chambers deployed at Site 6 over the period October 1994 - June 1995 are shown in Figures 26a - 26b.

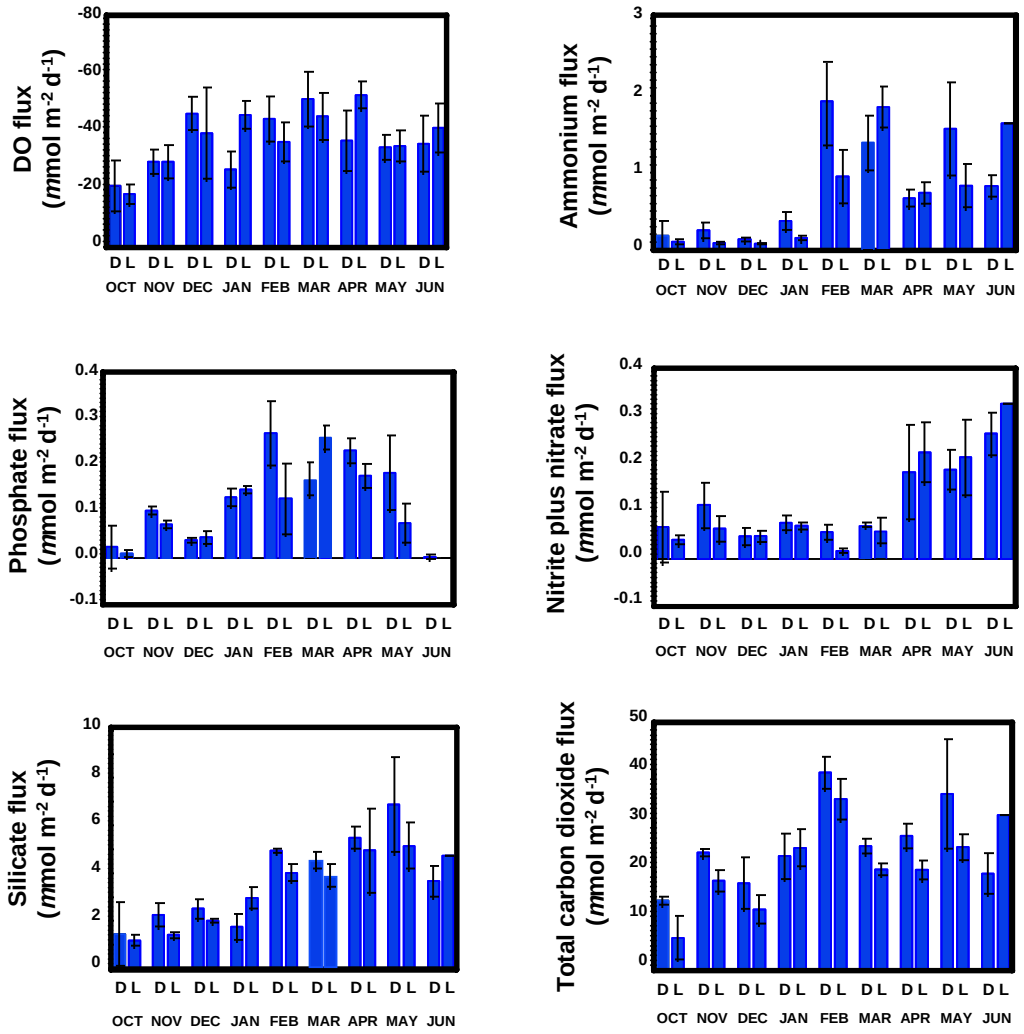

Figure 26a: Fluxes (*m*mol m^{-2} day^{-1}) of DO, ammonium, phosphate, nitrite plus nitrate, silicate and total carbon dioxide from dark (D) and light (L) chambers over nine monthly deployments beginning October 1994 at Site 6. The error bars indicate one standard deviation about the mean. The shorter term (5 hour) deployments with intermediate sampling were conducted during the months of April, May and June 1995.

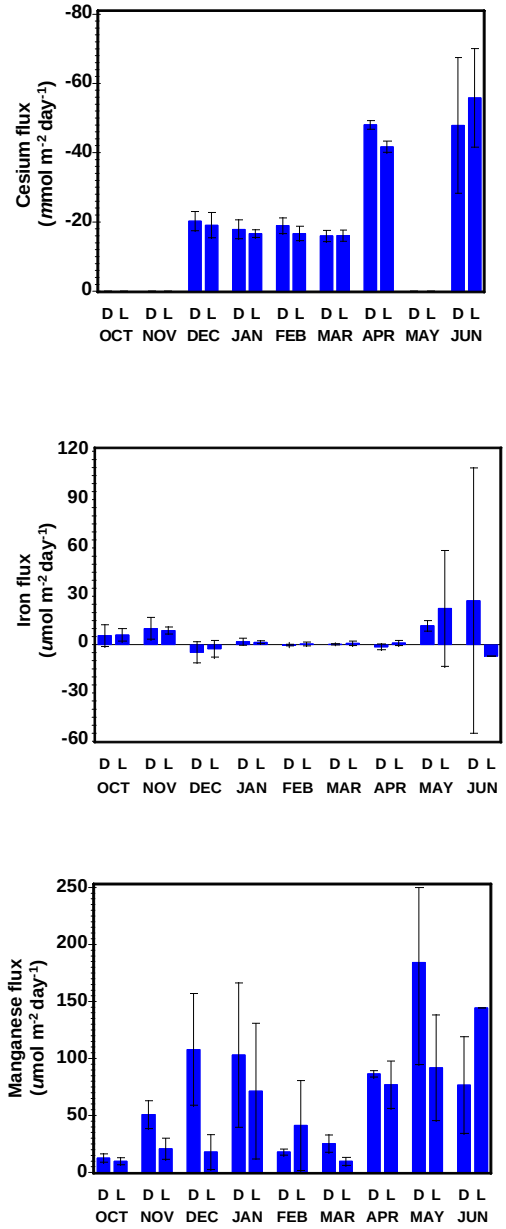

Figure 26b: Fluxes of cesium (*m*mol m^{-2} day^{-1}) and of iron and manganese (*u*mol m^{-2} day^{-1}) from dark (D) and light (L) chambers over nine monthly deployments at Site 6. The error bars indicate one standard deviation about the mean. The shorter term (5 hour) deployments with intermediate sampling were conducted during the months of April, May and June 1995. Cesium fluxes from those sampling periods of > 5 hours duration were estimated as if from 5 hours with the cesium concentration at that time obtained using an exponential function describing cesium loss from chambers (Berelson *et al.* 1996).

11 - 12 May 1995

As mentioned previously, this exercise utilised two sites where from a previous study it was known that while otherwise similar in depth, location, and soft sediment composition, there was a difference in diversity and abundance of benthic infauna. We wished to observe if differences in solute fluxes correlated with the benthic biomass. Site STL12 was expected to have the greater biomass. The fluxes are shown in Figure 27.

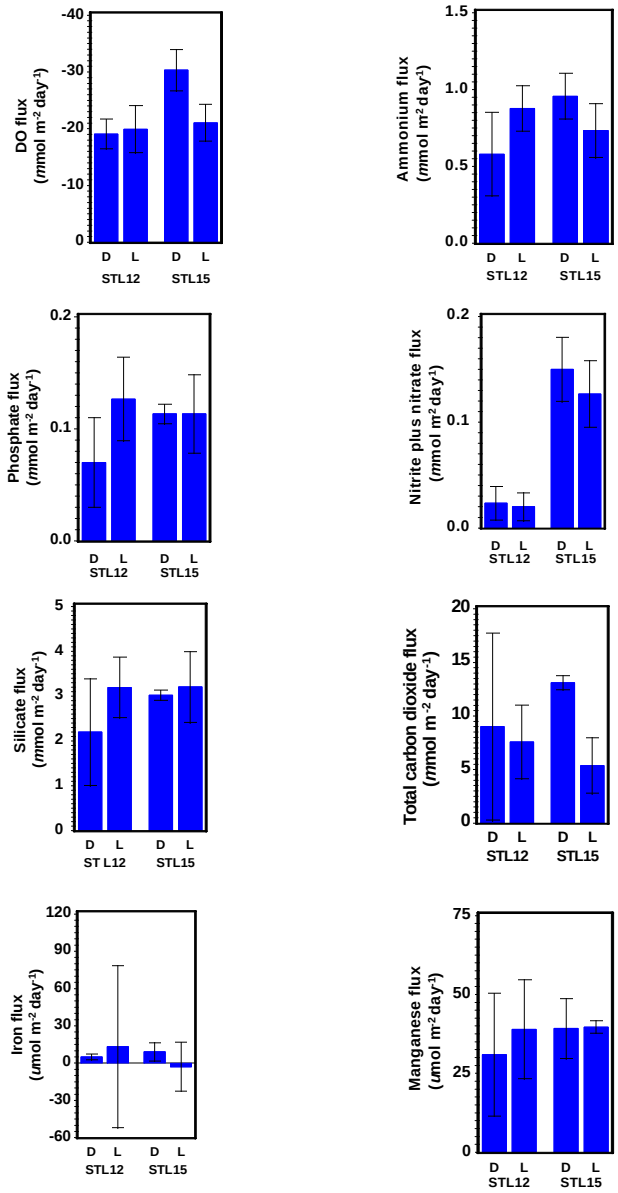

Figure 27: Fluxes (*m*mol m^{-2} day^{-1}) of DO, ammonium, phosphate, nitrite plus nitrate, silicate, total carbon dioxide, iron and manganese for dark (D) and light (L) chambers from two adjoining Sites STL12 and STL15. The error bars indicate one standard deviation about the mean.

30 August - 1 September 1995

Fluxes of DO, ammonium, phosphate, nitrite plus nitrate, silicate, total carbon dioxide and manganese, from Sites 16 and 37 during 30 August - 1 September 1995, are shown in Figure 28.

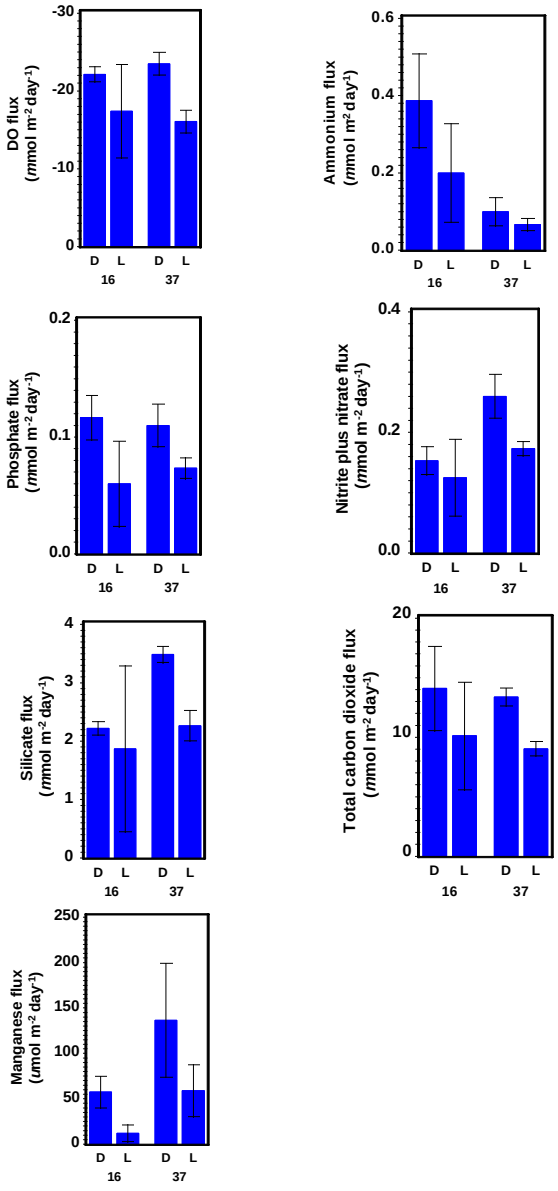

Figure 28: Fluxes (*m*mol m^{-2} day^{-1}) of DO, ammonium, phosphate, nitrite plus nitrate, silicate, total carbon dioxide and manganese at Sites 16 and 37 from dark (D) and light (L) chambers during August - September 1995. The error bars indicate one standard deviation about the mean.

18 January - 24 January 1996

Fluxes of DO, ammonium, phosphate, nitrite plus nitrate, silicate and total carbon dioxide from Sites 16 and 37 during 18 January - 24 January 1996, are shown in Figure 29.

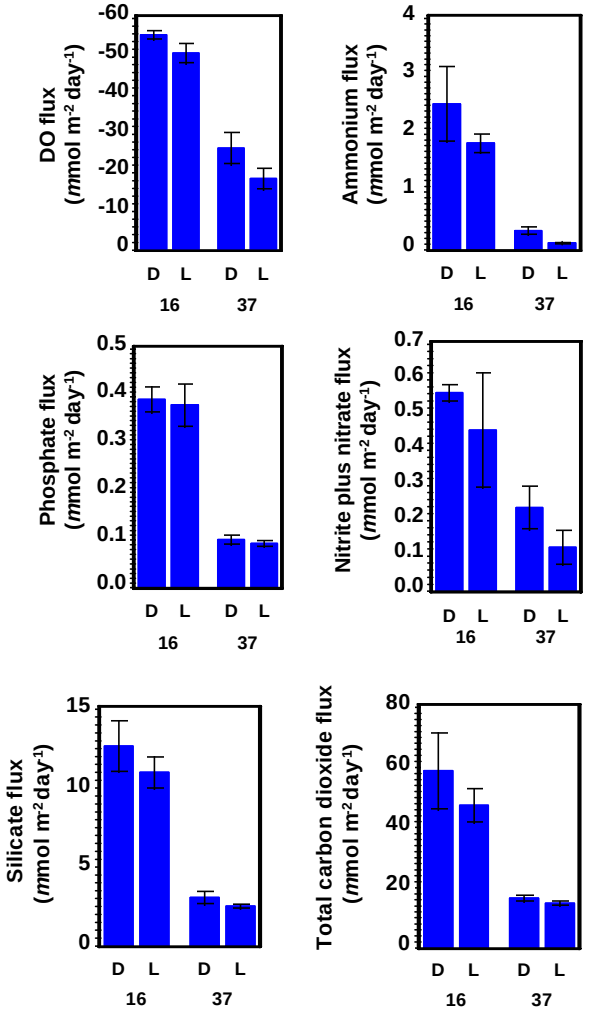

Figure 29: Fluxes (*m*mol m^{-2} day^{-1}) of DO, ammonium, phosphate, nitrite plus nitrate, silicate and total carbon dioxide at Sites 16 and 37 from dark (D) and light (L) chambers during January 1996. The error bars indicate one standard deviation about the mean.

BENTHIC CHAMBER FLUX COMPARISONS

Site 16:

Benthic chambers were deployed at Site 16 during October 1994, and March, August and January 1996. Water temperatures in the Bay were 12^{o}C, 20^{o}C, 11^{o}C and 19^{o}C respectively, and are typical of high and low temperatures within the Bay. The fluxes of DO, total carbon dioxide, ammonium, phosphate, nitrite plus nitrate, silicate and manganese from these four deployments are shown in Figure 30.

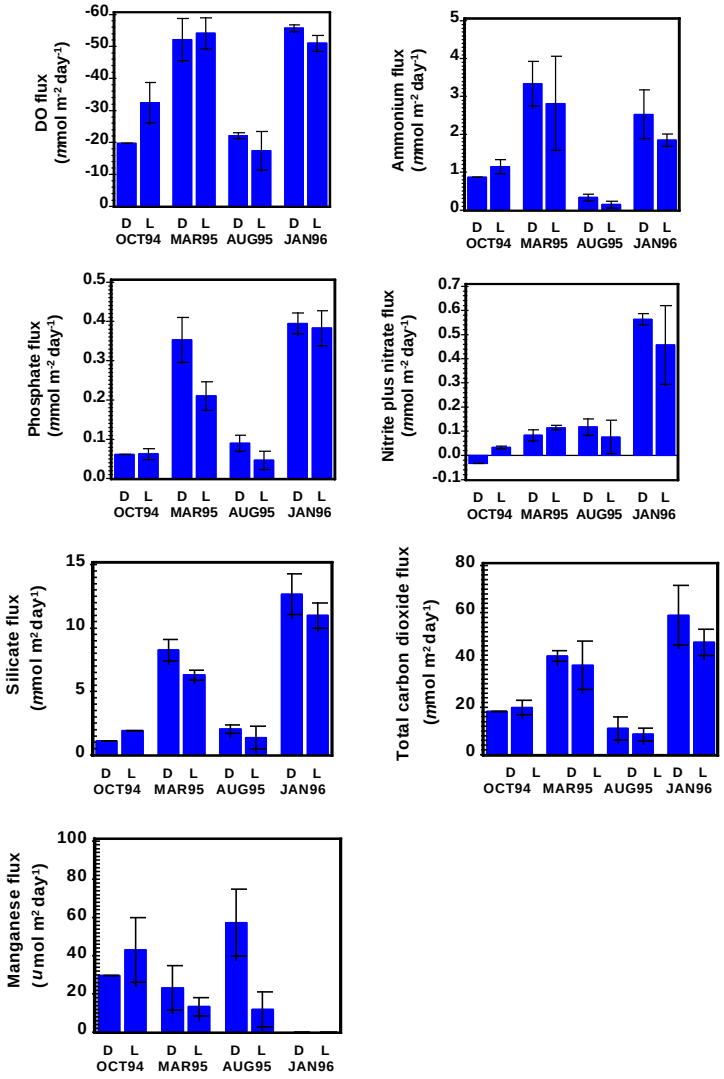

Figure 30: Fluxes (*m*mol m^{-2} day^{-1}) of DO, ammonium, phosphate, nitrite plus nitrate, silicate, total carbon dioxide and manganese (*u*mol m^{-2} day^{-1})at Site 16 during October 1994, and March, August and January 1996 from dark (D) and light (L) chambers. The error bars indicate one standard deviation about the mean.

Site 37: Benthic chambers have been deployed at Site 37 during October 1994, February-March and August 1995 and January 1996. Water temperatures in the Bay were 12^{o}C, 20^{o}C, 11^{o}C and 19^{o}C respectively, and are typical of high and low temperatures within the Bay. The fluxes of DO, total carbon dioxide, ammonium, phosphate, nitrite plus nitrate, silicate and manganese from these four deployments are shown in Figure 31.

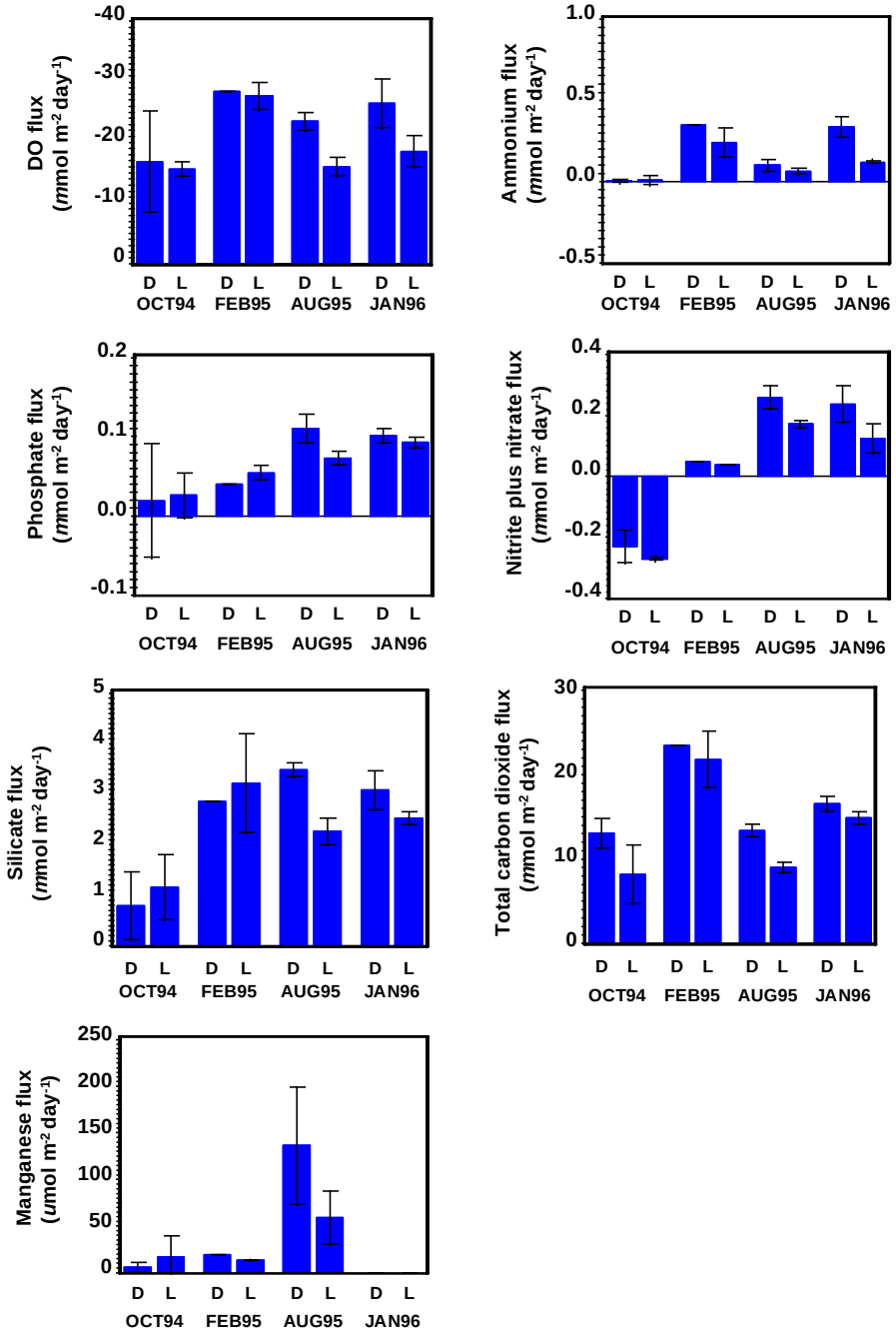

Figure 31: Fluxes (*m*mol m^{-2} day^{-1}) of DO, ammonium, phosphate nitrite plus nitrate, silicate, total carbon dioxide and manganese (*u*mol m^{-2} day^{-1}) at Site 37 during October 1994, February-March and August 1995 and January 1996 from dark (D) and light (L) chambers. The error bars indicate one standard deviation about the mean

COMPARISON WITH BERELSON BENTHIC CHAMBER

The benthic chamber of Berelson *et al.* (1994) was deployed in parallel with VFRI benthic chambers at Sites 6, 8, 16 and 37 during February and March 1995. The comparisons of fluxes of DO, ammonium, phosphate, nitrite, nitrite plus nitrate, silicate and total carbon dioxide from the (usually) single Berelson chamber and from six VFRI chambers is shown in Figure 32a.

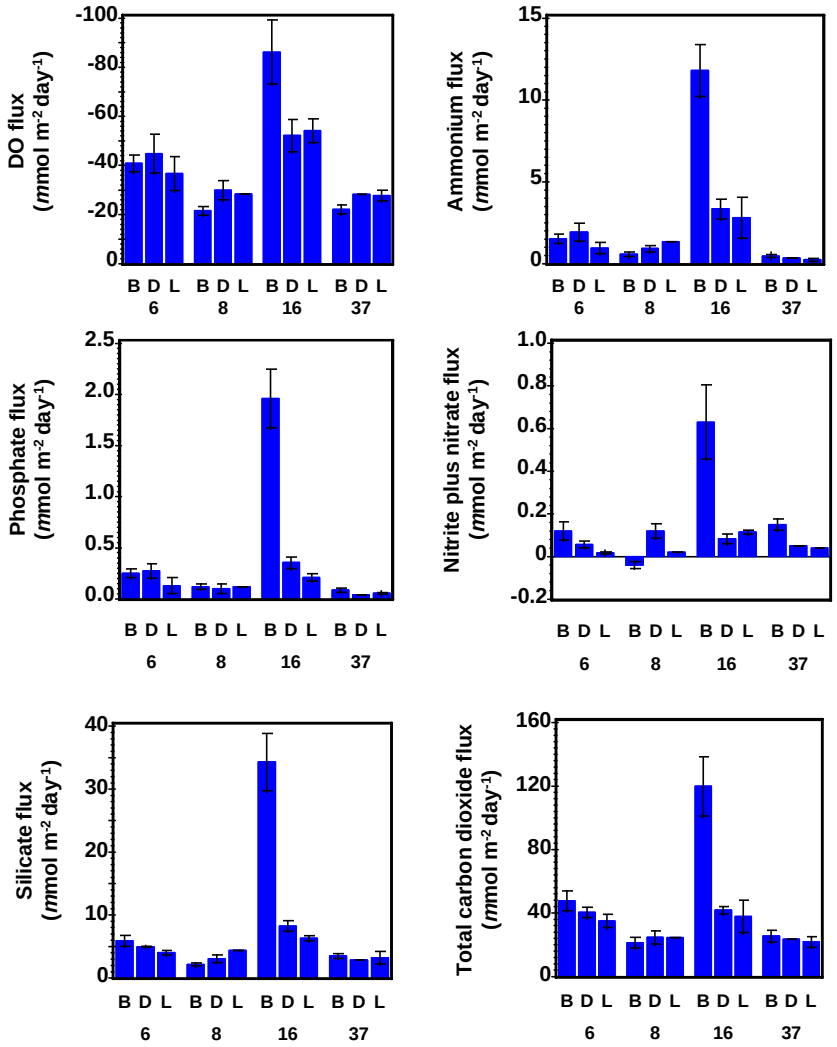

Figure 32a: Fluxes (*m*mol m^{-2} day^{-1}) of DO, ammonium, phosphate, nitrite plus nitrate, silicate and total carbon dioxide from the Berelson chamber (B) and from VFRI dark (D) and light (L) chambers from Sites 6, 8, 16 and 37. Error bars indicate one standard deviation about the mean.

The charts in Figure 32a show that other than at Site 16, Berelson chambers and VFRI chambers produced fluxes of similar magnitude. The method of determination of DO flux by the two chamber types is similar. The method of sample collection of other solutes is different between the two chamber types. A regression through zero of

Berelson chamber fluxes versus our mean chamber fluxes (including and excluding data from Site 16), with Berelson chamber fluxes as the independent variable, enabled a ratio to be calculated between the two benthic devices. These are shown in Table 7.

Table 7: Ratio of the flux values and standard error calculated from Berelson and from VFRI clear benthic chambers, inclusive and exclusive of data from Site 16. The regression used was of the form: Berelson = m * VFRI.

Flux	Berelson ratio			
	Incl 16	± S.E.	Excl 16	± S.E.
DO	1.2	0.2	0.9	0.1
CO_2	1.9	0.5	1.1	0.1
PO_4	4.8	1.8	1.3	0.2
NO_x	3.7	1.4	1.8	1.4
NH_4	3.0	0.8	0.8	0.2
SiO_4	3.0	1.1	1.2	0.2

Cesium chloride was introduced into chambers as a means of chamber volume determination by measuring the dilution of CsCl within 5 minutes of injection. Any further Cs decrease was interpreted as due to leakage or porewater irrigation. The loss of Cs from chambers in all cases follows a monotonic decrease with incubation time and is described in Berelson *et al* (1996) by the exponential function:

$$Cs = Cs_0 \, e^{(bt)}$$

where Cs is the concentration of Cs within the chamber at time = t, Cs_0 is the Cs concentration in the chamber within 5 minutes of injection, and b is the fitting parameter. Chambers with larger negative b values have the greatest Cs loss. If the Cs loss was due simply to chamber leakage, then chambers with largest negative b values would have lower fluxes of other solutes. However, chambers which have large negative b values and high fluxes of other solutes indicate higher rates of porewater irrigation. Comparisons of b values obtained from Berelson chambers and from VFRI chambers are shown in the following Figure 32b.

The greatest negative cesium fitting parameter (b) in Figure 32b is from the Berelson chamber at Site 16, and indicates the greatest rate of cesium dilution. As the greatest fluxes of other solutes also occur from the Berelson chamber at Site 16, the combination of both is an indication of greatest porewater irrigation occurring under this chamber at this site.

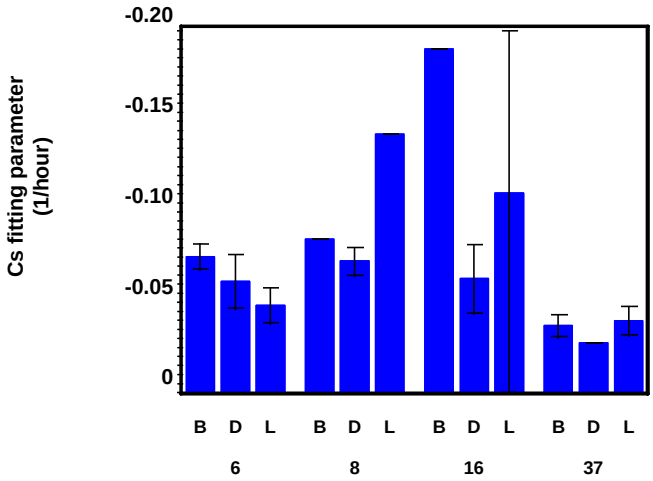

Figure 32b: Values of b, the Cs fitting parameter (1/hour) obtained from the Berelson chamber (B), and from VFRI dark (D) and light (L) chambers from Sites 6, 8, 16 and 37. Error bars indicate one standard deviation about the mean.

NITROGEN AND PHOSPHORUS BUDGETS

The results from all chamber deployments between October 1994 and August 1995 were used to estimate annual amounts of N and P liberated from the sediments of PPB. Sites located within each of the four regions of the Bay were considered typical of that region. If more than one sampled site was located in a region, the values from all sites were averaged for the region. Dissolved inorganic N flux to the water column was estimated both from chamber fluxes of NH_4 and NO_x, and a theoretical flux calculated from DO flux, assuming 16 mole of N is regenerated for each 138 mole of O_2 consumed. Phosphate flux to the water column was estimated from chamber fluxes of PO_4, and a theoretical flux calculated from DO flux, assuming 1 mole of P is regenerated for each 138 mole of O_2 consumed. The results are shown in Table 8.

Table 8: Nitrogen and phosphorus (tonne year^{-1}) liberated from the sediments within each region as estimated by chamber DIN and PO_4 fluxes, and by the DO flux and the Redfield ratio.

Region	Area	Estimated from DIN & PO_4 flux		Theoretical, estimated from DO flux	
	(km^2)	N (tonne yr^{-1})	P (tonne yr^{-1})	N (tonne yr^{-1})	P (tonne yr^{-1})
Central	506	700 ± 900	400 ± 250	6500 ± 2000	900 ± 300
Northern	240	2400 ± 1500	650 ± 400	6000 ± 3000	800 ± 300
Surround	919	3500 ± 2000	1000 ± 500	11000 ± 3500	1500 ± 500
Western	284	1500 ± 1700	400 ± 300	6500 ± 2000	900 ± 300
Total	1949	8100 ± 3200	2450 ± 750	30000 ± 5500	4100 ± 720

PROCESSES

There are two models available which represent organic carbon oxidation end-member scenarios (Berelson *et al.* 1996). One model accounts for all the measured alkalinity flux, after corrections for nitrite plus nitrate and ammonium fluxes, as derived from $CaCO_3$ dissolution; the second model accounts for all the corrected alkalinity flux as derived from sulphate reduction. If production or consumption of oxidised nitrogen species is neglected, and Redfield stoichiometry is assumed for the oxidation of organic matter, then equations that describe the two model scenarios are shown below (McCaffrey *et al*., 1980):

Calcium carbonate dissolution scenario:

$$(CH_2O)_{106}(NH_3)_{16}(H_3PO_4) + 106O_2 \Leftrightarrow 106CO_2 + 106H_2O + 16NH_3 + H_3PO_4;$$

$$CO_2 + CaCO_3 + H_20 \Leftrightarrow Ca^{2+} + 2HCO_3^-;$$

Sulphate reduction scenario:

$$(CH_2O)_{106}(NH_3)_{16}(H_3PO_4) + 53SO_4^{2-} \Leftrightarrow 106HCO_3^- + 53H_2S + 16NH_3 + H_3PO_4;$$

If marine phytoplankton is the dominant carbon source, the oxygen flux/carbon oxidation flux should be between 1.0 and 1.3. The calcium carbonate dissolution scenario typically yields ratios close to 1.0, while the sulphate reduction scenario yields ratios close to 1.3 (Berelson *et al.* 1994, Berelson *et al.* 1996). Table 9 gives the ratios of oxygen flux/carbon oxidation flux from both model scenarios for all chamber deployments carried out by VFRI. Most of the ratio values from both models are higher than 1.3. This is most likely due to some underestimation of fluxes other than DO because of the sampling for the other solutes could be done only between two to four times per deployment, depending upon the repetitive sampling diver accessibility to the site.

Table 9: Ratios of oxygen flux/carbon oxidation flux for carbonate dissolution model and for sulphate reduction model for all VFRI benthic chamber deployments.

Site	Mean carbonate dissolution model ratio	Mean sulphate reduction model ratio
6	1.83	2.09
8	1.20	1.30
16	1.39	1.70
19	1.46	1.88
37	1.62	1.80
STL12	1.54	1.65
STL15	2.69	3.06

CORRELATIONS

Site N:P ratios

Dissolved inorganic nitrogen flux and dissolved inorganic phosphorus flux were correlated at each site and overall. If Redfield stoichiometry is assumed during the breakdown of sedimented organic matter, then the predicted molar ratio of regenerated N:P is 16:1. The correlation was analysed with total nitrogen flux as the independent variable, and the results are shown in Table 10.

Table 10: Correlation coefficients, N:P ratio and standard error of the N:P ratio from DIN and phosphate fluxes from chamber deployments at all sites.

Site	r^2	N:P	Std error
6	0.28	6.0	1.2
8	0.91	9.6	1.7
14	0.73	10.7	3.3
16	0.89	9.5	0.8
19	0.98	4.2	0.3
37	0.64	4.3	0.9
STL12	0.94	8.1	0.7
STL15	0.94	8.4	0.9
all	0.41	6.9	0.7

The Site 6 correlation coefficient is much lower than that from all other sites, and the inclusion of Site 6 heavily skews the r^2 value when included in an analysis of all sites. The observations of N:P flux ratios less than 16:1 at all sites with high r^2 values at all but Site 6 indicate that denitrification occurs extensively within PPB.

SUMMARY

Results

1) Benthic chambers were placed on seafloor areas which, apart from burrows, were clear of epifauna or macroalgae. Profiles of DO concentration (Figs. 18 - 23) from within chambers at sample sites show a decrease with time, indicating oxygen consumption, and profiles from light and dark chambers tended to replicate well. Oxygen fluxes were calculated from the most linear part of the DO profiles, which usually occurred within the first few hours of deployment. However, in some instances oxygen concentrations within clear chambers increased for up to 8 hours following deployment (Figs. 18, 21a and 23). As the chambers were usually deployed between late morning and early afternoon, the DO increases coincided with daylight hours. As the breakdown of organic matter consumes oxygen, the DO increase must indicate the presence of photosynthesising benthic autotrophs. Fluxes of oxygen production in these chambers were estimated from the most linear rate of change of increasing DO with time. In fact, it is now known that production by microphytobenthos plays a significant role in the recycling of nitrogenous material in and on the sediments, especially through facilitating the all-important nitrification/denitrification processes (Harris *et al.* 1996). This is discussed further in point 6 in the following page.

2) During the June 1995 monthly deployment at Site 6 (Fig. 21c) when underwater visibility was very poor, one clear chamber was accidentally placed over an epi-benthic tube worm (*Sabella spallanzanii*), and the DO plot for this chamber was distinctive from the others. It also appeared that one dark chamber was placed on some type of epifauna during the August 1995 deployment at Site 37 (Fig. 22), as this profile is also distinct from the others. In both cases DO consumption was greatly increased.

3) Figures 24 - 29 show flux charts from deployments during October 1994, February - March 1995, October 1994 - June 1995 (Site 6), May 1995, August 1995 and January 1996. While there were some aberrations, the mean fluxes of DO, ammonium, phosphate, silicate, total carbon dioxide and manganese from dark and light chambers within sites replicated well.

Temporal patterns from chamber deployments at Site 6 between October 1994 - June 1995 (Figs. 26a - 26b), showed that fluxes of DO, ammonium, phosphate, silicate and total carbon dioxide increased during summer and autumn, whereas nitrite plus nitrate flux increased during the colder months. Iron and manganese fluxes increased during the colder months. Iron and manganese fluxes were near the lower limits of detection, and consequently cannot be considered with the same confidence as the other fluxes.

Spatial patterns from chambers deployed at a number of sites within sampling periods of between two days and two weeks showed that the greatest fluxes were from sites 16 and 6.

4) Comparisons of benthic fluxes from Sites 16 and 37 (Figs. 30 and 31 respectively) over cold and warm water sampling periods showed a trend of increased flux within a site for a number of solutes from warm water chamber deployments. Nitrite plus nitrate, SiO_4 and TCO_2 fluxes at Site 16 were greatest during January 1996. Ammonium flux during January 1996 was less than from the previous warm water period during March 1995 at Site 16 (Fig. 30).

5) There was good agreement between the VFRI dark and light chambers and the Berelson chamber at Sites 6, 8 and 37, but not at Site 16 (Fig 32), where the Berelson chamber has consistently higher flux values of all solutes. The Berelson and the VFRI chambers were placed about 20 m apart during the dual deployment at Site 16, which is within close proximity to the shipping channel of the Port of Melbourne. Any heterogeneity within the sediment at this site is likely to be enhanced due to shipping and dredging activity constantly remobilising local sediments. It would appear that the heterogenous nature of the sediment at this site is pronounced and is the cause of the large difference between both chamber types. Further evidence to support this supposition is that both the Cs dilution rate and the solute fluxes are greatest at this site from the Berelson chamber, which is an indication of an enhanced porewater irrigation rate. It is probable that the differences between chamber types noted at this site are a consequence of sediment heterogeneity.

6) The data in Table 8 shows estimates of N and P liberated from the sediments as calculated from DIN and PO_4 fluxes, and from the DO flux. The amount of N and P estimated from the DO consumption in the breakdown of organic matter is about 3.5 and 1.7 times as great, respectively, as the N and P estimated from DIN and PO_4 fluxes. This indicates that about 70% of the N mineralised undergoes denitrification and is liberated from the Bay as N_2 gas, and that approximately 40% of the mineralised P is adsorbed and trapped within the sediment. There is a discrepancy between the N and P loads liberated from the sediments as estimated from the DO flux, and terrestrial loads of organic matter to the Bay. Production of N_2 in chambers has now been directly demonstrated (Heggie *et al.*, in preparation).

7) Organic carbon oxidation scenarios are represented by either calcium carbonate dissolution or sulphate reduction, and sometimes a combination of both. Fluxes of DO, alkalinity, DIN and CO_2 were used to determine ratios of DO flux/carbon oxidation flux. These should be between 1 - 1.3, with calcium carbonate dissolution typically yielding ratios closer to 1, and sulphate reduction typically yielding ratios closer to 1.3. Most of the ratios shown in Table 9 exceeded the 1 - 1.3 range. It is most likely that the fluxes of alkalinity, DIN and CO_2 were under-estimated because they were calculated from only two samples, collected at the beginning and end of chamber deployment. Fluxes calculated from mid-term samplings during shorter term deployments commenced in April 1995 were under-estimated by 1.1 - 1.4 from fluxes calculated from full-term sampling. It is difficult to determine by which process organic matter undergoes diagenesis. However, Berelson *et al* (1996) suggests that as the nitrification of ammonia within the sediments of PPB is quite efficient, the sulphate reduction model is likely to more closely represent organic matter mineralisation, although the difference between the two models is not great, with a 20% difference at Site 16.

8) If the diagenesis of organic matter follows Redfield stoichiometry, then the N:P molar ratio as calculated from fluxes (Table 10) is much less than 16:1 and indicates that at all sites denitrification is efficient in removing N from PPB.

Statistics

The general linear models (GLM) procedure within the SAS system (SAS Institute Inc., Cary, North Carolina) was used for the testing of a number of hypotheses. In all cases the type III sums of squares were used to test the null hypothesis. A number of modelling scenarios were tested. Apart from the monthly deployment for 9 months at Site 6, Fe and Mn data was not available for some sampling periods. Consequently, Tables 11, 12 and 13 in the following text present results from the analysis of fluxes of DO, CO_2, NH_4, PO_4, NO_X and SiO_4.

1) Analysis of variance of the fluxes of DO, CO_2, NH_4, PO_4, NO_X and SiO_4 obtained from chamber deployments were tested for site and light and dark chamber differences as the main effects. The model used was:

flux = site + chamber type + site*chamber type

The results are shown in the following Table 11.

Table 11: The F ratio and level of significance ($P < 0.05$) for the effects of site, chamber type and the site and chamber type interaction on 6 fluxes for all sites and times is shown below.

Flux	Site	Type	Site* Type
DO			
F	9.29	0.73	0.37
P	*0.0001*	*0.3941*	*0.8965*
CO_2			
F	7.18	0.86	0.08
P	*0.0001*	*0.3573*	*0.9990*
NH_4			
F	4.73	0.04	0.17
P	*0.0001*	*0.8425*	*0.9906*
PO_4			
F	5.78	0.15	0.39
P	*0.0001*	*0.6947*	*0.9083*
NO_X			
F	1.61	0.38	0.28
P	*0.1409*	*0.5369*	*0.9601*
SiO_4			
F	5.89	0.00	0.21
P	*0.0001*	*0.9508*	*0.9827*

Table 11 indicates that there are significant site differences ($P < 0.05$) for all fluxes except NO_X. Chamber type had no significant effect for any flux. Site and chamber type interactions were also insignificant.

2) Results from all chamber deployments were investigated to determine the effects of site, chamber type and water temperature at time of sampling on 6 fluxes, with water temperatures at time of sampling being classified either as cold or warm in response to the particular season. The model to study these effects was:

flux = site + type + temp + site*type + site*temp + type*temp + site*type*temp.

The results are shown in Table 12.

Table 12: The F ratio and level of significance ($P < 0.05$) for the effects of site, chamber type, water temperature, and the interactions on 6 fluxes is shown below.

Flux	Site	Type	Temp	Site* Type	Site* Temp	Temp* Type	Site* Type* Temp
DO							
F	9.72	1.02	41.21	0.65	10.57	0.15	0.29
P	*0.0001*	*0.3142*	*0.0001*	*0.6914*	*0.0001*	*0.6975*	*0.7523*
CO_2							
F	5.23	1.31	36.05	0.10	18.22	0.02	0.49
P	*0.0001*	*0.2548*	*0.0001*	*0.9984*	*0.0001*	*0.9020*	*0.6131*
NH_4							
F	4.33	0.19	13.68	0.20	10.54	1.68	0.36
P	*0.0003*	*0.6617*	*0.0004*	*0.9858*	*0.0001*	*0.1984*	*0.6974*
PO_4							
F	6.37	0.47	41.34	0.48	17.10	0.04	0.20
P	*0.0001*	*0.4928*	*0.0001*	*0.8503*	*0.0001*	*0.8443*	*0.8200*
NO_x							
F	1.23	0.58	1.55	0.30	8.40	0.06	0.18
P	*0.2959*	*0.4501*	*0.2169*	*0.9507*	*0.0004*	*0.8122*	*0.8336*
SiO_4							
F	6.62	0.01	45.95	0.28	41.73	0.07	0.41
P	*0.0001*	*0.9054*	*0.0001*	*0.9612*	*0.0001*	*0.7883*	*0.6635*

Table 12 shows that site differences and water temperature difference (either warm water or cold water) were significant ($P < 0.05$) effects for all fluxes except NO_X, whereas chamber type effects were not significant for all fluxes. Site and temperature interactions were significant ($P < 0.05$) for all fluxes. Site and chamber type and temperature and chamber type interactions were interactions were not significant for all fluxes, while the interaction of the three main effects was not significant for any fluxes. *Post hoc* (ie Duncan's and Tukey's tests) testing indicated Site 16 to be the site most different to all other sites with respect to fluxes, and indicated that warm water corresponded to the greatest mean values for all the other solute fluxes.

3) A smaller scale deployment in cold water conditions at Sites 16 and 37 occurred in August 1995. These two sites were also among those sampled during October 1994 (cold water conditions) and February - March 1995 and January 1996 (warm water conditions).

Effects of site differences, water temperature differences and chamber type differences as well as their interactive effects on 6 fluxes were investigated in the following model:

flux = site + type + temp + site*type + site*temp + type*temp + site*type*temp

Two cold water periods in October 1994 and August 1995 were labelled "cold1" and "cold2" respectively, and the two warm water periods in February 1995 and January 1996 were labelled "warm1" and "warm2", respectively. The results from this model are shown in Table 13.

Table 13: The F ratio and level of significance ($P < 0.05$) for site, chamber type, water temperature, the interactions of site and type, site and temp, type and temp and site and type and temp on 8 fluxes sampled during October 1994, February - March 1995 and August 1995 from Sites 16 and 37.

Flux	Site	Type	Temp	Site* Type	Site* Temp	Temp* Type	Site* Type* Temp
DO							
F	85.52	1.56	39.19	4.05	24.44	3.58	0.52
P	*0.0001*	*0.2250*	*0.0001*	*0.0566*	*0.0001*	*0.0301*	*0.6734*
CO_2							
F	52.64	3.58	31.28	0.02	18.60	0.28	0.77
P	*0.0001*	*0.0717*	*0.0001*	*0.8769*	*0.0001*	*0.8370*	*0.5228*
NH_4							
F	93.56	2.00	19.17	0.19	15.94	0.65	0.38
P	*0.0001*	*0.1712*	*0.0001*	*0.6707*	*0.0001*	*0.5888*	*0.7718*
PO_4							
F	114.66	6.06	50.79	2.65	39.21	1.67	2.02
P	*0.0001*	*0.0221*	*0.0001*	*0.1177*	*0.0001*	*0.2033*	*0.1400*
NO_X							
F	23.80	2.35	53.48	1.44	15.76	1.36	0.24
P	*0.0001*	*0.1397*	*0.0001*	*0.2431*	*0.0001*	*0.2818*	*0.8641*
SiO_4							
F	105.75	2.92	84.18	0.70	63.18	1.28	1.39
P	*0.0001*	*0.1013*	*0.0001*	*0.4122*	*0.0001*	*0.3053*	*0.2721*

Site and temperature were found to be significant ($P < 0.05$) main effects for all fluxes. Chamber type was found to be a significant main effect ($P < 0.05$) for PO_4 flux. *Post hoc* testing recognised the four labelled temperatures as different for the fluxes of PO_4, NO_X and SiO_4, recognised the difference between the warm temperatures for DO and NH_4, and recognised the difference between the combined

warm and combined cold temperatures for CO_2. In all instances, greater means were acknowledged for the warmer temperature periods over the colder temperature periods. Site and chamber type interactions and site and chamber type and temperature interactions were not significant ($P < 0.05$) for any fluxes. Site and temperature interactions were significant ($P < 0.05$) for all fluxes. Chamber type and temperature interaction was significant ($P < 0.05$) for the DO flux.

4) Chambers were deployed at Site 6 once every month for 9 months. The two effects looked at in this situation were water temperature at time of sampling, and chamber type. The model used to investigate this was:

flux = temp + type + temp*type

The results from the model are shown in Table 14.

Table 14: The F ratio and level of significance ($P < 0.05$) of water temperature at time of sampling, chamber type and the interactions of temperature and type on 8 fluxes sampled monthly between October 1994 and June 1995 from Site 6.

Flux	Temp	Type	Temp* Type
DO			
F	4.19	0.47	1.44
P	*0.0015*	*0.4971*	*0.2165*
CO_2			
F	9.07	1.07	3.68
P	*0.0001*	*0.3086*	*0.0036*
NH_4			
F	8.03	0.11	4.09
P	*0.0001*	*0.7436*	*0.0018*
PO_4			
F	14.09	9.94	2.21
P	*0.0001*	*0.0034*	*0.0519*
NO_x			
F	6.83	2.48	2.57
P	*0.0001*	*0.1246*	*0.0267*
SiO_4			
F	13.81	0.86	1.56
P	*0.0001*	*0.3609*	*0.1749*
Fe			
F	0.44	0.00	0.05
P	*0.8898*	*0.9691*	*0.9999*
Mn			
F	4.45	1.30	1.69
P	*0.0010*	*0.2625*	*0.1370*

Temperature was a significant effect ($P < 0.05$) for all fluxes except Fe, whereas chamber type was significant only for PO_4 flux. Temperature and chamber type interaction was significant for CO_2, NH_4, and NO_x. Tukey's and Duncan's range tests on temperature effects on fluxes produced no discernible and consistent sequential pattern with respect to order of magnitude of temperature.

SECTION 3

BENTHIC CHAMBER AND DIFFUSIVE FLUX COMPARISONS

Fluxes of ammonium, phosphate, silicate and nitrite plus nitrate calculated from chamber deployments and from porewater profiles from July 1993 to August 1995 are shown in Figures 33a - 33d. Samples from different periods were grouped by water temperature. Chamber and sediment samples collected within a temperature range of 10.9 - 12.4^{o}C during July 1993, July 1994, October 1994 and August 1995, were considered as cold water samples. Chamber and sediment samples collected during January 1994, February/March 1995 and January 1996 within a temperature range of 18.9 - 20.5^{o}C were considered as warm water samples.

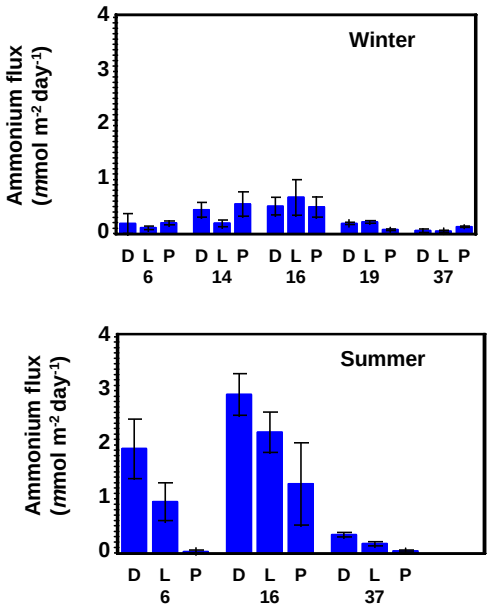

Figure 33a: Fluxes (*m*mol m^{-2} day^{-1}) of ammonium calculated from the deployment of dark (D) and light (L) chambers and porewater profiles (P) from sediment coring at common sites during cold water sampling (top) and warm water sampling (bottom). The error bars indicate one standard deviation about the mean.

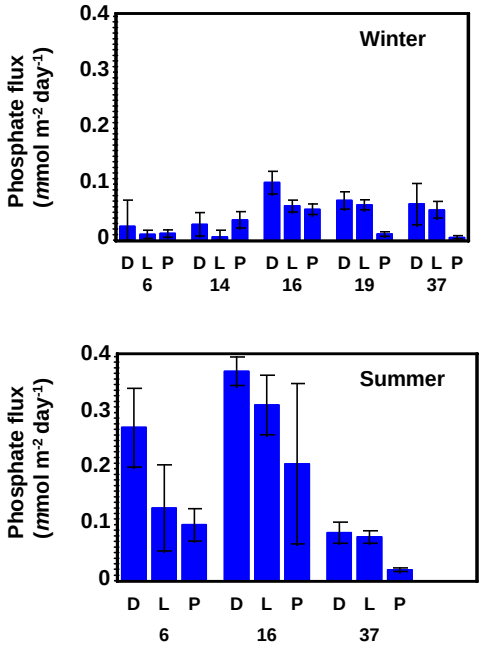

Figure 33b: Fluxes (*m*mol m^{-2} day^{-1}) of phosphate calculated from the deployment of dark (D) and light (L) chambers and porewater profiles (P) from sediment coring at common sites during cold water sampling (top) and warm water sampling (bottom). The error bars indicate one standard deviation about the mean.

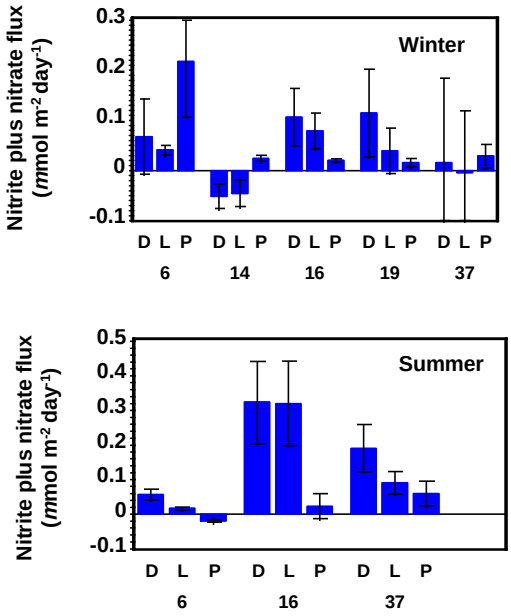

Figure 33c: Fluxes (*m*mol m^{-2} day^{-1}) of nitrite plus nitrate calculated from the deployment of dark (D) and light (L) chambers and porewater profiles (P) from sediment coring at common sites during cold water sampling (top) and warm water sampling (bottom). The error bars indicate one standard deviation about the mean.

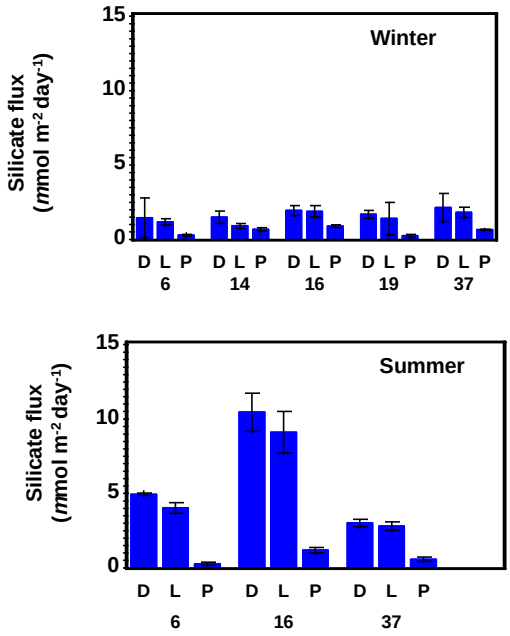

Figure 33d: Fluxes (*m*mol m^{-2} day^{-1}) of silicate calculated from the deployment of dark (D) and light (L) chambers and porewater profiles (P) from sediment coring at common sites during cold water sampling (top) and warm water sampling (bottom). The error bars indicate one standard deviation about the mean.

SUMMARY

Results

1) Chamber fluxes and diffusive fluxes were of similar magnitude during cold water sampling periods, but chamber fluxes were greater than diffusive fluxes during warm water sampling periods.

2) Site (spatial) effects were apparent during both cold water and warm water sampling periods.

Statistics

1) Diffusive and net fluxes, estimated from both porewater solute profiles and benthic chambers were tested to determine whether there was an effect due to site and to the method of flux estimation. Data was split into cold water and warm water sampling periods and the following model was tested within each sampling period, with the assumption that chamber type was not an effect. Origin was the term used to discriminate between benthic chamber fluxes and diffusive fluxes:

$$\text{flux} = \text{site} + \text{origin}$$

The output from the model is shown in Table 15.

Table 15: The F ratio and level of significance ($P < 0.05$) for NH_4, PO_4, NO_X and SiO_4 chamber and diffusive fluxes from cold water and warm water sampling periods.

Flux	Cold Water			Warm Water		
	Site	Origin	Site* Origin	Site	Origin	Site* Origin
NH_4						
F	6.49	0.23	0.96	9.75	17.27	2.91
P	*0.0003*	*0.6330*	*0.4364*	*0.0001*	*0.0002*	*0.0691*
PO_4						
F	7.11	10.66	3.95	11.02	11.94	0.57
P	*0.0001*	*0.0020*	*0.0074*	*0.0001*	*0.0016*	*0.5704*
NO_X						
F	1.71	0.39	1.43	1.19	5.78	1.57
P	*0.1630*	*0.5358*	*0.2400*	*0.3320*	*0.0221*	*0.2230*
SiO_4						
F	2.73	44.98	1.04	6.10	60.50	8.00
P	*0.0395*	*0.0001*	*0.3967*	*0.0009*	*0.0001*	*0.0015*

Site was a significant effect ($P < 0.05$) except for NO_X from both the cold and warm water sampling periods. Advection (the enhancement of diffusive fluxes by bioturbation and represented in origin) was a significant effect ($P < 0.05$) for the fluxes of PO_4 and SiO_4 in cold water, and for all fluxes in warm water sampling periods (Table 15).

OVERALL SUMMARY

The various diagrams and statistics in the preceding pages indicate the following trends.

1) There was a significant spatial pattern in the magnitude of nutrient fluxes calculated by diffusion.

2) There was a significant sampling date effect, but not a consistent warm water/cold water sampling period effect on the magnitude of diffusive nutrient fluxes calculated from porewater profiles.

3) There was a significant spatial pattern in the magnitude of fluxes estimated from the deployment of benthic chambers.

4) There was a significant consistent warm water/cold water sampling period effect on the magnitude of fluxes estimated from the deployment of benthic chambers.

5) There was a significant temporal effect on the magnitude of fluxes estimated from the deployment of benthic chambers during the monthly sampling periods at Site 6.

6) There was no significant difference between the magnitude of silicate and nitrite plus nitrate fluxes estimated by diffusion and from the deployment of benthic chambers during the cold water sampling period.

7) Bioturbation enhanced the fluxes of ammonium, silicate and nitrite plus nitrate during the warm water sampling period.

8) Benthic oxygen production was occasionally observed at Sites 16, 6 and 37, from within clear chambers during daylight hours.

DISCUSSION

The porewater profiles of ammonium, phosphate and silicate obtained during the sampling periods of July 1993, January 1994 and July 1994 are characteristic indicators of benthic animal activity and the mineralization of recently deposited fine-grained material rich in organic matter (Van Der Loeff 1980, Callender & Hammond, 1982, Emerson *et al.* 1984, Viel *et al.* 1991). Subsurface maxima of ammonium, phosphate and silicate in porewater profiles were observed at all periods of the year in samples collected from the southern Bight of the North Sea, although no significant seasonal variations were found in the interstitial nutrient concentrations (Van Der Loeff 1980). However, other workers have found seasonal changes in pore water profiles and benthic fluxes (Lerat *et al.* 1990; Barbanti *et al*. 1995). Variance analysis of sampling period effects on nutrient concentrations within the porewater to a depth of 20 cm in PPB found time to be a significant effect, but did not translate into consistent seasonal (or temperature) patterns.

Many coastal and estuarine benthic environments exhibit pronounced seasonality in rates of benthic metabolism, nutrient regeneration and sediment-water chemical exchange. Seasonality is almost entirely a biological response of the system to an annual oscillation in temperature. Incubation experiments showed that at > 15^{o}C microbially mediated reaction rates caused detectable solute concentration changes over a few days rather than a few months (Klump & Martens 1989). Yoon & Benner (1992) considered that temporal variations in rates of denitrification and total DO consumption were dominated by temperature. Reduced benthic fluxes of nitrite plus nitrate and manganese with increased temperature may indicate that anaerobic processes are not a major diagenetic pathway during the colder months, at least at Site 6, in PPB.

Regression between the methods of estimation of the four common nutrient fluxes from cold water and warm water samplings used the flux from chambers as the independent variable, and the regression was forced through zero (Table 16). The warm:cold ratio of the flux enhancement factor for NH_4, PO_4 and SiO_4 (Table 16) is between about 1.3 to 3.2 over a temperature difference of about 8^{o}C, while NO_X is about 12. Aller & Aller (1992) note that meiofaunal activity can increase solute transport in surface muds by between 1.7 to 2.3 times for temperatures between 10^{o}C - 25^{o}C, with the magnitude of the effect varying predominantly with temperature.

Table 16: Regression of chamber flux versus diffusive flux for NH_4, PO_4, NO_X and SiO_4, showing goodness of fit, the flux enhancement factor and the standard error, and the water temperature at sampling. The flux enhancement factor is the ratio of chamber flux:diffusive flux.

Flux	r^2	Flux Enhancement Factor	Std Error	Water Temp
NH_4	0.8304	0.82	0.19	cold
	0.7834	2.07	0.77	warm
PO_4	0.5602	1.36	0.60	cold
	0.9802	1.75	0.18	warm
NO_X	0.1728	0.27	0.30	cold
	0.3959	3.29	2.88	warm
SiO_4	0.8615	2.46	0.49	cold
	0.9339	7.96	1.44	warm

However, temperature was not considered the driving factor controlling ammonium production in the sediments in the southern part of San Francisco Bay, but rather the timing of organic inputs, with primary production and subsequent organic deposition greatest in the spring (Caffrey 1995). In PPB, preliminary data analysis indicates that most primary production occurs during summer, and is about five times greater than winter levels (Beardall *et al.* 1996). Benthic chamber deployment periods at times coincided to within two weeks with sampling cruises of the PPBES task investigating phytoplankton productivity. A number of sites from both programs were similar. Data collected from both programs within similar temporal and spatial frameworks was used to provide the plot of sediment C flux (as CO_2) versus water column C production shown in Figure 34, and indicates a good relationship (r^2 = 0.6552) between sediment CO_2 flux and primary production within the water column.

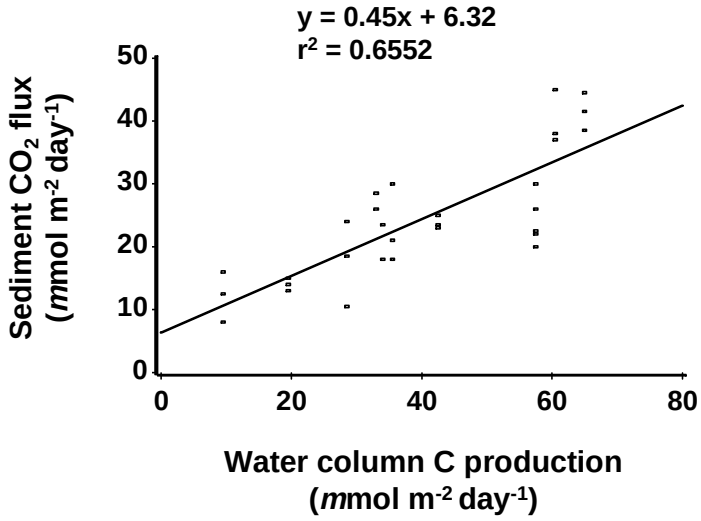

Figure 34: Sediment CO_2 flux versus water column C production (courtesy Dr. R. Royle, Monash Uni.).

The magnitude of solute fluxes within PPB are affected by proximity to source of terrestrial nutrient inputs, bioturbation and the effect of temperature on bioturbation. The intensity and type of diagenetic processes have been noted elsewhere as a function of the distance from riverine input (Barbanti *et al.* 1995). Sites 16 and 6 in PPB have the greatest fluxes; both of these sites are near major terrestrial nutrient inputs. Bird (1994) and Smith (1996) have indicated that burrowing animals turn over large amounts of porewater and sediments, to at least 10 cm depth, within PPB. *Neocallichirus limosus*, a burrowing shrimp, is estimated to process 8 x 10^5 tonne of sediment daily in PPB; irrigation rates of burrowing organisms may overturn the water volume of PPB almost once a month.

More study of the data is required to define pathways of organic matter diagenesis. The sulphate reduction pathway model of Berelson *et al* (1996) accounts for 5 - 50% of total organic carbon oxidation, but is adopted as the diagenesis model because 1000 tonne day^{-1} of carbonate shell material within the Bay would have to dissolve to fit the interpretation of the calcium carbonate dissolution model.

It is interesting to note that the intercept from Figure 34 gives an instantaneous CO_2 flux of about 6 *m*mol m^{-2} day^{-1}. This could be viewed as flux emanating from the dissolution of $CaCO_3$, and if this value is applied to the total Bay area of 1950 km^2, the daily $CaCO_3$ dissolution amount is about 1200 tonne. However, it is likely that both processes occur, and the difference in the calculated amounts of total carbon oxidised is not great, with a maximum of a 20% difference between the two models at Site 16. Yoon & Benner (1992) note that sulphate reduction is typically the predominant process responsible for the mineralization of organic carbon in anaerobic marine sediments and accounts for about 50% of the total mineralization in shallow coastal sediments.

The N:P ratio expected if the diagenesis of organic matter follows Redfield stoichiometry is 16:1. Nitrogen to P ratios at all sites throughout the Bay determined from measured DIN and PO_4 fluxes were considerably lower than this, ranging from 4.3 - 10.7:1 (Table 10), with a trend of lowest N:P ratios originating from sites which have the lowest fluxes of DIN and PO_4, or the lowest rates of organic carbon mineralisation. A large portion of the mineralized N is escaping the Bay as gaseous N through denitrification, and the data shown in Figure 35 supports this assertion. Each of the three graphs has a solid 1:1 ratio line drawn in it, as well as a dashed line of best fit forced through zero. It can be seen that the obtained N flux as measured from DIN flux is very much less than what would be expected when calculated from the total carbon dioxide flux. The regression estimate, with a correlation of 0.7474, shows the obtained N flux is 0.31 of the expected flux, and this can be translated into an estimated baywide denitrification of 69%. The obtained P flux as measured from PO_4 flux is also less than the expected P flux when calculated from the total carbon dioxide flux. The regression estimate, with a correlation of 0.7444, shows the obtained P flux is 0.53 of the expected flux, which could be considered as an indication that about 47% of the baywide mineralised P is adsorbed onto sediment particles. A good relationship can be observed between the baywide measured DO flux and the calculated DO flux determined from the CO_2 flux, with a regression estimate of 0.98 and a correlation of 0.8519. As CO_2 is the common parameter used in these assertions, and as there appears to be no reference in the literature to CO_2 being locked in the sediments in an adsorptive relationship, this result could be considered as a validation that N and P expected fluxes are much greater than those measured. As it appears that N is the limiting nutrient in PPB, any perturbation of the denitrification process which leads to less N_2 being liberated will likely have major deleterious effects associated with increased production within the Bay.

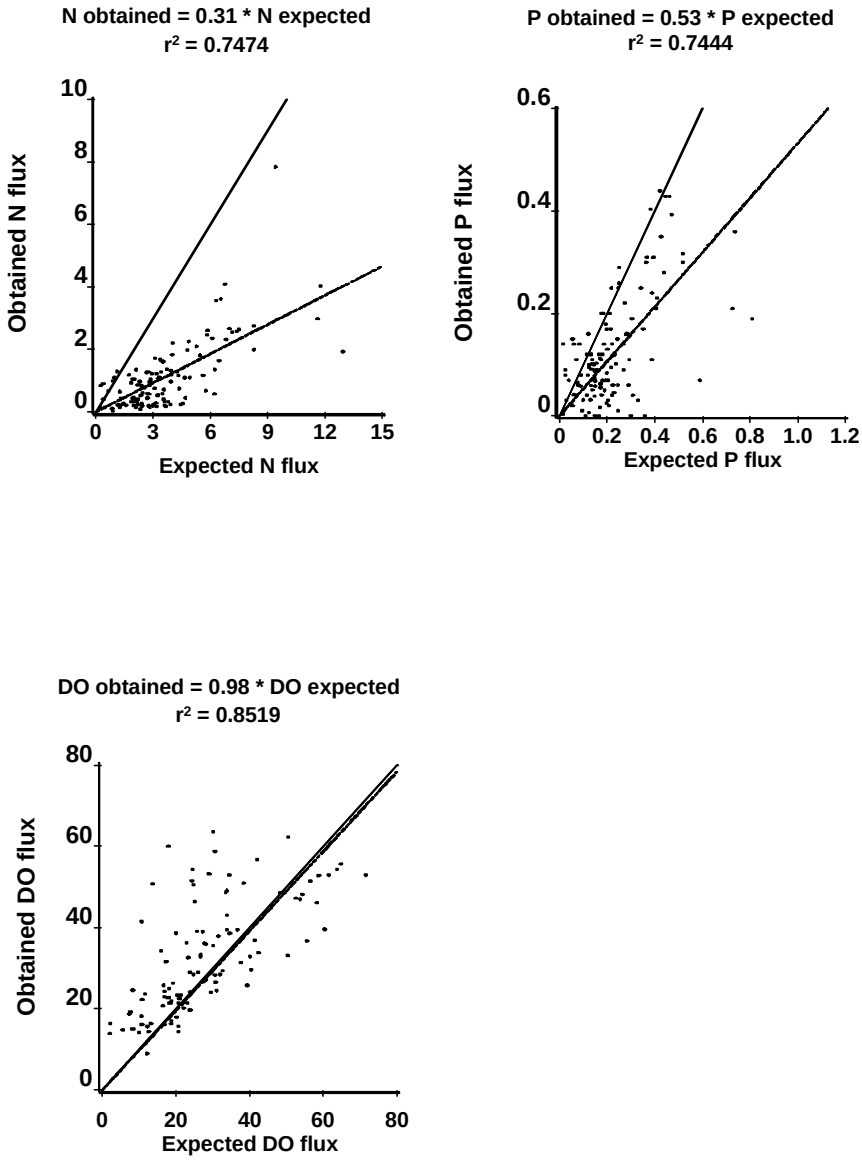

Figure 35: Plots of baywide measured fluxes of inorganic N, inorganic P and DO versus expected fluxes of inorganic N, inorganic P and DO as calculated from the CO_2 flux. The solid line is the expected 1:1 ratio, and the broken line is the line of best fit of the data when forced through zero.

A number of shorter duration VFRI chamber deployments of between 5 to 6 hours, with mid-term solute sampling, were undertaken during the later stages of this program at Sites 6, 16 and STL12. The data presented in Figure 36 are plots of DO concentrations versus nutrient concentrations at time of sampling for all short deployments.

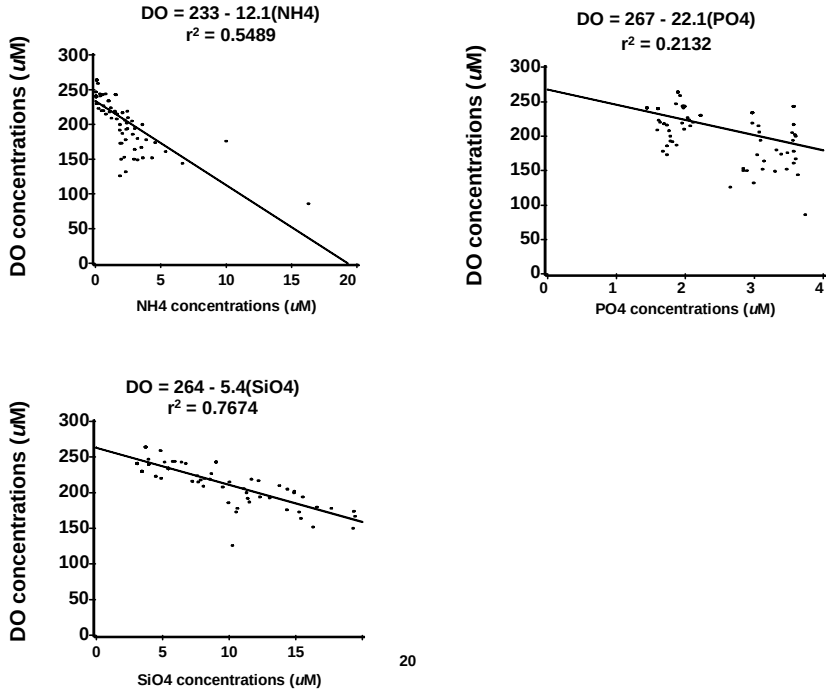

Figure 36: Plots of concentrations of DO versus NH_4, PO_4 and SiO_4 at time of sampling from all short-term deployments.

The data shown in Figure 36 suggests a number of points. The generally linear relationship from all of the plots indicates that the bulk of the DO consumed within the chamber is used for the breakdown of sedimented organic material. The poorest relationship occurs with PO_4 and most likely is indicative of the adsorptive effects of sediment on mineralised P, and also that differing sediment types found within the Bay have different characteristics with respect to adsorptive processes. The NH_4 relationship is probably reflective of denitrifying processes differing between sites, but not as greatly as site effects on P adsorption, with an average N loss from the system of about 50%. The best relationship occurs with SiO_4 and the slope of the line (5.4) is close to the Redfield estimate of 6.6 between O_2 and Si, and indicatives that site location has little effect on the mineralisation of Si, as well as the absence of processes removing Si.

The estimated terrestrial inputs of N and P are shown in the introductory section of this report and there is a large discrepancy in the budget between terrestrial input of N and P to the Bay and the amount of N and P released by the sediments as estimated by Redfield stoichiometry of DO fluxes. Also, the amount of N and P flux measured

from the chambers are about 70% and 50% respectively less than expected when estimated from DO, which could be indicative of high denitrification and high sediment adsorption, respectively. Part of the budgeting problem is associated with the boundaries of the nominal regions of the Bay. A suggested review of the regional boundaries is shown in Figure 37.

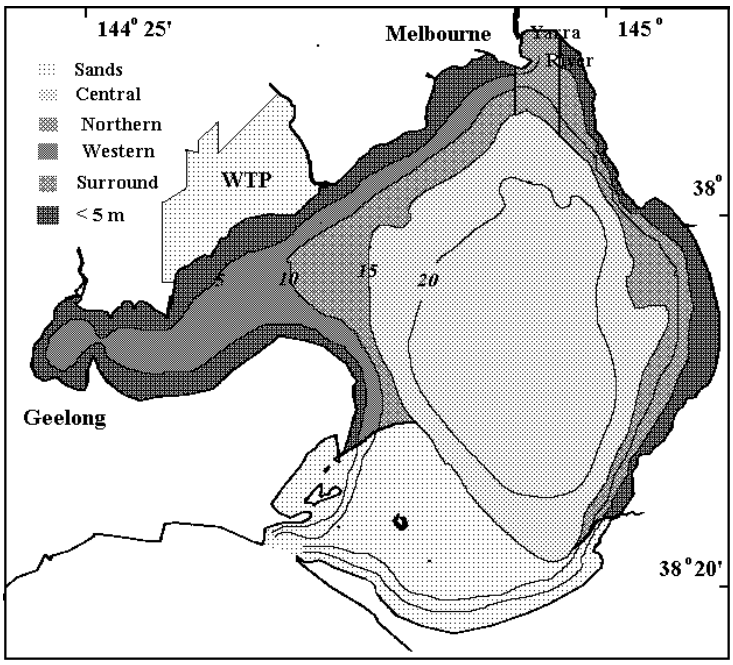

Figure 37: Suggested reworking of regional area boundaries. The sands and area less than 5m depth are excluded. The central region has been increased, while the other 3 remaining regions have been decreased.

It is likely the large sandy southern region of the Bay (~ 340 km^2) within the Surround region termed the 'Great Sands' (Port Phillip Bay chart Aus 143) and under tidal influence from Bass Strait has little sedimented organic material and contributes little in the way of N and P fluxes to the water column. Similarly, the area of the Bay between the shoreline and the 5 m depth contour (~ 190 km^2 from Surround region and ~ 90 km^2 from the Western region) is likely to have little sedimented organic matter due to constant resuspension from wave action and would also contribute little in the way of N and P output. The Central region boundary has been changed to follow the 15 m depth contour, as the sediment found at this depth and greater appears to be similar in nature. This has increased the area from ~500 km^2 to ~900 km^2. The Western region has been reduced in area and is that region within the 5 m and 10 m contour, and bounded by the sands in the south and the Northern region in the north. The Northern region has been greatly reduced in area and the boundaries chosen to the 15 m contour were based on sediment characteristic and selected area affected by the Yarra. The Surround region is that area remaining between the 10 m and 15 m depth contour. Even with these boundary reworkings (Table 17) there is still a large imbalance in the budget between terrestrial inputs and sedimentary outputs.

Table 17: Nitrogen and phosphorus (tonne year^{-1}) liberated from the sediments within each reworked region as estimated by chamber DIN and PO_4 fluxes, and by the DO flux and the Redfield ratio (cf. Table 8).

Region	Area	Estimated from DIN & PO_4 flux		Estimated from DO flux	
	(km^2)	N (tonne yr^{-1})	P (tonne yr^{-1})	N (tonne yr^{-1})	P (tonne yr^{-1})
Central	800	1100 ± 1400	650 ± 400	10300 ± 4000	1400 ± 500
Northern	40	400 ± 250	100 ± 70	800 ± 400	110 ± 50
Surround	290	1100 ± 650	320 ± 200	3500 ± 1100	500 ± 200
Western	185	1000 ± 1100	250 ± 200	4000 ± 1300	550 ± 200
Total	1315	3600 ± 1900	1320 ± 500	18600 ± 4000	2500 ± 600

The O_2 production noticed occasionally in clear chambers during deployments would have a modifying effect on nutrient budget estimates. Broad coverage of the sediment surface by some type of benthic (phytoplanktonic) mat was noticed at Site 37, which has a depth of 24 m, during January 1996. Estimates of DO production from Sites 6, 16 and 37 can vary between ~1 - 26 *m*mol m^{-2} day^{-1}. Estimates of N flux to the sediments in the Central region, assuming an area of ~800 km^2 and a N flux of 3.3 *m*mol m^{-2} day^{-1}, can be up to 900 tonne year^{-1}.

ACKNOWLEDGMENTS

The advice and assistance of Will Berelson, Graham Skyring, David Heggie, Anne Gason and Technical Operations staff at VFRI is appreciated. Brian Newell and Doug Hall of the PPBES office did the final edit of the manuscript and Rob Molloy and Colin Arrowsmith helped with the data. Also appreciated is the comments from other members of the PPBES Technical Group and task officers for ideas and suggestions.

Melbourne Water is thanked for the financial assistance, without which this work would not have been done.

REFERENCES

Aller, R.C. and Aller, J.Y. (1992). Meiofauna and solute transport in marine muds. *Limnol. Oceanogr*. **37**, 1018-1033.

Axelrad, D.M., Poore, G.C.B., Arnold, G.H., Bauld, J., Brown, V., Edwards, R.R.C. and Hickman, N.J. (1981). The effects of treated sewage discharge on the biota of Port Phillip Bay, Victoria. In *Proceedings of the First International Symposium on Nutrient Enrichment of Estuaries*. Editors: B.J. Neilson and L.E. Cronic, Virginia, USA.

Barbanti, A., Bergamini, M.C., Frascari, F., Miserocchi, S., Ratta, M. and Rosso, G. (1995). Diagenetic processes and nutrient fluxes at the sediment-water interface, Northern Adriatic Sea, Italy. *Mar. Freshwater Res.* **46**, 55-67.

Bauld, J. and Millis, N.F. (1977). *Role of bacteria in nitrogen cycling in the Werribee zone*. Environmental Study Series No. 166, Ministry for Conservation, Victoria.

Beardall, J., Roberts, S. and Royle, R. (1996). *Phytoplankton productivity in Port Phillip Bay: seasonal and spatial distributions.* . Technical Report 35, CSIRO INRE, Port Phillip Bay Environmental Study, Melbourne, Australia..

Beasley, A.W. (1966). Port Phillip Bay survey, 1957-1963: bottom sediments. *Memoirs of the National Museum of Victoria*, **27**, 69-105.

Bendschneider , K. and Robinson, R.J. (1952). A new spectrophotometric method for the determination of nitrite in seawater. *J. Mar. Res.*, **11**, 87-96.

Berelson, W.M., Kilgore, T.E. and Heggie, D.T. (1994). *Benthic chambers, nutrient fluxes and the biogeochemistry of the seafloor from Port Phillip Bay, Australia.* AGSO Record 1994/16, Australian Geological Survey Organisation, Canberra, ACT, Australia.

Berelson, W., Kilgore, T., Heggie, D., Skyring, G. and Ford, P. (1996). *Benthic chambers, nutrient fluxes & the biogeochemistry of the seafloor of Port Phillip Bay, 1995 & 1996.* AGSO Record 1996/17, Australian Geological Survey Organisation, Canberra, ACT, Australia.

Bird, F.L. (1994). *The effects of bioturbation in Port Phillip Bay.* Technical Report 14, CSIRO INRE, Port Phillip Bay Environmental Study, Melbourne, Australia..

Bray, J.T., Bricker, O.P. and Troup, B.N. (1973). Phosphate in interstitial waters of anoxic sediments: oxidation effects during sampling procedure. *Science*. **180**, 1362 - 1364.

Burke, C.M. (1995). *Microprofiles of oxygen concentration in Port Phillip Bay*. Report, Department of Aquaculture, University of Tasmania at Launceston, Launceston, Tasmania, Australia. 7250.

Caffrey, J. M. (1995). Spatial and seasonal patterns in sediment nitrogen remineralization and ammonium concentrations in San Fransisco Bay, California. *Estuaries* **18**, 219-233.

Callender, E and Hammond, D. (1982). Nutrient exchange across the sediment-water interface in the Potomac River estuary. *Est., Coast Shelf Sci.* **15**, 395-413.

Cody, R.P. and Smith, J.K. (1991). *Applied Statistics and the SAS Programming Language. Third Edition.* Prentice-Hall Inc., Englewood Cliffs, New Jersey, USA.

Crum, L., Editor (1986). SAS system for linear models. SAS Institute Inc., Cary, NC, USA. p 86.

Currie, D.R. and Parry, G.D. (1995). *The effect of scallop dredging on a soft sediment community: A large scale experimental study.* Early draft Internal Report, July. Victorian Fisheries Research Institute, Department of Conservation and Natural Resources, Victoria, Australia.

Dickson, A.G. (1981). An exact definition of total alkalinity and a procedure for the estimation of alkalinity and total inorganic carbon from titration data. *Deep-Sea Res.,* **28A**, 609-623.

Emerson, S., Jahnke, R. and Heggie, D. (1984). Sediment-water exchange in shallow water estuarine sediments. *J. Mar. Res.* **42**, 709-730.

Fisher, T.R., Carlson, P.R. and Barber, R.T. (1982). Sediment nutrient regeneration in three North Carolina estuaries. *Est., Coast. Shelf Sci.*, **14**, 101-116.

Gorfine, H.K., Longmore, A.R. and Abbott, B.D. (1996). *Sediment oxygen demand in Port Phillip Bay.* Publication no. 495 , Environment Protection Authority, Victoria, Australia.

Harris, G., Batley, G., Fox, D., Hall, D., Jernakoff, P., Molloy, R., Murray, A., Newell, B., Parslow, J., Skyring, G. and Walker, S. (1996*). Port Phillip Bay Environmental Study Final Report.* CSIRO, Canberra, Australia.

Hecky, R.E., Campbell, P. and Hendzel, L.L. (1993). The stoichiometry of carbon, nitrogen and phosphorus in particulate matter of lakes and oceans. *Limnol. Oceanogr.*, **38**(4), 709-724.

Hunter, J.R. (1992). *Review of physical process.* In *Port Phillip Bay Environmental Study: Status Review.* D.N. Hall: (Ed), Technical Report 9, CSIRO INRE, Port Phillip Bay Environmental Study, Melbourne, Australia..

Jorgensen, B. and Revsbech, N. (1985). Diffusive boundary layers and the oxygen uptake of sediments and detritus. *Limnol. Oceanogr.* **30**, 111-122.

Justic, D., Rabalais, N.N. and Turner, R.E. (1995). Stoichiometric nutrient balance and origin of coastal eutrophication. *Mar. Pollut. Bull.* **30**, 41-46.

Klump, J. and Martens, C. (1989). The seasonality of nutrient regeneration in an organic-rich coastal sediment: Kinetic modelling of changing pore-water nutrient and sulfate distributions. *Limnol. Oceanogr.* **34**, 559-577.

Koroleff, F. (1972). Determination of reactive silicate. In *New Baltic Manual*. (Editor S. Carlberg). ICES Charlottenlund Slot, Denmark.

Krom, M.D. and Berner, R.A. (1980). The diffusion coefficients of sulphate, ammonium, and phosphate ions in anoxic marine sediments. *Limnol. Oceanogr.*, **25**, 327 - 337.

Lerat, Y., Lasserre, P. and le Corre, P. (1990). Seasonal changes in pore water concentrations of nutrients and their diffusive fluxes at the sediment-water interface. *J. Exp. Mar. Biol. Ecol.* **135**, 135-160.

Longmore, A.R., Cowdell, R.A. and Gibbs, C.F. (1989). *Monitoring of water quality in Port Phillip Bay, 1985-86.* SRS 89/003, Environment Protection Authority, Victoria, Australia.

Longmore, A.R., Cowdell, R.A. and Abbott, B. (1994). *Water quality in Port Phillip Bay 1990 - 94: Program 700 interim report*. Internal Report No. 212. Victorian Fisheries Research Institute, Department of Conservation and Natural Resources, Victoria, Australia

Longmore, A.R., Cowdell, R.A. and Flint, R. (1996). *Nutrient status of the water in Port Phillip Bay*. Technical Report 24, CSIRO INRE, Port Phillip Bay Environmental Study, Melbourne, Australia..

Marinelli, R.L. (1992). Effects of polychaetes on silicate dynamics and fluxes in sediments: Importance of species, animal activity and polychaete effects on benthic diatoms. *J. Mar. Res.*, **50**, 745 - 779.

McCaffrey, R.J., Myers, A.C., Davey, E., Morrison, G., Bender, M., Luedtke, N., Cullen, D., Froelich, P. and Klinkhammer, G. (1980). The relation between pore water chemistry and benthic fluxes of nutrients and manganese in Narragansett Bay, Rhode Island. *Limnol. Oceanogr.*, **25**, 31-44.

Morris, A.W. and Riley, J.P. (1963). The determination of nitrate in seawater. *Anal. Chim. Acta.*, **29**, 272-279.

Murray, A.G. (1994). *Western treatment plant outputs to Port Phillip Bay.* Technical Report 15, CSIRO INRE, Port Phillip Bay Environmental Study, Melbourne, Australia..

Murphy, J. and Riley, J.P. (1962). A modified single solution method for the determination of phosphate in natural waters. *Anal. Chim. Acta*, **27**, 31-36.

Nicholls, K.H. (1975). A single digestion procedure for manual determination of Kjeldahl nitrogen and total phosphorus in natural waters. *Anal. Chim. Acta.*, **76**, 208-212.

O'Leary, T., Leeming, R., Nichols, P.D. and Volkman, J.K. (1994). *The distributions and concentrations of biomarkers for sewage, primary producers and bacteria in the major sediment types of Port Phillip Bay.* Technical Report 17, CSIRO INRE, Port Phillip Bay Environmental Study, Melbourne, Australia..

Otto, C.J. (1992). *Literature and information review of groundwater input of nutrients and toxicants to Port Phillip Bay.* Technical Report 4, CSIRO INRE, Port Phillip Bay Environmental Study, Melbourne, Australia..

Revsbech, N.P., Sorenson, J., Blackburn, T.H. and Lomholt, J.P. (1980). Distribution of oxygen in marine sediments measured with microelectrodes. *Limnol. Oceanogr.*, **25,** 403-411.

Rosenberg, M, Black, K. and Parry G. (1992). *Scallop dredging and sedimentation in Port Phillip Bay. Volume 1: Sediment and hydrodynamic measurements: Field data collection and analysis.* Victorian Institute of Marine Sciences Working Paper No. 24, 78 pp. Victoria, Australia.

Santschi, P., Hohener, P., Benoit, G. and Buchholtz-ten Brink, M. (1990). Chemical processes at the sediment-water interface. *Mar. Chem.* **30**, 269-315.

Skyring, G.W., Longmore, A.R., Chiffings, A.W. and Crossland, C.J. (1992). *Nutrients.* In *Port Phillip Bay Environmental Study: Status Review.* D.N. Hall: (Ed), Technical Report 9, CSIRO INRE, Port Phillip Bay Environmental Study, Melbourne, Australia..

Smith, D. (1996). Port Phillip Bay. Lead-210 in sediment profiles. Technical Report 41, CSIRO INRE Port Phillip Bay Environmental Study, Melbourne, Australia.

Solorzano, L. (1969). Determination of ammonia in natural waters by the phenol hypochlorite method. *Limnol. Oceanogr.* **14**, 799-801.

Standard Methods. (1992). Standard Methods. 18th Edition. *For the examination of water and wastewater.* A.E. Greenberg, L.S. Clesceri and A.D. Deaton (Eds.). American Public Health Association, Washington, USA.

Statham, P.J. (1985). The determination of dissolved Mn and Cd in sea water at low nmol l^{-1} concentrations by chelation and extraction followed by electrothermal atomic absorption spectrometry. *Anal. Chim. Acta.* **169**, 149-159.

Stookey, L.L. (1970). Ferrozine - a new spectrophotometric reagent for iron. *Anal. Chem.* **42**, 779-781.

Strickland, J.D.H. and Parsons, T.R. (1968). *A Practical Handbook of Seawater Analysis*. Fisheries Research Board of Canada, Ottowa, Canada.

Sweerts, J.R.A. (1991). Similarity of whole-sediment molecular diffusion coefficients in freshwater sediments of low and high porosity. *Limnol. Oceanogr.*, **36**, 335 - 342.

Tabatabai, M.A. (1974). Determination of sulphate in water samples. *Sulphur Institute Journal*. **10**, 11-13.

Technicon (1972). Nitrate and nitrite in seawater. Industrial method No. 158-71W. Technicon Instrument Corporation, Tarrytown, New York.

Technicon (1973a). Ammonia in water and seawater. Industrial method No. 154-71 W. Technicon Instrument Corporation, Tarrytown, New York.

Technicon (1973b). Orthophosphate in water and seawater. Industrial method No. 155-71W. Technicon Instrument Corporation, Tarrytown, New York.

Technicon (1973c). Silicates in water and seawater. Industrial method No. 186-71W. Technicon Instrument Corporation, Tarrytown, New York.

Ullman, W.J. and Aller, R.C. (1982). Diffusion coefficients in nearshore marine sediments. *Limnol. Oceanogr.*, **27,** 552-556.

Valiela, I. (1984). *Marine Ecological Processes.* Springer-Verlag, New York, USA.

Van Der Loeff, M.M.R. (1980). Nutrients in the interstitial waters of the Southern Bight of the North Sea. *Neth. J. Sea Res.*, **14**, 144-171.

Van Hall, C.E., Safranko, J. and Stenger, V.A. (1963). Rapid combustion method for the determination of organic substances in aqueous solution. *Anal. Chem.* **35**, 315-319.

Varian. (1979). Analytical methods for flame spectroscopy. Publication No. 85-100009-00, Varian Techtron Pty. Ltd., Springvale, Australia.

Viel, M., Barbanti, A., Langone, L., Buffoni, G., Paltrinieri, D. and Rosso, G. (1991). Nutrient profiles in the pore water of a deltaic lagoon: Methodological considerations and evaluation of benthic fluxes. *Est., Coast Shelf Sci.* **33**, 361-382.

Walpole, R.E and Myers, R.H. (1978). *Probability and Statistics for Engineers and Scientists. Second edition.* Macmillan Publishing Co., Inc., New York, USA.

Yoon, W. and Benner, R. (1992). Denitrification and oxygen consumption in sediments of two south Texas estuaries. *Mar. Ecol. Prog. Ser.* **90**, 157-167.

Zar, J.H. (1984). Biostatistical Analysis. Second edition. Prentice-Hall, Inc., Englewood Cliffs, New Jersey, USA.

APPENDICES

Appendix 1: Visual observations by divers during attendance at 10 sites sampled during January 1994. See Figure 2 for site locations.

Site	Diver observations
3	Soft clay/mud sediment with some shell grit present. The sediment was soft enough for a diver to insert arm to the shoulder. Many large burrows present. A lot of mussels, oysters and fan worms (*Sabellids*) were noticed. There were also patches of clear sediment with no apparent micro algal mats.
6	Soft sand/silt/clay mixture. There was probably complete coverage of bottom with filamentous green and red/brown algae and a thin reddish tinged layer which may have been settled dead diatoms from recent *Nitzchia* blooms. A lot of burrows, worms crawling over the benthic mat and crustaceans evident.
8	Bottom type was predominantly sandy/shelly and very bumpy. Large clumps of cunjevoi, macro and filamentous red-brown algae and fan worms. There was an incomplete benthic mat coverage.
11	Soft muddy/silty sediment with many burrows of various diameters and filamentous micro-algae present.
13	Very soft unconsolidated flocculent sediment, very easy to push arm fully into. Burrows were evident but no mats were noticed.
14	Soft more consolidated sediment of mud/silt/clay mixture. Some burrows and isolated mussels and oysters were noticed but no benthic mats.
16	Very soft unconsolidated sediment to a depth of about 35 cm above a hard clay-like layer. Very few burrows evident and no benthic mats.
19	Predominantly sandy with some clay/silt. Scallops, mussels and cunjevoi and a few burrows noticed, although no benthic mats were seen.
22	Clear sandy rippled bottom in tidal current scoured area. Little evidence of burrowing animals.
37	Very soft sediment. Burrows were evident.

Appendix 2: Mean pooled values with one standard deviation from the sediment of dissolved inorganic nitrogen (DIN), DIP, DON, DOP, SedN, SedP and SOC in tonnes from all regions and the baywide total in PPB from July 1993, January 1994 and July 1994, and the mean pooled values with one standard deviation of DIN, DIP, DON and DOP in tonnes in the water column obtained from the concurrently run PPBES task N2.1 (Longmore *et al*., 1996).

Program source	Region (km^2)	DIN (tonnes)	DIP (tonnes)	DON (tonnes)	DOP (tonnes)	SedN (tonnes)	SedP (tonnes)	SedC (tonnes)
N3.1	Central (506)	25 ± 15	20 ± 10	60 ± 45	1.5 ± 1	40,000 ± 9,000	14,000 ± 3,000	480,000 ± 110,000
N3.1	Northern (240)	60 ± 55	45 ± 30	130 ± 50	3 ± 1.5	29,000 ± 3,000	12,000 ± 2,000	315,000 ± 55,000
N3.1	Surround (919)	45 ± 20	25 ± 15	150 ± 55	3 ± 2	37,000 ± 5,000	30,000 ± 10,000	270,000 ± 270,000
N3.1	Western (284)	30 ± 10	35 ± 15	120 ± 75	3 ± 4	41,000 ± 6,000	15,000 ± 2,000	360,000 ± 80,000
N3.1	Baywide (1949)	160 ± 60	125 ± 35	460 ± 115	10.5 ± 5	147,000 ± 12,000	71,000 ± 11,000	1,425,000 ± 310,000
N2.1	Baywide (1949)	270 ± 210	1270 ± 130	2600 ± 320	130 ± 60			